

**University of Alberta**

Using 5.9 GHz DSRC to Aid the Elderly in Vehicular Environments

by

Fraaz Kamal

A thesis submitted to the Faculty of Graduate Studies and Research  
in partial fulfillment of the requirements for the degree of

Master of Science

in

Computer, Microelectronic Devices, Circuits and Systems

Department of Electrical and Computer Engineering

©Fraaz Kamal  
Spring 2013  
Edmonton, Alberta

Permission is hereby granted to the University of Alberta Libraries to reproduce single copies of this thesis and to lend or sell such copies for private, scholarly or scientific research purposes only. Where the thesis is converted to, or otherwise made available in digital form, the University of Alberta will advise potential users of the thesis of these terms.

The author reserves all other publication and other rights in association with the copyright in the thesis and, except as herein before provided, neither the thesis nor any substantial portion thereof may be printed or otherwise reproduced in any material form whatsoever without the author's prior written permission.

## **Abstract**

This thesis investigated the feasibility of using the Dedicated Short Range Communication (5.9 GHz) protocol as a vehicular wireless system for transmitting elderly drivers' vital signs in medical emergencies. Existing vehicular communication systems, physiological monitors, and low-power wireless protocols were researched. An integrated in-car system that combined DSRC and physiological monitoring was developed. The DSRC system was tested for latency, packet loss, and range. The physiological monitor was tested for accuracy of its sensors. Finally, the integrated system was tested for its success rate in a vehicular environment. The DSRC system communicated between moving vehicles with an average latency of  $1.450 \pm 0.415$  ms, and it transmitted from a vehicle to roadside infrastructure at a maximum range of 460 m. The physiological monitor collected accurate heart rate, SpO<sub>2</sub>, and body temperature measurements. Finally, the integrated system transmitted physiological parameters from one moving vehicle to another with a 95% success rate.

## **Acknowledgements**

My two supervisors - Dr. Edmond Lou and Dr. Vicky Zhao - deserve immense credit for their hard work throughout these past two and a half years. They were always accessible when I needed help and were constantly providing valuable feedback. They kept me on track every step of the way, and for this, I am grateful.

I would like to thank my entire family for their love and encouragement. My parents are particularly deserving of recognition for instilling a great respect towards education within me from a young age. They gave me the freedom to choose my own career path, but were constantly ensuring that I was fully exerting myself in my educational endeavors. In short, they are the best parents that a student could ask for.

The students and staff of the Glenrose Rehabilitation Hospital provided me with plenty of advice, assistance, and good conversation during my years as a student. I would like to thank every student of past and present who has ever assisted in a test or proofread a paper on my behalf. The best way to ensure your own success is to surround yourself with people smarter than you are, and within the walls of our research lab, such people are never in short supply.

I would like to thank the AUTO21 research consortium for providing me with funding as well as the initial inspiration for this project. The research coming out of AUTO21 from its various university and industry partners is of incredible importance, and this research will make our roads much safer and our environment much more sustainable in the long run.

Finally, I would like to thank my two closest friends - Ryan Caskey and Ravi Chahal - for keeping me sane throughout my undergraduate and graduate programs. They are encouraging, funny, smart, and almost as good at Halo as I am. Almost.

# Table of Contents

<b>CHAPTER 1: INTRODUCTION.....</b>	<b>1</b>
1.1. Application of DSRC and Physiological Monitors to the Safety of Elderly Drivers	3
1.2. Objectives.....	5
1.3. Scope of Work.....	6
1.4. Thesis Overview.....	9
<b>CHAPTER 2: BACKGROUND .....</b>	<b>11</b>
2.1. Motor Vehicle Accidents Among Elderly Drivers.....	11
2.2. Literature Review of Vehicular Communication .....	18
2.3. Literature Review of Physiological Monitoring.....	24
2.3.1. Ambulatory Monitors .....	26
2.3.2. In-car Physiological Monitors .....	32
<b>CHAPTER 3: WIRELESS COMMUNICATION SYSTEMS FOR HEALTH CARE OF ELDERLY DRIVERS.....</b>	<b>38</b>
3.1. DSRC .....	38
3.2. The Four Most Prevalent Low-Power Wireless Communication Systems .....	47
3.2.1. Bluetooth .....	47
3.2.2. ZigBee .....	50
3.2.3. ANT .....	54
3.2.4. Bluetooth Low Energy.....	57
<b>CHAPTER 4. SYSTEM DESIGN .....</b>	<b>62</b>
4.1. System Overview .....	62
4.2. DSRC Vehicular Communication System .....	64
4.2.1. Hardware Selection.....	64
4.2.2. DSRC Radio Driver.....	72
4.2.3. In-car User Interface.....	74
4.3. Physiological Monitoring System .....	76
4.3.1. Bluetooth Low Energy Radio .....	77
4.3.2. Sensors.....	78
4.3.3. Data Acquisition System .....	80
4.3.4. Firmware Design .....	82
4.4. Integrated System.....	86

<b>CHAPTER 5: SYSTEM VALIDATION AND RESULTS.....</b>	<b>89</b>
5.1. DSRC System Test Methods.....	89
5.1.1. DSRC Frequency Spectrum Test.....	89
5.1.2. Indoor Test.....	90
5.1.3. Vehicle-to-Vehicle Tests .....	91
5.1.4. Vehicle-to-Infrastructure Tests .....	93
5.2. Physiological Monitor Test Methods .....	96
5.2.1. Skin Temperature Test.....	96
5.2.2. Heart Rate and SpO <sub>2</sub> Test .....	97
5.2.3. Current Consumption Test.....	97
5.2.4. Bluetooth Low Energy Frequency Spectrum Test.....	98
5.2.5. Bluetooth Low Energy Range Test.....	98
5.2.6. Long-Term Sampling Test.....	98
5.3. Integrated System Test Methods .....	99
5.4. DSRC System Test Results .....	100
5.4.1. DSRC Frequency Spectrum Test Results .....	100
5.4.2. Indoor Test Results .....	103
5.4.3. Vehicle-to-Vehicle Test Results .....	104
5.4.4. Vehicle-to-Infrastructure Test Results .....	105
5.5. Physiological Monitor Test Results .....	109
5.5.1. Skin Temperature Test Results .....	109
5.5.2. Heart Rate and SpO <sub>2</sub> Test Results .....	112
5.5.3. Current Consumption Test Results .....	112
5.5.4. Bluetooth Low Energy Frequency Spectrum Test Results .....	113
5.5.5. Bluetooth Low Energy Range Test Results .....	114
5.5.6. Long-Term Sampling Test Results .....	114
5.6. Integrated System Test Results .....	116
<b>CHAPTER 6: CONCLUSIONS AND RECOMMENDATIONS .....</b>	<b>118</b>
6.1. Conclusions .....	118
6.2. Future Recommendations.....	122
<b>REFERENCES.....</b>	<b>125</b>

## List of Tables

Table 3-1: IEEE 802.11p OFDM parameters .....	40
Table 3-2: Comparison of low-power wireless communication systems .....	61
Table 4-1: Comparison of embedded computers .....	68
Table 4-2: Comparison of antennas .....	71
Table 4-3: Comparison of Bluetooth Low Energy radios.....	78
Table 5-1: Received signal power for DSRC spectrum analysis .....	103
Table 5-2: Recorded latencies for indoor test .....	103
Table 5-3: Latency test results for V2V Test 2, Part A .....	105
Table 5-4: Latency test results for V2I Test 1 .....	106
Table 5-5: Latency test results for V2I Test 3, Part A .....	108
Table 5-6: Mean and standard deviation of pulse oximeters .....	112
Table 5-7: Long-term sampling test results .....	115

## List of Figures

Figure 1-1: Percentage of elderly drivers in Canada .....	1
Figure 2-1: Probability of fatality in a motor-vehicle collision relative to a 20-year old male .....	13
Figure 2-2: Ratio of fatalities to injuries from motor-vehicle collisions in Canada .....	15
Figure 2-3: Deaths per 1,000 deaths in crashes in the United States .....	15
Figure 2-4: Example of a wireless body-area network .....	26
Figure 3-1: DSRC frequency spectrum.....	39
Figure 3-2: DSRC packet structure.....	41
Figure 3-3: Example of an infrastructure BSS.....	42
Figure 3-4: Example of an ad-hoc BSS .....	43
Figure 3-5: DSRC OBU/RSU example .....	44
Figure 3-6: Bluetooth scatternet example .....	49
Figure 3-7: Bluetooth packet structure .....	49
Figure 3-8: ZigBee stack (simplified view).....	51
Figure 3-9: ZigBee tree topology.....	53
Figure 3-10: ZigBee packet structure .....	54
Figure 3-11: ANT starbus network example .....	55
Figure 3-12: ANT packet structure.....	56
Figure 3-13: Bluetooth Low Energy packet structure.....	59
Figure 4-1: Block diagram of in-car integrated system .....	63
Figure 4-2: Block diagram of developed DSRC system.....	65
Figure 4-3: RF system for DCMA-86P2 DSRC radio.....	67
Figure 4-4: Alix 1D with DSRC radio and CF card .....	69
Figure 4-5: Keypad for developed DSRC system.....	70
Figure 4-6: Complete DSRC system.....	72
Figure 4-7: In-car user interface .....	75
Figure 4-8: Block diagram of physiological monitor .....	76
Figure 4-9: Physiological monitor PCB with battery .....	81

Figure 4-10: BLE stack OSAL task loop.....	83
Figure 4-11: Physiological monitor application layer .....	85
Figure 5-1: Spectrum analyzer test setup for DSRC system.....	90
Figure 5-2: Environment for V2V Test 1, Part A .....	92
Figure 5-3: Environment for V2I Test 1 .....	94
Figure 5-4: Physiological monitor on volunteer .....	99
Figure 5-5: Frequency spectrum of DSRC radio at 5.86 GHz.....	101
Figure 5-6: Frequency spectrum of DSRC radio at 5.90 GHz.....	102
Figure 5-7: Frequency spectrum of DSRC radio at 5.92 GHz.....	102
Figure 5-8: Temperature data for temperature test 1 (heat lamp).....	110
Figure 5-9: Temperature data for temperature test 2 (arm) .....	111
Figure 5-10: Frequency spectrum for Bluetooth Low Energy radio.....	114
Figure 5-11: Skin temperature of subject 1 during long-term trial.....	115
Figure 5-12: Temperature data for integrated system test .....	117

## **List of Abbreviations**

3GPP: 3<sup>rd</sup> Generation Partnership Project

4G: 4<sup>th</sup> Generation

A/D: Analog-to-Digital

APS: Application Support Sublayer

BLE: Bluetooth Low Energy

BPSK: Binary Phase Shift Keying

BSS: Basic Service Set

CCIS: Cooperative Crash Injury Study

CRC: Cyclic Redundancy Code

CRDA: Central Regulatory Domain Agent

DSRC: Dedicated Short Range Communication

DSSS: Dynamic Sequence Spread Spectrum

ECDH: Elliptic Curve Diffie Hellman

ECG: Electrocardiogram

EDR: Enhanced Data Rate

EEG: Electroencephalogram

EMG: Electromyograph

EMI: Electromagnetic Interference

EMS: Emergency Medical Services

EVDO: Evolution-Data Optimized

FARS: Fatality Analysis Reporting System

FCC: Federal Communications Commission

FCS: Frame Control Sequence

FEC: Forward Error Correction

FIPS: Federal Information Processing Standards

FHSS: Frequency Hopping Spread Spectrum

FPGA: Field Programmable Gate Array

GPIO: General Purpose Input/Output

GPS: Global Positioning System

GUI: Graphical User Interface  
HAL: Hardware Abstraction Layer  
HF: High Frequency  
HRV: Heart Rate Variability  
IBSS: Independent Basic Service Set  
ICI: Inter-Carrier Interference  
IDE: Integrated Development Environment  
ISI: Inter-Symbol Interference  
ISM: Industrial, Science, and Medical band  
JDK: Java Development Kit  
JRE: Java Runtime Environment  
LF: Low Frequency  
LTE: Long Term Evolution  
MAC: Medium Access Control  
MAIS: Maximum Abbreviated Injury Scale  
MBMS: Multimedia Broadcast/Multicast Services  
MICS: Medical Implant Communications Service  
MMCX: Micro Miniature Coaxial  
NWK: Network  
OBU: On-board unit  
OFDM: Orthogonal Frequency Division Multiplexing  
O-QPSK: Offset Quadrature Phase Shift Keying  
OSAL: Operating System Abstraction Layer  
PAN: Personal Area Networks  
PCB: Printed Circuit Board  
PHY: Physical (Layer)  
PLL: Phase Locked Loop  
PPV: Positive Predictive Value  
QAM: Quadrature Amplitude Modulation  
QPSK: Quadrature Phase Shift Keying  
RTC: Real-Time Clock

RSU: Roadside Unit

SIG: Special Interest Group

SNR: Signal-to-noise ratio

STA: Station

UDP: User Datagram Protocol

UMTS: Universal Mobile Telecommunications System

V2I: Vehicle-to-Infrastructure

V2V: Vehicle-to-Vehicle

VANET: Vehicular Ad-Hoc Network

VLf: Very Low Frequency

WAVE: Wireless Access in Vehicular Environment

WBAN: Wireless Body Area Network

# CHAPTER 1: INTRODUCTION

Motor vehicle traffic collisions are a prevalent cause of injury and death in modern society. In 2009, motor vehicle traffic collisions killed 2,011 people in Canada and 30,797 people in the United States [1], [2]. These collisions pose a significant danger to drivers of all ages, but they are particularly hazardous for elderly drivers. Using data from the United States government’s Fatality Analysis Reporting System (FARS), it has been estimated that a given impact sustained by a 50-year-old male driver has double the probability of resulting in a fatality when compared to a 20-year-old male driver (2.34 times in the case of a 50-year-old female driver) [3]. Using the same relations, an 80-year old male driver has quadruple the probability of dying in an accident when compared to a 20-year-old male driver (4.24 times for a female driver).

This issue becomes more concerning when looking at the annual increase in the number of elderly drivers. From Figure 1-1, it is clear that the elderly are forming a larger percentage of Canada’s overall population of licensed drivers [1]. In 2003, 26.3% of all licensed drivers were aged 50 and over. However, this percentage has increased every year since, and by 2009, 29.8% of all licensed drivers were 50 and over.

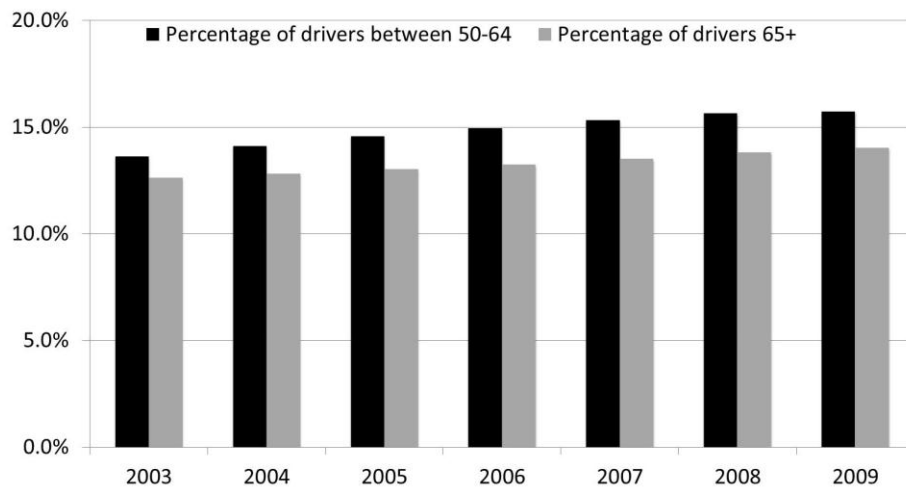


Figure 1-1: Percentage of elderly drivers in Canada [1]

Driving cessation is sometimes necessary in the case of an elderly driver whose ability has declined. However, if an elderly driver's senses are still strong, it is preferable to keep them on the road. A survey from Adler and Rottunda [4] revealed that many elderly people who were forced to stop driving suffered a large decline in their sense of independence and their self-esteem. For these elderly drivers who are still on the road but more vulnerable in the case of an accident, there should be safeguards in place that allow them to receive prompt medical attention in the event of a motor vehicle accident. There have been numerous research studies that investigate the use of physiological sensors in a vehicle ([5], [6], [7], and [8] are a few examples), but there have been very few studies investigating the use of vehicular communication to transmit these physiological parameters to emergency medical services (EMS) or to other vehicles in the event of a car accident. A combined physiological monitoring and vehicular communication system could allow elderly drivers to receive medical attention quickly, which would potentially lower the number of fatalities that occur due to motor-vehicle traffic collisions. Additionally, the vehicular communication network could allow vehicles to be more aware of one another, which could lead to collision prevention applications that prevent elderly drivers from ending up in a life-threatening motor vehicle accident in the first place.

At present, there is no ideal communication system in place to facilitate the requirements for collision prevention applications. Some researchers have looked at the possibility of using existing cellular communication systems such as UMTS [9] or WiMAX [10] to implement vehicular communication, but a vehicular network is intrinsically ad-hoc, and these cellular communication systems are not designed for ad-hoc communication. Communicating with a cellular tower leads to packet latencies that are unacceptable for collision prevention applications where the driver and/or the vehicle only has a very small amount of time to respond to the environment. This has motivated the creation of the IEEE 802.11p communication system for vehicle-to-vehicle (V2V) and vehicle-to-infrastructure

(V2I) communication. IEEE 802.11p is more commonly referred to as Dedicated Short Range Communication (DSRC), and it is has been designed for the exclusive purpose of ad-hoc vehicular communication. DSRC avoids the congestion experienced by cellular or WLAN communication by communicating inside the 5.9 GHz frequency band [11], and it avoids the high latency of cellular networks by utilizing ad-hoc communication. There is a possibility that DSRC could be useful for both collision prevention applications and the transmission of a vehicle occupant's physiological parameters in the event of an accident. In particular, the ad-hoc capability of DSRC could allow these parameters to be transmitted to nearby vehicles following an accident, thereby allowing nearby drivers to provide care if they are qualified to do so.

This thesis seeks to determine whether 5.9 GHz DSRC is a viable system for transmitting a vehicle occupant's vital signs in the event of a car accident or a medical emergency. The final goal of this research is to investigate whether DSRC could prove beneficial for elderly drivers, either through facilitating faster and more effective emergency response after an accident or through preventing accidents from occurring altogether. Although DSRC sounds promising as a communication system for this application, there has been no research that looks at the combination of DSRC and in-car physiological monitoring. In order to evaluate the viability of this application, it will be necessary to create an integrated system that combines V2V/V2I communication through DSRC with a physiological monitoring system that can track the vital signs of a driver or passenger.

### **1.1. Application of DSRC and Physiological Monitors to the Safety of Elderly Drivers**

Ambulatory physiological monitoring has been explored extensively in the literature as a way of providing preventative health care to the elderly as well as other at-risk populations. Such a system is beneficial because it captures the

physiological parameters of a patient in their day-to-day activities and logs them for later analysis by a health care professional. This is especially useful when attempting to diagnose a condition like atrial fibrillation and flutter, in which the symptoms (fibrillation patterns in a patient's heartbeat) are intermittent [12]. Ambulatory monitors are also useful in instances where it is difficult to attain accurate readings in a clinic. For example, a patient receiving a blood pressure check at a clinic may be anxious and measure a higher blood pressure than what is actually present during daily activities [13]. As the elderly population increases worldwide, the need for preventative health care measures is becoming increasingly important, and physiological monitoring has emerged as a promising means of providing preventative health care to the elderly.

Physiological monitoring also has potential for specific applications outside of preventative health care or long-term monitoring. With respect to the application being discussed in this thesis, in-car physiological monitoring can be helpful for determining a person's physiological parameters in the event of a medical emergency. This medical emergency could be a car accident or even something unrelated, such as a heart attack or stroke. Additionally, in-car physiological monitoring can also be used to provide a real-time assessment of the driver's stress level by using sensors for parameters such as body temperature or galvanic skin response (which increases as the driver perspires). If the system detects an excessive amount of stress in the driver, the automobile could take measures to alleviate that stress level, such as altering the temperature inside the vehicle.

The combination of DSRC with physiological monitoring can potentially be used for a number of safety applications. The most important application with respect to this thesis is the use of in-car physiological monitoring to notify EMS in the event of an accident. If EMS can arrive to the scene of an accident with the physiological parameters of each crash victim, they can prioritize their emergency response in favour of those victims whose vital signs are the most severe. This would be especially beneficial for elderly drivers, who are at a greater risk of

dying from motor vehicle collisions. In addition to transmitting parameters to EMS, the system could also be used to transmit parameters to nearby vehicles if an accident occurs. Since DSRC creates a vehicular ad-hoc network (VANET) with cars in the vicinity, it would be much easier to send a broadcast transmission to nearby vehicles with DSRC than it would be with a cellular communication system like UMTS or WiMAX. If anybody in the vicinity of a car accident is capable of providing care, and if they are aware of the declining vital signs of one of the crash victims, they may be able to provide medical attention while EMS is en route. This integrated DSRC physiological monitoring system could also utilize the GPS capabilities that are present in many modern vehicles, thereby allowing EMS to easily locate accidents with injured victims as soon as they occur.

The in-car DSRC physiological monitoring system being discussed in this thesis is a research tool. While DSRC has the potential to improve the safety of elderly drivers through the aforementioned techniques, its effectiveness has yet to be proven. This thesis seeks to answer the question of whether or not 5.9 GHz DSRC is a viable communication system for this particular application.

## **1.2. Objectives**

The objectives of this thesis are:

- To determine whether 5.9 GHz DSRC is a viable system for transmitting a vehicle occupant's vital signs in the event of a car accident or a medical emergency.
- To evaluate the use of 5.9 GHz DSRC in a vehicular setting with both vehicle-to-vehicle (V2V) and vehicle-to-infrastructure (V2I) communication.
- To design and validate a 5.9 GHz communication system that can communicate in both V2V and V2I settings. The system should be able to

communicate with low latency and packet loss, and it should fully conform with the IEEE 802.11p DSRC standard.

- To evaluate in-car physiological sensors that could provide useful information to EMS in the event of a car accident. These sensors should also be able to measure the physiological parameters of a vehicle driver at all times. Additionally, the sensors should be unobtrusive in order to avoid creating a potentially hazardous distraction for the driver while they focus on the road.
- To design and validate an in-car physiological monitor for elderly drivers and passengers. The monitor should be able to measure, store, and transmit physiological parameters using low-power wireless communication.
- To design an in-car user interface for controlling the physiological monitoring system and DSRC communication on both the driver side and the EMS side. The interface should have commands for sending physiological parameters, requesting parameters (for use by EMS), storing parameters for future analysis, and other functions. The interface should use low-power wireless for communicating with the monitor and 5.9 GHz DSRC for communicating with other vehicles.

### **1.3. Scope of Work**

As previously mentioned, there have been numerous studies investigating the use of other wireless systems in the context of vehicular communication. This includes cellular systems such as WiMAX and UMTS. Additionally, researchers have also looked at the possibility of using WLAN systems such as 2.4 GHz 802.11b in vehicular environments. It will be important to perform an in-depth literature review of these proposed systems in order to determine whether 5.9 GHz DSRC can give any improvements over these existing systems. Additionally, it will be important to perform a review of existing physiological monitoring systems, including both ambulatory and in-car systems. Although there has not

been any investigation performed to date on the use of DSRC for physiological monitoring, there have been studies that looked at the possibility of in-car vehicular monitoring for applications such as stress measurements, long-term health monitoring, or assessing driver aptitude. The monitoring systems created for these studies could provide useful information for determining which sensors are appropriate for in-car health monitoring of the elderly, and where sensors should be placed in order to avoid creating unwanted distractions for the driver.

An investigation of wireless communication systems for physiological monitoring will also be required. In order to avoid creating distractions for the driver, it is absolutely necessary for the physiological monitoring system to be wireless. Although the physiological monitor may inevitably have wires leading to individual sensors (such as a heart rate sensor), these should be avoided whenever possible by utilizing sensor nodes in a scatternet or mesh network. Furthermore, the connection from the sensor node(s) to the in-car DSRC system must be wireless. A wired connection between the worn system and the in-car system would be hazardous for the driver as they attempt to operate the vehicle, thereby defeating the purpose of using a safety system. Within the literature, several different communication systems have been used for wireless body sensor networks, including Bluetooth, ZigBee, customized IEEE 802.15.4 systems, and even proprietary 2.4 GHz systems. It will be necessary to look at these wireless systems and determine which one would be the most appropriate for an in-car physiological monitoring system with low power and small size requirements.

Once the appropriate physiological sensors have been chosen along with the wireless protocol, the integrated in-car system will need to be created in order to evaluate DSRC as a vehicular communication protocol for aiding elderly drivers. The DSRC vehicular communication system and the wireless physiological monitor will need to be created individually and then integrated together through software and hardware on the in-car system side.

The DSRC communication system will be required to conform with the IEEE's 802.11p communication standard. Specifically, it must be able to communicate in the frequency range of 5.850 – 5.920 GHz with seven 10 MHz channels. DSRC is a new communication system that has been recently ratified by the IEEE, and there are very few commercial or prototype DSRC systems available for comparison. Therefore, it is difficult to set requirements on specific communication characteristics such as range, latency, and throughput. However, it will be important to choose system components that maximize the performance of the system. The latency in particular is very important, as low latency is the key advantage that DSRC is intended to have over existing systems such as WiMAX or UMTS. Low packet loss is another very important feature for a vehicular communication system, especially one that is going to be used for safety applications in emergency situations where an elderly driver may be involved in a serious crash.

With regards to the physiological monitoring system, the most important requirement of the system is comfort during driving. As previously stated, the system must be able to work with no distractions to the driver, which means that a wireless communication system from the worn monitor to the in-car DSRC system will be essential. The use of a wireless system will lead to increased power consumption and lower battery life, and therefore steps must be taken to find a wireless system that minimizes power consumption as much as possible. While inside of a vehicle, the range requirements are small – less than five metres of transmission distance from one sensor node to another. However, a high success rate of packet reception is very important in emergency situations where the driver's life may be in danger.

The integration of the physiological monitor with the DSRC system will require both software and hardware on the DSRC system side. For whichever wireless communication system is chosen for the physiological monitor, a transceiver will have to be installed on the DSRC system side in order to read packets from the

physiological monitor in real-time. Furthermore, although the system should ideally perform many of its functions automatically, there are instances where user intervention may be required. Therefore, the DSRC system will need to have a user interface designed for certain simple functions such as manually transmitting physiological parameters. These functions should be very simple in nature and easy to perform, in order to minimize any focus that has to be diverted away from the road environment.

The created system will have to be tested in order to determine the accuracy and reliability of the physiological sensors over long periods of time. Most importantly, the integrated in-car system will have to be tested in a vehicular environment to determine whether DSRC is a viable system for transmitting a vehicle occupant's physiological parameters.

#### **1.4. Thesis Overview**

This thesis consists of six chapters. It begins by identifying and discussing the previously used methods of aiding elderly drivers. After this, an investigation of 5.9 GHz DSRC as a potential communication system for aiding elderly drivers in medical emergencies will be performed. This investigation requires the creation of a combined DSRC and physiological monitoring system and testing of the system in both laboratory and vehicular environments.

Chapter 1 contains an introduction to the problem of improving vehicle safety for elderly drivers and passengers, and then it proposes an investigation of DSRC as a possible means of improving safety through physiological monitoring and the transmission of physiological parameters.

Chapter 2 discusses the challenges associated with motor vehicle accidents among elderly drivers. From here, it goes into an in-depth literature review of vehicular communication and physiological monitoring (both ambulatory and in-car).

Chapter 3 describes various wireless communication systems that can be used for applications of health care among elderly populations. These include currently used systems such as Bluetooth, ZigBee, and ANT. The chapter also contains in-depth descriptions of the two wireless systems being used in this thesis: 802.11p DSRC and Bluetooth Low Energy.

Chapter 4 discusses the design of the system being used to perform the investigation of DSRC for physiological monitoring. This includes the design of the DSRC vehicular communication system, the Bluetooth Low Energy-based physiological monitor, and the integration of the two components into a combined system for vehicular safety.

Chapter 5 reports the test results for each module of the designed system as well as test results for the integrated system. These tests results determine whether DSRC vehicular communication is a viable method for improving the safety of elderly vehicle occupants.

Chapter 6 provides a summary of the thesis work, concluding remarks about the research, and then some future recommendations for improving the DSRC physiological monitoring system.

## **CHAPTER 2: BACKGROUND**

This chapter contains background information required to understand the motivation behind the research topic of this thesis. The chapter begins with a discussion about the dangers of motor vehicle collisions among elderly drivers and the challenges involved with preventing or mitigating these collisions. As previously mentioned, vehicular communication has the potential to aid elderly drivers in these collision scenarios, and therefore a literature review of vehicular communication is included in this chapter. Lastly, a literature review of state-of-the-art physiological monitoring will be discussed, as in-car monitoring is an important aspect of this research.

### **2.1. Motor Vehicle Accidents Among Elderly Drivers**

Though all drivers are at risk of serious injury or death from a motor vehicle collision, there is much evidence to suggest that the elderly face a greater risk than younger drivers due to their fragility. Welsh et al. [14] looked at data from the UK Co-operative Crash Injury Study (CCIS) and found that older drivers were far more susceptible to serious chest injuries from frontal impact than younger drivers. The study looked at 1,541 collisions involving vehicles that were manufactured post-1991, and it focused predominantly on crashes that were considered to be “serious” or “fatal” according to the UK government’s classifications. It was found that in frontal impacts, elderly drivers (defined in this study as those over 65 years old) suffered fatalities in approximately 15% of instances, whereas young drivers (defined as 17-39 years old) and middle aged drivers (defined as 40-64 years old) both suffered fatalities in less than 5% of instances. Furthermore, serious but non-fatal injuries in frontal impacts occurred in about 35% of instances for elderly drivers, compared to about 28% for young drivers. When using maximum abbreviated injury scale (MAIS) scores (where 1 represents a minor injury and 6 represents a maximum life-threatening injury), it was found that although elderly drivers suffer serious head injuries (MAIS of 3 or

greater) with roughly the same probability as other drivers, they have approximately triple the likelihood of suffering a serious chest injury as compared to young or middle-aged drivers. The authors noted that for serious chest injuries among elderly drivers, fractures were more frequently caused by the seatbelt than the steering wheel. A similar study was performed using collision data from northern Sweden over a ten-year period [15], and the authors reached a similar conclusion. Namely, the elderly had a greater representation in serious traffic collisions than younger drivers, and serious chest injuries were more common than head injuries, although the data did not include any reliable data on the specific causes of the chest injuries (seatbelt, steering wheel, other cause).

Another study based on data from the United States' Crash Injury Research and Engineering Network (CIREN) [16] looked exclusively at elderly (65-79 years old) and extreme elderly ( $\geq 80$  years old) vehicle occupants. In frontal impacts involving these two groups, the seat belt was the largest cause of rib and sternum fractures. Specifically, 40.9% of fractures among elderly occupants and 57.4% of fractures among extreme elderly occupants were caused by the seat belt, which is consistent with what was found in [14]. In [17], data from the California Office of Statewide Planning and Development Hospital Discharge Database in 1994 was analyzed to see the frequency and severity of injuries among people 65 years old or older. Although their analysis did not account for the fact that older drivers typically drive less than younger drivers, they found that the risk of hospitalization was 1.80 times greater for an 80-84 year old driver when compared to a 65-69 year-old driver. Furthermore, the severity of those injuries became greater at older ages, particularly once drivers exceeded the age of 80. As also observed in [14], [15], and [16], neck and trunk injuries occurred more often than injuries to other parts of the body, though the authors did not provide any discussion on the specific causes of these injuries.

The aforementioned studies suggest that elderly drivers are much more susceptible to motor vehicle injuries – particularly chest fractures – than younger

drivers, whether these injuries are caused by the seatbelt, the steering wheel, or other parts of the vehicle. Using data from the United States government’s FARS database, Evans created mathematical relations in order to quantify the fragility that a driver’s body experiences with age [3]. For male and female drivers, these relations are as follows:

$$R_{\text{males}}(A) = \exp[0.0231(A-20)] = 0.630\exp(0.0231A) \quad (2-1)$$

$$R_{\text{females}}(A) = 1.3\exp[0.0197(A-20)] = 0.877\exp(0.0197A) \quad (2-2)$$

Where A is the age of the driver and R is the probability that a given collision will prove fatal relative to the probability that a similar collision will kill a 20-year-old male. These relations are shown in Figure 2-1. From the figure, it is clear that that elderly males face an increased risk of fatality from motor vehicle collisions, and this risk is even greater for elderly females. Specifically, a 50-year old male has double the probability of dying and a 50-year old female faces 2.35 times the risk of dying when compared to a 20-year old male. These relative probabilities increase to 3.17 and 3.48 for 70-year-old drivers, and they increase even further to 4.00 and 4.24 for 80-year-old drivers.



Figure 2-1: Probability of fatality in a motor-vehicle collision relative to a 20-year old male [3]

Statistics collected by Transport Canada in 2009 [1] also suggest a greater level of driver fragility with age. Figure 2-2 shows the ratio of fatalities to injuries in motor vehicle collisions across Canada. In this figure, we can see that the ratio increases in every age range starting from 35-44 years and onward. Specifically, when looking at the 35-44 year age range, there were a total of 26,148 motor vehicle injuries and 244 fatalities, for a ratio of 0.0093. When moving up to the 45-54 age range, there were 26,205 injuries and 355 fatalities, for a ratio of 0.0135, which represents a 45.16% increase. When reaching the 65+ age group, there were 13,922 injuries and 389 fatalities, for a ratio of 0.0279, which is a 200% increase over the 35-44 age group. In other words, elderly drivers who were involved in a motor vehicle accident on Canadian roads in 2009 stood a greater chance of dying than younger drivers, particularly when compared to those in the 35-44 year old age range (presumably where drivers have an optimal combination of skill and physical strength). Li et al. [18] performed a similar analysis using data from the United States government's FARS database from 1993 to 1997. As a marker for fragility, they observed the amount of deaths per 1,000 drivers in crashes across various age groups, and the results are shown in Figure 2-3. In the case of both males and females, the number of deaths per 1,000 drivers in crashes increased in every single age range starting from the 30-59 year range. For males, the 65-59 year old group experienced a 53.7% increase in deaths over the 30-59 year old group. For females, this increase was 109.5%. The increased probability of fatality that older drivers experience is a convincing indicator of their increased fragility.

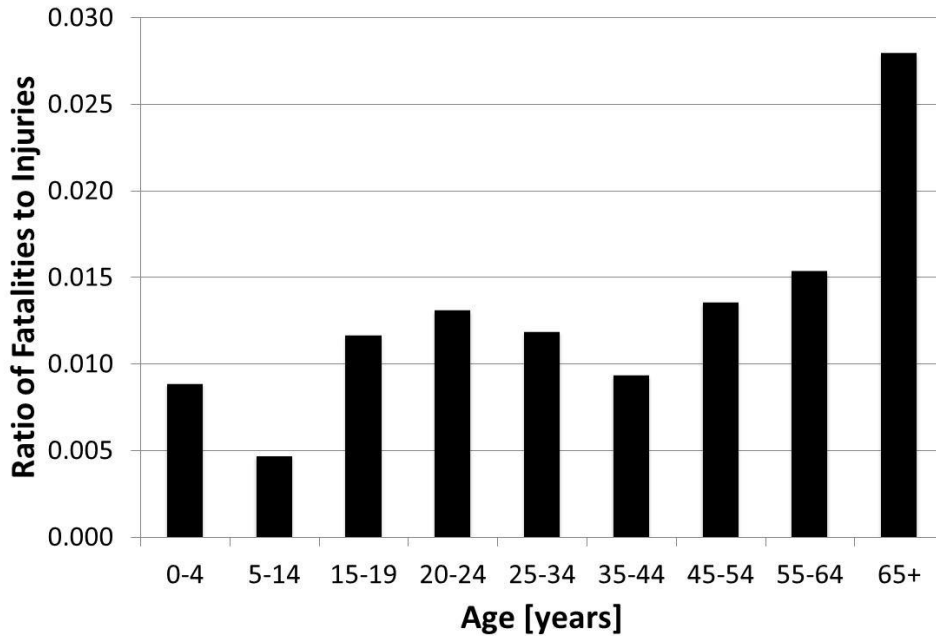


Figure 2-2: Ratio of fatalities to injuries from motor-vehicle collisions in Canada [1]

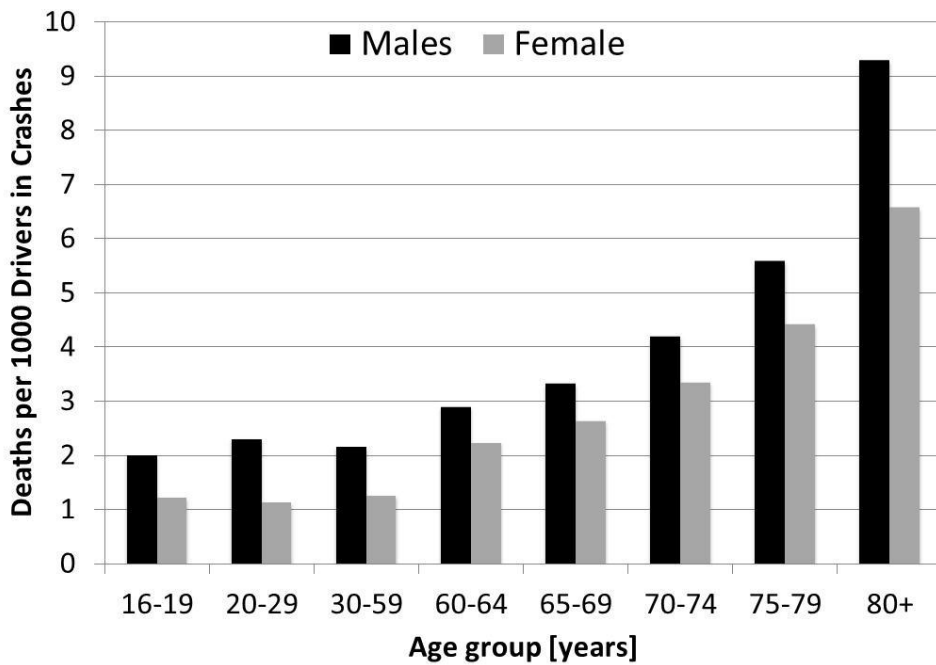


Figure 2-3: Deaths per 1,000 deaths in crashes in the United States [17]

Society often evaluates older drivers with skepticism, and there is an assumption that renewing the license of an elderly person creates a danger to their fellow

drivers and pedestrians due to their cognitive impairment. The various news stories about unintended acceleration by senior drivers resulting in the deaths of pedestrians has reinforced this skepticism towards older drivers [19]. In a study by Leonard Evans [20], this belief is examined in detail, and he concluded that renewing the license of an older driver does not pose a greater threat to other road users and pedestrians. In fact, when looking at data taken between 1994 and 1996, Evans found that there were approximately 20 pedestrian fatalities per million licensed drivers when looking at accidents involving drivers aged 80 or older. This value is lower than the approximately 30 pedestrian fatalities per million drivers at the age of 40 and over 50 pedestrian fatalities per million drivers at the age of 20 (these numbers only account for male drivers, though a similar trend exists for female drivers). It was also found that a 20-year-old male is over 100% more likely to be involved in a crash in which a pedestrian is killed than a male driver over the age of 70. Evans ultimately concluded that licensing an older driver does not pose a greater risk to other drivers or pedestrians, and it actually presents a much lower risk than renewing the license of a driver in their twenties.

If an elderly person is still capable of operating a vehicle to an acceptable standard, it is preferable to keep them on the road as long as they feel safe and confident in their driving ability. In a study by Adler and Rottunda [4], it was found that elderly people (defined in that study as people over the age of 60) who gave up driving experienced a loss of independence and the added stress of having to constantly rely upon their family and friends for rides whenever they needed to get groceries or run other errands. In particular, males who gave up driving experienced a loss in self-esteem, and some of them felt as though their driving cessation indicated a loss of masculinity. When asked about the possibility of using public transportation, many elderly people reacted negatively, describing public transportation as inconvenient and dangerous. Additionally, many elderly people live in areas where public transport is either not available at all or very inconvenient to use [21].

Some in-car systems have appeared promising for improving the conditions of elderly drivers, but it is important to create systems that this particular demographic will be receptive to. Older drivers typically have slower response times than younger drivers, and these differences are even more drastic if the driver in question does not frequently use their vehicle [22]. Additionally, older drivers also tend to have less physical strength, which makes gripping certain controls more difficult as a driver ages. For these reasons, Shaheen and Niemeier suggested various guidelines to follow when designing an in-car system for elderly drivers [22]. These guidelines include using large knobs and handles, textures that are easy to grip and hold, and controls that facilitate single-handed tasks. It is also important to note that some elderly drivers may be skeptical towards adopting new technologies. In a study by Sixsmith and Sixsmith [23], it was found that warning systems with the potential to startle the driver (often through the use of sound) were evaluated negatively. The survey group felt that driving on its own was demanding enough, and the need to focus on a control system only added to the difficulty. The authors recommended a system that does not present non-critical information to the driver while they are performing certain tasks such as turning or braking. Furthermore, it was also recommended to use large distinguishable buttons as opposed to turning knobs in order to account for drivers with limited manual dexterity.

It is clear based on the literature that there is a large and growing segment of the elderly population that still possesses excellent driving ability, though they are far more susceptible to serious injuries and fatalities from motor vehicle collisions. Collision prevention and response applications based on vehicular communication have the potential to improve the safety of elderly drivers. The next section investigates the various wireless communication protocols that have been proposed for vehicular environments.

## 2.2. Literature Review of Vehicular Communication

Although DSRC has recently emerged as one of the more promising technologies for vehicle-to-vehicle communication, it is not the only protocol that has been explored in the literature. Cellular systems have been proposed as a platform for future vehicular applications, primarily because the infrastructure for these systems is already in existence, whereas the roadside infrastructure for DSRC has yet to be deployed. Valerio et al. [9] proposed the use of the Universal Mobile Telecommunications System (UMTS) for the implementation of an intelligent road safety system. Specifically, this study looked at the Multimedia Broadcast/Multicast Services (MBMS) capability that the 3<sup>rd</sup> Generation Partnership Project (3GPP) (a collection of telecommunications associations from Asia, Europe, and North America) added to UMTS in 3GPP Release 6. It was believed that the broadcast capabilities of MBMS would be ideal for a vehicular communication system, since safety messages could be broadcast from a cellular communication tower to the user equipment in each vehicle (though this requires that each vehicle have MBMS-capable user equipment installed). Though no physical system was created in this study, simulations were run using an MBMS multicast system and a regular UMTS unicast system, and it was found that when there were few cars on the road, the use of MBMS was unjustified due to the extra power required for transmission. However, in a scenario with many cars on the road, MBMS could improve the capabilities of UMTS in a vehicular scenario.

A different study from Mangel et al. [24] compared the use of UMTS and 4<sup>th</sup> generation (4G) Long Term Evolution (LTE) for vehicular communication. LTE is one of the most promising 4G technologies due to its very high throughput capabilities, but the authors wanted to see how well it would perform in a vehicular environment where many small packets are sent out at high frequencies. It is important to note that this is different from a typical LTE usage scenario, in which a large file is being downloaded by a small number of users in a given cell. In their simulations, the authors assumed that each vehicle on the road would be

sending out Cooperative Awareness Messages (CAMs) at a high frequency. These CAMs would contain information regarding the vehicle's location, its trajectory, its speed, and other information. By receiving CAMs from all vehicles in the vicinity at a high frequency, vehicles would be able to estimate a reasonably accurate model of the environment, thereby allowing for greater movement prediction and hopefully a decreased likelihood of collisions. The comparison of DSRC, UMTS, and LTE showed that LTE allowed for the greater number of CAMs transmitted per intersection per second. Specifically, LTE allowed for 1,700-3,400 CAMs per intersection per second, whereas DSRC could transmit 1,000 CAMs per second, and UMTS could only transmit 300 CAMs per second when assuming a packet size of 250 bytes with a 70 byte payload and 150 byte security overhead. This high rate of CAMs was due to the high throughput capabilities of LTE in comparison to DSRC and UMTS. However, despite LTE's impressive throughput, DSRC was the best system in the simulation when looking at the latency of each system. This is due to the fact that DSRC is an ad-hoc communication system, whereas UMTS and LTE must operate within cells in which all communication must pass through a cellular tower. It is important to note that [24] performs their simulations based on LTE Release 8, which has support for scalable bandwidths up to 20 MHz and theoretical data rates up to 300 Mb/s (hence why it is able to send so many CAMs within a single cell). However, telecommunications companies in the United States and Canada (among other countries) are preparing to deploy LTE Release 10 [25]. LTE Release 10 is also known as LTE-Advanced, and it allows deployment bandwidths of up to 100 MHz, which could facilitate theoretical data rates that are over 1 Gb/s. If such a system were deployed in a vehicular setting, it would increase the frequency of CAMs even further, though each individual CAM would still have to go through a cellular tower before being direct to the target vehicle, so even this improved version of LTE does not necessarily solve the latency issue.

In addition to UMTS and LTE, the other existing communication system that has been proposed for vehicular communication is WiMAX. Although the original

IEEE 802.16 specification offered support for WiMAX in fixed metropolitan area networks, the newer 802.16e standard created Mobile WiMAX, which was intended to facilitate communication in environments with vehicle speeds of up to 125 km/h at frequencies ranging from 2-6 GHz [26]. WiMAX has shown promise due to its large range spanning several kilometres in a line-of-sight scenario. Furthermore, WiMAX contains quality of service routines in its medium access control (MAC) layer that allow for packets of different priority levels to be easily implemented with minimal routine requirements in higher level layers. Costa et al. [10] performed a preliminary assessment of WiMAX in a vehicular environment using both on-board and roadside units, though all of the hardware used in their tests were built for fixed WiMAX as opposed to Mobile WiMAX. In these tests, the lowest latencies that were experienced were around 50 ms, though packets that were allocated to lower priorities took 200 ms at data rates of 4,000 kbps. Elsewhere, Chou et al. [27] performed experiments to create a comparison between WiMAX and 802.11b/g WiFi. Specifically, they compared the signal characteristics of a DL-624 WiFi device (D-Link, Taiwan) and a MP16 3500 WiMAX device (Proxim, USA) in a stationary environment at distances of up to 900 m. It was found that while the WiFi device offered lower latencies ( $< 10$  ms) and higher throughputs at distances less than 200 m, the signal was lost at higher distances. Conversely, WiMAX had high latencies between 30 and 40 ms, but it was able to transmit up to 900 m without experiencing a significant increase in latency.

As previously stated, vehicular communication is intrinsically ad-hoc, and this has made IEEE 802.11b/g WiFi a popular research topic when discussing vehicle-to-vehicle communication. Prior to the allocation of the 5.9 GHz band by the Federal Communications Commission (FCC) and the IEEE's ratification of the 802.11p standard, 802.11b/g was explored as a potential standard for vehicular communication. In [28] and [29], vehicle tests were performed using Orinoco WLAN cards (Proxim, USA) in both multi-car V2V and V2I scenarios. It was found that when travelling at 50 km/h, the communication experienced a 1.99%

packet loss, versus 3.48% packet loss when travelling at 90 km/h. However, changing speeds was found to have a minimal impact on the latency of packets, as 50 km/h speeds resulted in an average latency of 1.97 ms while 90 km/h speeds produced an average latency of 2.04 ms. Furthermore, these latencies were found to be much lower than what is typically experienced in a cellular network, thereby making ad-hoc communication beneficial for V2V communication. A similar test was performed in [30] and [31], in which Orinoco WLAN cards were placed inside two vehicles while one vehicle streamed user datagram protocol (UDP) packets to the other. This setup was tested in three environments - a suburban environment with 64 km/h speeds, an urban environment with 40 km/h speeds, and a freeway with 105 km/h speeds. It was found that the urban environment was the most hostile to the communication performance, which was likely due to the large amount of building constructions and the high volume of vehicles on the road. In freeway and suburban settings, communication could be maintained at distances of up to 1000 m, though throughputs were less than 100 kbps at these distances, and the packet size could not exceed 256 bytes. Ott and Kutscher [32] also performed several tests using laptops with 802.11b cards installed, and they found that similar to [31], they could achieve distances above 700 m, though the throughput of the communication became very poor. Furthermore, many of their packet losses at long distances were over 50%. Gass et al. [33] also performed tests with 802.11b, though they were concerned with how different vehicle speeds would affect packet loss. When moving from 8 km/h to 120 km/h, they found that packet loss tripled, though the actual losses were less than 1% even in the worst case scenario. From these results, 802.11-based protocols were capable of operating in vehicular environments with low latencies, though they use heavily congested frequency bands such as 2.4 GHz. Combining the ad-hoc capabilities of the 802.11-based protocols with a less congested frequency band was the primary motivation behind DSRC.

The 5.9 GHz frequency band was allocated for vehicular applications in 1999, but the 802.11p DSRC standard was not ratified by the IEEE until June of 2010 [34].

Until now, there have been very few DSRC radios available on the market. This has resulted in researchers taking varied approaches to creating DSRC systems. In a study conducted by Fuxjager et al. [35], a software radio solution was created using GNURadio along with a USRP2 software radio kit (Ettus Research, USA). The software radio solution was compared with a prototype 802.11p chipset, both of which transmitted at 5.88 GHz. It was found that the power spectrum produced by the software radio was comparable to that of the prototype radio, though this study did not look at testing the GNURadio system in an actual vehicular environment. Elsewhere, Xiang et al. [36] tuned a MAX2829 802.11a chipset (Maxim, USA) for use at 5.9 GHz. This tuned RF front end was used in conjunction with a software radio, which was then integrated with a tablet PC. Their system was tested by performing a video stream between two on-board vehicle units, though they did not report any specific parameters of their test (bit rate, throughput, packet loss, proximity, etc.). An 802.11a chipset was also modified in [37] in order to make it compliant with 802.11p standards. The resulting system was tested in a road environment between an on-board unit and a roadside unit. Using this approach, the system was able to transmit at distances of up to 300 m with acceptable performance. Specifically, the packet loss in unicast conditions was below 5% and the latency was between 1-3 ms. However, once the distance between the two units exceeded 300 m, the packet loss of the system immediately spiked, reaching 100% loss between 300-350 m.

Some researchers tested the capabilities of DSRC by using supplied prototype systems. In [38], a DSRC radio created by Savari Networks was used for their studies, and their work focused primarily on developing useful testing techniques for DSRC systems. Using one on-board unit and one roadside unit, they measured latency and packet loss in a stationary setting at distances of up to 500 m. In these tests, latency ranged from 0.519 ms to 15.163 ms, whereas packet loss ranged from 0% to 100%, though it varied based on the direction of the vehicle with respect to the roadside unit. In moving tests, the vehicle travelled as fast as 99 km/h, at which point the communication experienced latencies of 5.030 ms and

packet losses of 33%. In a different study, Bai and Krishnan [39] used in-car DSRC systems provided by General Motors in order to perform V2V tests in a freeway and an open field. The systems sent out packets containing their GPS coordinates, speed, heading, and other information every ten seconds. In the freeway environment, the authors reported a packet delivery ratio over 90% at distances of up to 100 m, but then it began to decrease until reaching its lowest point of about 50% at 425 m. In the open field environment, the system maintained a packet delivery ratio above 80% from 25 m to 450 m, thereby implying that the environment of the freeway had a much greater impact on the packet delivery ratio than the distance between vehicles. Furthermore, the packet delivery ratio did not decrease monotonically in the open field environment, which the authors attributed to roadway reflections that were prominent in the test track.

One particular study by Msaada et al. [40] performed a comparison between DSRC and WiMAX. The two technologies tend to complement each other, as DSRC is suitable for medium range applications where delay times need to be as small as possible, whereas WiMAX is capable of much longer ranges, though it is not capable of the low latency times that DSRC can achieve. In order to compare the two communication systems, a simulation of a highway scenario with one vehicle and several base stations was created. In coverage tests, the 3.5 GHz WiMAX system unsurprisingly outperformed the 5.87 GHz DSRC system by an approximate factor of ten, though the WiMAX base station had a higher antenna height and greater transmission power (as would be expected when comparing a roadside base station with a cellular tower). When measuring latency, the DSRC system outperformed WiMAX, but this advantage was negated once the source data rate exceeded 1.2 Mbps. These simulation results imply that DSRC is best suitable for low-throughput applications in order to maintain its latency advantage over WiMAX. Another comparison was performed in [41], though that study looked at simulations between DSRC and UMTS in V2I scenarios. As others have shown, DSRC was coverage limited due to the small range of its roadside units,

especially when compared to the large UMTS cellular towers. However, DSRC was capable of a much higher downlink cell capacity per roadside unit. As a result, the simulations showed that in a 1,500 km coverage area with  $10^5$  users, UMTS required 8,000 cells in order to provide service, whereas DSRC only required 4,000 roadside units. From these results, it can be concluded that if adequate coverage could be provided, DSRC would be a more appropriate choice in high-traffic scenarios (traffic jams, large urban environments, etc.) than UMTS, thanks to its much higher downlink capacity.

Compared to the other wireless communication protocols discussed in this section, DSRC has advantages that would be beneficial in a vehicular environment. WiMAX and LTE are capable of very high data rates, but results from the literature have shown that DSRC is capable of achieving lower latencies due to its ad-hoc network topology. Moreover, while UMTS is capable of higher communication ranges, DSRC has a much higher downlink capacity, and it would therefore need much fewer road-side units in heavily congested urban environments. In Canada and the United States, the 5.9 GHz frequency band is reserved exclusively for DSRC applications, which greatly reduces the congestion issues of 2.4 GHz systems such as 802.11b WiFi.

### **2.3. Literature Review of Physiological Monitoring**

With respect to the topic of this thesis, physiological monitoring of elderly vehicle occupants is important because the physiological parameters that are collected need to be transmitted to EMS with DSRC. There have been many different physiological monitors discussed in the literature, and this section will attempt to highlight some of them in order to create a picture of the current state-of-the-art for ambulatory and in-car systems. From the literature, there are very few studies that have explored the possibility of using vehicular communication to transmit physiological parameters out of the vehicle, and there are no systems that use DSRC for this purpose. Additionally, many of the in-car physiological monitoring

systems were created in order to log physiological parameters only while driving, and not while the driver is potentially incapacitated. This involves the placement of sensors in areas that would only be used during regular driving, such as the steering wheel.

Many of the physiological monitoring systems that are described in this section are implemented in the form of Wireless Body Area Networks (WBAN). From Ullah et al. [13], a WBAN is a collection of lightweight wireless sensor nodes that either monitor specific parameters on the human body or the surrounding environment. A simple example of a WBAN with several nodes and a base station is shown in Figure 2-4. One of the most common applications of WBAN is in long-term patient monitoring. From [13], the example is given of a patient visiting a doctor for a blood pressure check. In that particular scenario, the patient may be nervous, due to the setting, the physician, or some other environmental factor. That additional anxiety would likely alter the patient's blood pressure, thereby resulting in a reading that is not indicative of what the patient actually experiences in their day-to-day environment. Such monitoring systems are also useful for detecting symptoms that a patient may try to conceal, as is often the case with conditions like idiopathic toe-walking [42]. WBAN systems have been used in these cases in order to gain a more accurate picture of the patient's physiological parameters, though they also have applications that are less clinical in nature, such as athletic training and monitoring of military personnel [43].

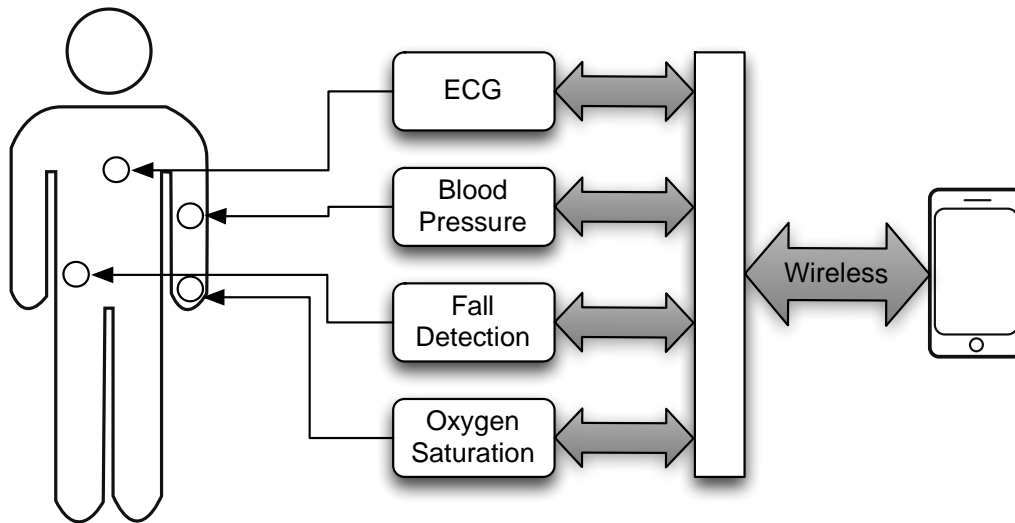


Figure 2-4: Example of a wireless body-area network

### 2.3.1. Ambulatory Monitors

Many researchers have created ambulatory monitors that focus on the use of Bluetooth for communication between sensor nodes and the base station. This is often done for reasons of interoperability, since Bluetooth radios are prevalent in most modern cellphones, computers, and tablets. One such example of a Bluetooth-based monitoring system is the HealthGear system created by Oliver and Flores-Mangas [44]. This system was created in order to find correlations between heightened blood oxygen saturation and sleep apnea, and for this reason it used a classic Bluetooth transceiver along with an XPod pulse oximetry system (NONIN, USA) and a fingertip sensor for collecting pulse signals. Using two AAA batteries, the monitor could only operate for twelve hours, but this was sufficient for the purposes of monitoring volunteers with sleep apnea, since the monitor only needed to collect data at night. Their system communicated over Bluetooth to a mobile phone that ran a custom application designed for the Windows Mobile operating system. Their system was evaluated by the subjects very positively - none of the twenty volunteers experienced any technical problems, and they were all able to collect a night of data successfully. Furthermore, the algorithms that were used to detect sleep apnea were successful

in 100% of instances, and they were even able to distinguish between mild and major cases of sleep apnea. This is similar to the system created by Rofouei et al. [45], though that system detected sleep apnea through a microphone installed in the diaphragm of a neck cuff. In addition to the microphone-diaphragm assembly, the neck cuff also had an off-the-shelf Bluetooth module, an MSP430 microcontroller (Texas Instruments, USA), a NONIN OEM III pulse oximetry module, a pulse sensor that clipped to the user's ear, and a 1000 mAh lithium polymer battery that was capable of powering the device for nine hours. Much like the HealthGear system, this system transmitted data via Bluetooth to a mobile phone for the end user, but it also had a Windows-based desktop application for the clinician to use. The microphone in the neck cuff captured the user's breathing at a rate of 2 KHz, and the frequency response of the resulting waveform and the recorded blood oxygen saturation ( $SpO_2$ ) data were analyzed at the base station for signs of sleep apnea. Their overall system was able to detect the amount of apnea events that occurred in a given subject, and through analyzing the characteristics of these events, the clinician could assign an apnea-hypopnea index that identified the severity of their sleep apnea.

Bluetooth was also used in [46] in order to detect stress during ambulatory activities. The built system had sensors to measure electrocardiogram (ECG), skin temperature, skin conductance, respiration, and activity (through accelerometry), and these sensors were isolated into separate Bluetooth nodes to form a true WBAN system. Each sensor connected to individual Bluetooth sensor nodes. The node used in this study was called the Mulle (Lulea Institute of Technology, Sweden), which included a Bluetooth controller, a microcontroller with an 8 channel analog-to-digital (A/D) converter, and a rechargeable lithium polymer battery. The individual sensors connected to the microcontroller through the A/D converter, and the parameters captured by each sensor were transferred back to a base station for analysis. The individual sensors were compared against "gold standard" measurements and were found to be accurate, though this particular study did not involve any clinical trials or volunteer trials. The idea of using a

Bluetooth-based WBAN to identify situations of stress was also pursued in [47], though that system was being targeted towards bomb disposal technicians who are required to wear heavy explosive ordinance disposal suits and are therefore very susceptible to heat stress. The created system had temperature sensors that were placed on the neck, chest, biceps, abdomen, thighs, and lateral calf muscle. These sensors connected to three Gumstix Connex Bluetooth microcontroller boards (Gumstix, USA), which wirelessly output temperature data to a remote station for analysis. Using this system along with a mathematical model for thermal sensation, the authors were able to assess and quantify the level of discomfort experienced while wearing an explosive ordinance disposal suit during various activities.

Elsewhere, Xu et al. [48] created a Bluetooth-enabled physiological monitor with real-time cuff-less blood pressure monitoring. In order to capture blood pressure without the use of an inflatable cuff, ECG and PPG sensors were used together in a method similar to that described in [49]. That is, ECG and PPG waveforms were measured to find the pulse travel time, and this value was used to estimate the systolic blood pressure of the wearer. This method had the advantage of not requiring an uncomfortable cuff that required a large amount of power consumption to inflate and deflate, but the PPG waveforms were greatly influenced by motion, which consequently had an adverse impact on the resulting blood pressure calculations. These sensors were integrated into a wrist-worn device that communicated with a mobile phone via Bluetooth, though there were no volunteer or clinical trials performed in this study.

Park and Kang created an expandable WBAN sensor system in [50]. Their paper focused mainly on the development of the system and the ad-hoc communication that would take place between modules. Consequently, there was no discussion on actual physiological parameters that would be monitored, and there were no clinical results from their system. Regardless, their system consisted of 25 mm x 25 mm modules that each contained a rechargeable lithium-ion battery (the size

could vary based on the power requirements), a Bluetooth module, and a 10-pin header for connecting the communication module to a sensor. The module consumed 26.5 mW while transmitting and 3.5 mW while idle, though these numbers do not account for any power that may be consumed by the sensor itself. These various communication modules all communicated to a Linux-based PDA, which served as the base station for the system. The overall system was able to support a total of 56 sensor nodes, though as the authors pointed out, the network management becomes very complex with such a large number of nodes.

In many cases, physiological parameters were extracted from a patient for the purposes of being logged in a database where they could be easily recalled, even if that patient visits a different medical facility from the one that they were originally admitted to. The system created by Yu and Cheng [51] was created in order to implement this feature by using Bluetooth to communicate from the worn monitor to a local monitoring unit stored in the hospital. From here, the local monitoring unit used WiFi to transmit these parameters to a control centre and a web page where ECG and blood pressure data could be recalled for future analysis.

There have also been studies that look at wearable Bluetooth-based sensor units for non-physiological parameters. One example of this is [52], in which a wearable sensor was created for the purpose of detecting organic pollutants in the atmosphere. The wearable sensor worked by passing air through an inlet and a series of filters. The resulting compound reacts with the polymer coating on a series of tuning forks, thereby changing the resonant frequency of those tuning forks. The resulting frequency change over time was transmitted to a Windows Mobile-based cellphone for data storage and analysis. In experimental tests, the sensor was able to detect the presence of benzene in the environment with the proper exposure levels, even when other odours such as perfume and mouth wash were present at the same time.

Bluetooth is not the only wireless communication protocol being used in the literature for ambulatory monitors. ZigBee is a very popular choice as well, due to its low power consumption. One example of a Zigbee-based monitor was researched in [53]. The authors combined their physiological monitoring system with an XBee (Digi International, USA) ZigBee transceiver in order to create a complete system that could be used to monitor patients as they leave the hospital but are still at risk. Their physiological monitoring system consisted of a temperature sensor, an accelerometer to detect falls, and a custom heart rate sensor that connected to the bottom of the user's ring finger. The combined sensor/ZigBee system consumed 60 mA during transmission, though the XBee radio could be put to sleep when not in use. Despite using the ZigBee communication system, the system could only run continuously for twenty-five hours before requiring a recharge. This system is very similar to the systems built in [54] and [55], though both of these papers placed the ZigBee radio and the microcontroller system on the same board, thereby eliminating the need for a ribbon cable connecting the physiological monitor and the radio. Additionally, the former system had its own SpO<sub>2</sub> module created from off-the-shelf components, and the latter system contained a purchased pulse oximeter.

In a different study, a patient monitoring and tracking system developed at the Johns Hopkins University in the United States used a proprietary communication protocol based on the same IEEE 802.15.4 standard utilized by ZigBee [56]. The system was built for the purpose of providing physiological monitoring of victims in a massive disaster scenario. The physiological sensors included a fingertip pulse oximeter sensor and a conventional blood pressure cuff, and the information extracted from these sensors was transmitted to a tablet PC carried around by the emergency service team members using 802.15.4 communication. In addition to physiological sensing, the monitor units also had GPS modules, thereby allowing EMS to find patients quickly if their physiological parameters reached a critical state. The tablet PCs used by EMS were also capable of transmitting the captured physiological parameters to a server using cellular Evolution-Data Optimized

(EVDO) communication. This system was created for a similar application to the one being explored in this thesis, though this particular system was meant for use by patients in a mass disaster incident who have already been tagged and triaged. It was not used in a moving vehicle, and it does not utilize any vehicular communication.

In addition to Bluetooth and ZigBee, there have been several physiological monitors that use different communication protocols entirely. Some of them such as [57] are proprietary systems that still use the 2.4 GHz Industrial, Science, and Medical (ISM) frequency band, but some of them opt for different frequencies entirely. For instance, Yoo et al. [58] created a continuous health monitoring system that used dry ECG electrodes placed at several locations on a patient's chest. These electrodes transmitted their ECG data to a chest belt using wireless communication that operated in the High Frequency (HF) band at a center frequency of 13.56 MHz. Furthermore, the dry electrodes harvested power from the HF transmissions sent out by the chest belt with an adaptive threshold rectifier that was built into each individual electrode's flexible printed circuit board (PCB). Furthermore, the electrodes and the chest belt also had the capability of transmitting in the 400 MHz Medical Implant Communications Service (MICS) band, thereby allowing the electrodes to be repurposed as implantable sensors. The authors stated two primary reasons for using these communication systems. First, they considered communication within the ISM band of 2.4 GHz to be a security risk, since somebody with a packet sniffer could theoretically bypass the encryption on the individual data packets and read the patient's physiological parameters. Second, placing batteries on patch sensors that would be placed directly on the user's skin with no protective casing was considered to be a safety risk, hence the use of adaptive power rectifiers, power extraction, and batteries placed on a separate chest belt that is worn over the patch sensors. The system created in this study was compared against other systems that utilized rectifiers, and it was found that this system's efficiency of 54.9% was better than any other rectifier system used in previous works.

There have been many wireless ambulatory monitors researched in the literature, and the majority of these systems use either Bluetooth or ZigBee as the wireless protocol. However, in-car physiological monitors have different requirements from ambulatory monitors, in that they must operate without creating distractions for the driver and they must monitor parameters that are useful either for determining a driver's mental state while driving (stress level, distraction level, etc.) or their physical state following a collision.

### **2.3.2. In-car Physiological Monitors**

There have been several implementations of in-car physiological monitoring systems in the literature, and many of these systems have been used in order to identify states of driver vigilance. One example of such a system comes from the FZi Research Center in Germany [6], in which the steering wheel of a car was fitted with a microcontroller system and several different sensors. Specifically, the wheel contained sensors for heart rate, SpO<sub>2</sub>, skin conductivity, and ECG. Additionally, the seat of the vehicle had non-contact electrodes for ECG that could collect data through the clothing of the patient (successfully demonstrated on a subject wearing a cotton shirt and denim jeans). The microcontroller system communicated with the in-car navigation system via Bluetooth in order to provide graphs of the physiological parameters. Though no full system testing had been performed in that particular study, the system was seamless with the wheel, and it presented no visible distractions to the driver (no protruding wires, etc.). However, the placement of various sensors into the steering wheel meant that it would be unable to log any parameters from the driver in the event of a car accident when the driver is potentially incapacitated and no longer gripping the wheel.

A similar study was conducted in [7] using ECG and photoplethysmogram (PPG) sensors that were attached to the steering wheel of a car. The authors wanted to

use the ECG and PPG sensors in order to measure the heart rate variability (HRV) of the driver, which would potentially provide an indication of the driver's level of fatigue. These sensors were connected to the analog-to-digital converter of a microcontroller, and the values from the sensors were transmitted to a PC using a ZigBee-based 2.4 GHz transceiver. Two volunteers operated the vehicle while rested and again while drowsy, and it was found that when decomposing the HRV signal's power spectrum into very low frequency (VLF), low frequency (LF), and high frequency (HF) components, the ratio of the LF to HF signal powers was higher in the drowsy state than it was in the normal state. Like the system from [6], this system required the driver to have their hands on the steering wheel at all times, therefore making it unsuitable for collision scenarios.

In [8], the goal of the system was to determine vigilance by identifying states where the driver may be asleep or where the driver may be spending too much time interacting with in-vehicle controls. In order to accomplish this, a garment with six textile ECG electrodes and a three-axis accelerometer was created for use inside of a vehicle. All of these sensors interfaced with a microcontroller system using an analog-to-digital converter, and the samples were then transmitted to a PDA using Bluetooth. Through experiments in a road setting at speeds of 30-50 km/h, it was found that the textile-based electrodes exhibited slightly worse signal-to-noise ratios than conventional ECG electrodes, but they were still sufficient in order to determine the posture of the driver. The accelerometer was able provide an assessment of the terrain conditions in order to prevent the system from sending false alarms when atypical ECG measurements were detected. Though the authors mention the possibility of transmitting this information to a remote monitoring location, no remote monitoring features were developed in this particular study.

In a different study, Lin et al. [59] also created a system to determine driver drowsiness, though their system used electroencephalogram (EEG) data in order to quantify this. In addition to the EEG electrodes, the system also had a

microprocessor unit, and the complete system was integrated into a headband that was worn by the driver. The data captured by the microprocessor unit was transmitted to a signal processing module using Bluetooth. When the signal processing module detected a drowsy state based on the EEG data, it sounded a warning tone from a speaker. The system was tested using a driving simulator with ten subjects, and it was able to quantify driver drowsiness with a positive predictive value (PPV) between 75% and 80%. The use of a driving simulator system to determine vigilance was also explored in [60] and [61], though those studies monitored the heart rate, body temperature, and galvanic skin response (GSR) of several drivers while they operated the simulator system. In the authors' subject trials, they were able to determine that heart rate and body temperature decrease when the driver is at risk of falling asleep, whereas the galvanic skin response increases. Although this study did not involve installing sensors into an actual vehicle, it does explore the possibility of using an evolving algorithm with a neural network in order to improve the likelihood of detecting a sleep risk while decreasing the occurrence of false positives.

Another major application of in-car physiological monitoring systems is the detection of driver stress. Furthermore, there have been several research studies that have attempted to correlate different driving conditions (weather conditions, night driving, etc.) with heightened states of stress. Baek et al. [62] installed physiological sensors inside of a car in order to measure driver stress during various scenarios. The steering wheel of the car contained sensors for GSR, PPG, and ECG. The seatbelt had a piezoelectric sensor that measured respiration, and the driver's seat contained a capacitive ground for the steering wheel-mounted ECG sensor. When volunteers drove around the city, they were subjected to various forms of stress such as being forced to drive in narrow alleys and being forced to perform mathematical calculations while driving. The system had high correlation with a reference physiological monitor and was capable of quantifying driver stress, though the driver was required to keep their hands on the steering wheel at all times in order to ensure continuous monitoring of parameters.

A similar system for determining stress was created by Healey and Picard in [63] and [64], though their setup used skin conductivity sensors on the hands and feet, ECG electrodes on the chest, electromyography (EMG) sensors on the shoulders, and a Hall effect sensor around the diaphragm to determine the rate of respiration. From the results gathered from driving around a city environment, it was found that heart rate (through ECG) and skin conductivity were the best parameters to determine a driver's stress level, and with these results, the authors explored the possibility of adjusting in-car functionality based on a driver's stress level. This is similar to the approach taken in [65] and [66], although that study integrated their physiological sensor unit with another unit that logged data from the vehicle itself, including relative speed, cruise control status, pedal depression, and turn signal usage. In that study, the authors wanted to create a system that could find correlations between certain driving situations and heightened states of stress.

Some in-car monitoring systems have been created in order to perform continuous monitoring for potential diseases, much like many of the ambulatory monitoring systems discussed in the previous section. One example of such a system can be seen in [5], in which D'Angelo et al. placed a physiological sensor unit on the steering wheel of a driving simulation system in order to monitor the physiological parameters of elderly drivers. The unit contained sensors for heart rate, SpO<sub>2</sub>, and skin conductivity. The sensor unit communicated with a windshield-mounted receiver unit using a proprietary 2.4 GHz communication protocol. The receiver unit contained a 2.1" TFT display for showing the driver's parameters as well as a micro SD card for saving the data. The simulation system was tested with twenty-four volunteers, and it was found that the heart rate and SpO<sub>2</sub> sensor had an availability of 91% and the skin conductivity sensor had an availability of 73%.

In-car systems to measure the intoxicated state of the driver have also been very popular in the literature. According to data from the United States Government's

FARS system, 32% of all crashes in 2007 involved alcohol-impaired driving [2], so it is easy to understand why this is such a significant research topic. Murata et al. [67] created a system consisting of air packs that are installed in the back of a car seat, and these air packs generated waveforms from the respiration of the driver. When performing an FFT analysis on the waveforms generated from several volunteers, it was found that the FFT experienced a frequency shift when the driver was drinking, although it required baseline data from the specific driver in order to identify intoxication. Furthermore, the driving period needed to be sufficiently long in order to generate a useful waveform. Another anti-drunk driving system was created in [68], although the main motivation in this paper was to create a system that could not be circumvented by having a sober passenger test in place of the drunk driver. The system used a CCD camera system along with a sensor that detected the alcohol concentration of the air around the driver. If the alcohol content of the air rose or fell by a certain amount, the camera system would ensure that the driver had not switched places with somebody else. The system was based around an ARM microprocessor, though there were no test results for the system in that particular study. In [69], a similar system was proposed, though this system didn't use a camera system to confirm the identity of the driver. Rather, the system used an off-the-shelf alcohol sensor. The authors planned to create a system that can detect the alcohol level of the driver's breath and stop the car (or prevent it from starting) if it detected an unsafe level, though this study did not have any test results to discuss.

Though there have been no investigations in the literature on the use of DSRC to transmit physiological parameters out of the vehicle, some researchers have looked at the possibility of using other communication systems for this purpose or similar purposes. Durrezi et al. [70] proposed using an inter vehicle ad-hoc communication network in order to transmit a driver's physiological parameters to a medical facility or to other doctors who may be travelling nearby at the time. Their proposed protocol was called Adaptive Inter Vehicle Communication (AIVC), and it used ad-hoc communication and priority scheduling to

differentiate between normal and urgent medical situations. The authors simulated AIVC using non-preemptive scheduling (in which normal and urgent cases go into different queues) and preemptive scheduling (where urgent cases assume higher positions in a shared queue with non-urgent cases) and found that the latter was more appropriate for handling urgent medical situations, though this created delays for non-urgent cases. Elsewhere, Kerr and Olateju discuss the possibility of using an existing in-car system like OnStar to transmit the blood glucose levels of diabetic drivers. The authors raised the possibility of using the wireless communication to transmit a driver's blood glucose levels to a health care centre in the event of a hypoglycaemia emergency, though they did not build a system or perform any tests. In [71], the authors proposed using a cellular network to connect an in-car physiological monitoring system to a sensor data management server in order to store the parameters of a senior driver and have those parameters accessible by the driver's family members. In their prototype system, a laptop with a USB GPS sensor was connected to a cellphone via Bluetooth, and this system transmitted data to a terminal for viewing. The trial system did not incorporate any physiological sensors or vehicle-to-vehicle communication.

Though there have been several implementations of in-car physiological monitoring in the literature, very few studies have explored the possibility of using vehicle-to-vehicle or vehicle-to-infrastructure communication to transmit physiological parameters. Furthermore, there have been no investigations regarding the use of DSRC in health care applications. With respect to the in-car monitors discussed in this section, many of them require constant contact with the steering wheel in order to record the driver's physiological parameters. These systems would be unsuitable for collision scenarios where the driver is no longer holding on to the wheel. Additionally, these steering wheel systems are unavailable for passengers. As discussed in Section 2.1, elderly passengers are equally susceptible to seat-belt injuries from frontal impacts, and therefore a monitoring system should ideally be usable by any vehicle occupant regardless of whether they are a driver or a passenger.

# **CHAPTER 3: WIRELESS COMMUNICATION SYSTEMS FOR HEALTH CARE OF ELDERLY DRIVERS**

From the literature, it is clear that a number of wireless communication systems are suitable for health care applications. However, providing health care for the elderly in an automotive setting requires specific wireless characteristics, and it is therefore important to choose wireless systems that can perform well in this environment. This chapter begins with a discussion of DSRC in order to understand its potential benefits for health care of elderly drivers. A low-power wireless communication system is essential to integrate the physiological monitor with the in-car DSRC system. For this reason, the four most prevalent low-power wireless communications systems in the health monitoring field – Bluetooth, ZigBee, ANT, and Bluetooth Low Energy – have been discussed. This discussion allows for a selection and justification of the most suitable wireless protocol for in-car physiological monitoring.

## **3.1. DSRC**

In 1999, the Federal Communications Commission (FCC) in the United States allocated 75 MHz of bandwidth in the 5.9 GHz spectrum for use in vehicle-to-vehicle (V2V) and vehicle-to-infrastructure (V2I) communication. The primary motivation of the allocation was to facilitate various traffic safety and traffic convenience applications. Some of the potential applications listed by the FCC included traffic congestion detection, automatic toll collection, and the ability for emergency vehicles to trigger traffic lights. However, in the FCC's press release, they also encouraged other applications of the DSRC frequency spectrum [72]. The IEEE developed a communication system around this frequency spectrum, and in July 2010, the standard governing this system was ratified as IEEE 802.11p [34], though it is more commonly referred to as Dedicated Short Range

Communication (DSRC) or Wireless Access in Vehicular Environments (WAVE). The spectrum has been divided into seven 10 MHz channels that are shown in Figure 3-1. Many additional applications of DSRC/WAVE have been proposed in the literature, including street lamp control [73], route optimization for lowering fuel consumption [40], and for-pay services from private companies [74].

	Ch 172	Ch 174	Ch 176	Ch 178	Ch 180	Ch 182	Ch 184
	5.86 GHz	5.87 GHz	5.88 GHz	5.89 GHz	5.90 GHz	5.91 GHz	5.92 GHz

Figure 3-1: DSRC frequency spectrum

The IEEE 802.11p protocol is based heavily on the existing 802.11 standard that is most commonly associated with 802.11a/b/g/n WiFi. In fact, DSRC is very similar to 802.11a, with the biggest differences being the slightly higher operating frequency spectrum of 5.9 GHz and the lower channel bandwidth of 10 MHz, which leads to a higher symbol interval of 8  $\mu$ s [35]. The symbol interval refers to the amount of time required to transmit one Orthogonal Frequency Division Multiplexing (OFDM) symbol, regardless of how many bits are in each symbol (which is defined by the modulation technique as discussed below). From Chapter 2, it was shown that 802.11b WiFi has been tested in vehicular settings with varying degrees of success. However, it is important to note that 802.11a/b/g/n radios operate in the unlicensed 2.4 GHz and 5 GHz frequency ranges, and these highly popular frequency bands (particularly the 2.4 GHz band) are susceptible to congestion, especially in densely populated urban environments where vehicular communication infrastructure would typically be installed. In Canada and the United States, DSRC has exclusive use of the 5.9 GHz frequency band, and this helps to alleviate the congestion issues commonly found in the 2.4 GHz ISM band. Furthermore, operating at a bandwidth of 10 MHz results in less noise at a given spectral density when compared to a 20 MHz 802.11a channel. Another advantage of the lower bandwidth is a greater tolerance for delay spread, which

results in a smaller probability of experiencing inter-symbol interference (ISI) on the channel. However, the use of 10 MHz channels in 802.11p has been a point of contention in the literature, with some researchers pointing out that 20 MHz channels have a faster symbol time, which would result in a decreased likelihood of packet collisions on highly active channels [75].

DSRC uses a similar OFDM scheme as 802.11a, the parameters of which are listed in Table 3-1 [75]. OFDM divides the transmitted signal into a number of different subcarriers, where each individual subcarrier occupies a small portion of the total channel bandwidth. The motivation behind using OFDM is to use a subcarrier frequency that is less than the coherence bandwidth of the channel, thereby ensuring that each subcarrier experiences flat-fading (as opposed to frequency-selective fading), which results in a significant reduction of ISI when compared to using a single carrier that spans the full bandwidth of the channel [76]. In the case of DSRC, the channel is divided into 64 subcarriers, where 48 transmit actual data, 12 are zeroed to reduce inter-carrier interference (ICI) from adjacent subcarriers, and 4 are pilots used for channel estimation purposes. Each subcarrier has a 1.6  $\mu$ s guard interval in the form of a cyclic prefix, which further prevents any ISI from occurring.

<b>Parameter</b>	<b>Value</b>
Number of data subcarriers	48
Number of pilot subcarriers	4
Number of zeroed subcarriers	12
Total number of subcarriers	64
Subcarrier frequency spacing	156.25 KHz
Guard interval	1.6 $\mu$ s
Symbol interval	8 $\mu$ s

Table 3-1: IEEE 802.11p OFDM parameters

Within each of the individual OFDM subcarriers, there are four different modulation techniques that can be used. Binary Phase Shift Keying (BPSK) offers the lowest data rate due to its encoding of only one bit per symbol. If all 48 data subcarriers are modulated with BPSK and if a coding rate of 1/2 is used (i.e. half

of the bits are useful information and half are redundant for the purposes of forward error correction), then the resulting data rate from this configuration is 3 Mbps (assuming a DSRC symbol duration of 8  $\mu$ s). Quadrature PSK (QPSK) offers the next highest data rate due to its encoding of two bits per symbol, which results in a data rate of 6 Mbps with a coding rate of 1/2. 16-Quadrature Amplitude Modulation (QAM) has four bits per symbol, resulting in a data rate of 12 Mbps with a coding rate of 1/2, and 64-QAM provides the best rate of 27 Mbps with a coding rate of 3/4.

Looking beyond the physical layer of 802.11p and into the MAC layer, the packet structure for DSRC is shown in Figure 3-2 [77]. The packet begins with a two-byte frame control field that indicates the type of frame (control, data, or management), the duration field is four bytes and it includes the physical transmission time of the packet, the next three six-byte address fields include the MAC addresses of the transmitting and receiving devices (respectively) along with the cell ID of the ad-hoc network (or the basic service set in the case of a managed network). Each data packet transmitted by an 802.11p device is assigned a sequence number and a fragment number, and these are stored in the Sequence Control (Seq Ctrl) field. Likewise, the QoS field contains various information pertaining to quality of service. The frame body contains the payload, and the frame check sequence uses a cyclic redundancy code (CRC) in order to check for errors caused by channel distortion.

2	4	6	6	6	2	2	Variable	4
FC	Duration	Transmit MAC Address	Receive MAC Address	Network Address	Seq Ctrl	QoS	Frame Body	FCS (CRC)

Figure 3-2: DSRC packet structure

Devices in 802.11 networks typically communicate using a Basic Service Set (BSS). In a WiFi network such as a public hotspot, the BSS is a managed network that consists of an infrastructure station along with a number of client stations

(note that “station” is the terminology used by the IEEE in [77] to describe either a client or infrastructure member of a network). As shown in Figure 3-3, any communication taking place in this network must be sent through the infrastructure in a routing technique similar to the one used by cellular networks. However, as previously stated in Chapter 1, vehicular networks are intrinsically ad-hoc, and in a fast-moving environment where low latency communication is essential to provide safety applications, it is preferable to use an ad-hoc communication system that does not rely on routing from infrastructure stations. For this reason, DSRC uses the Independent BSS (IBSS) local area network (LAN) defined in the 802.11 standard [77]. IBSS allows stations to communicate with each other without the need for access points or infrastructure, as shown in Figure 3-4. It is clear from the figure that an IBSS would be ideal for a vehicular system due to the close proximity of one vehicle to another in relation to an access point situated on the side of the road. IBSS existed in the 802.11 standard prior to the ratification of DSRC, and this existing system of ad-hoc communication is one of the key advantages of adopting the 802.11 framework for vehicular communication.

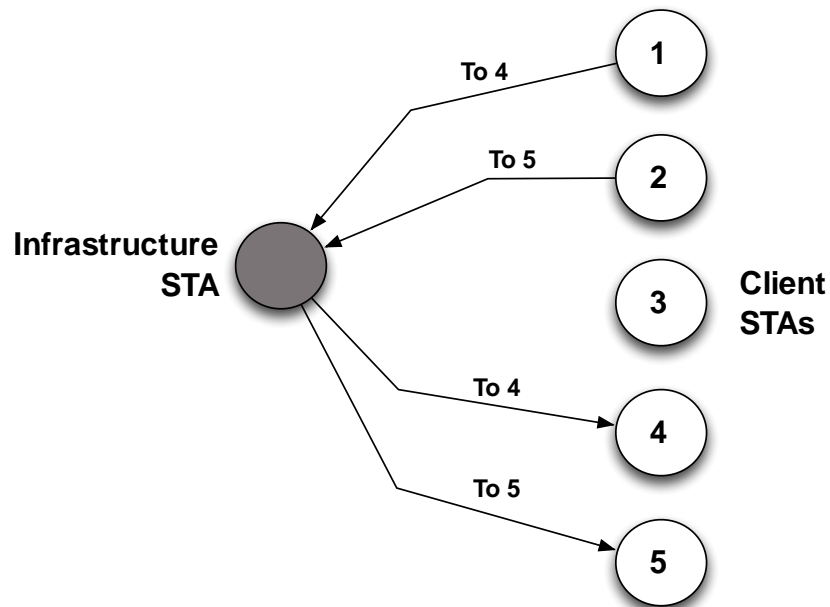


Figure 3-3: Example of an infrastructure BSS

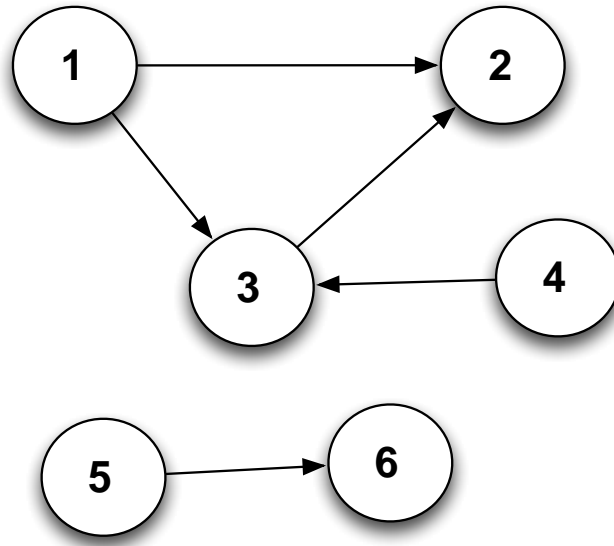


Figure 3-4: Example of an ad-hoc BSS

In DSRC, a vehicular ad-hoc network consists of on-board units (OBU) that are installed into vehicles and roadside units (RSUs) that are installed on the side of the road. However, the RSUs in DSRC serve a very different purpose than the cellular towers described in Chapter 2. In DSRC, OBUs do not subscribe to an RSU in the same way that a mobile phone subscribes to a cellular tower. Rather, the RSUs exist to provide complete coverage down the roadway, and they participate in ad-hoc communication with other OBUs and RSUs. The FCC stated that the maximum transmission range of a DSRC transmitter would be 1000 m at a Tx power of 28.8 dBm [75], though multipath interference and free space loss in the 5.9 GHz spectrum cause a great reduction in the maximum range. By installing RSUs in city and highway environments, it can be ensured that there is no loss in DSRC coverage. The RSUs will also be connected to a larger core network that contains authentication information and may also connect with certain emergency services [78]. There are a number of different ways that OBUs and RSUs can co-exist in a network, and these various examples are all application specific, though Figure 3-5 contains one particular example of a DSRC application that utilizes OBUs and RSUs. In this example, the black car

travelling westbound is about to run a red light, so RSU 2 servicing the east side of the intersection captures the speed and trajectory of the vehicle and sends a warning to RSUs 1 and 4 serving the at-risk directions (the north and south sides, respectively) which in turn warn any incoming vehicles of the collision risk.

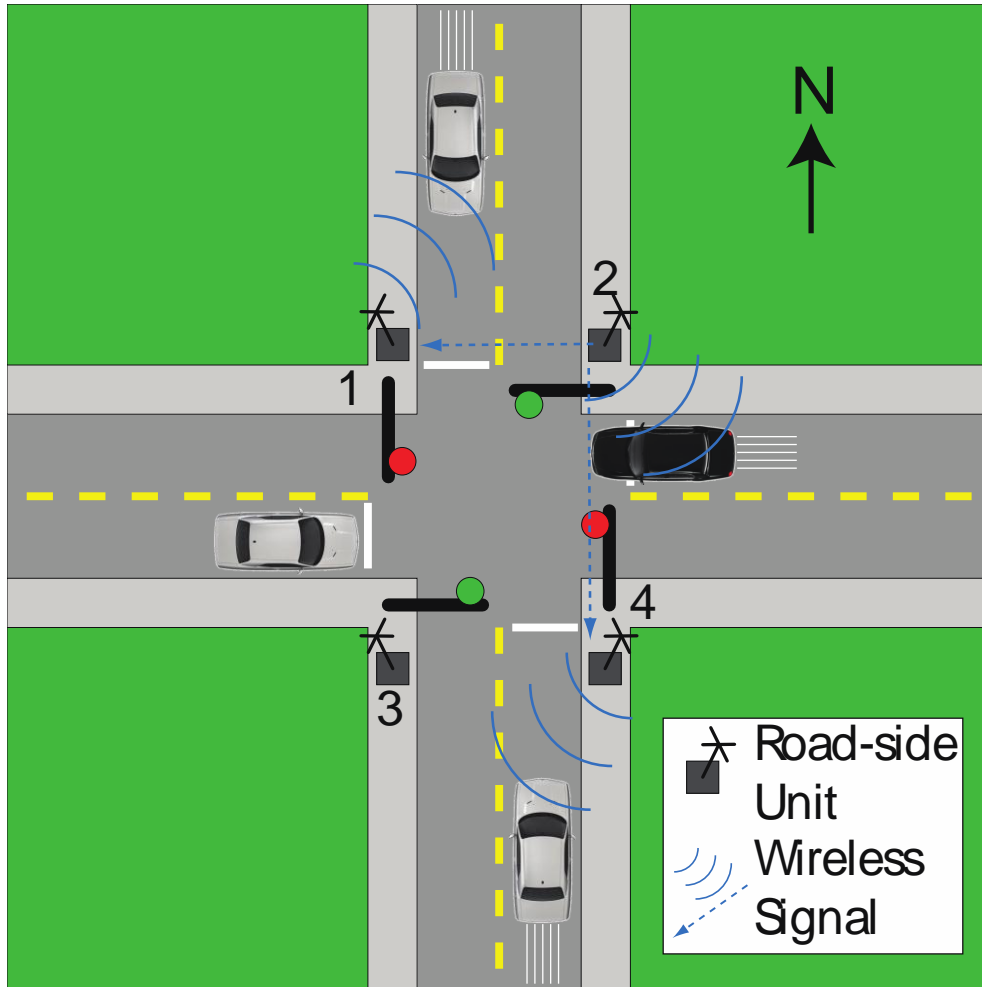


Figure 3-5: DSRC OBU/RSU example

The security protocols present in the current iteration of the IEEE 802.11 standard were not designed for the specific case of a Vehicular Ad-Hoc Network (VANET). The security standards typically seen in an 802.11 network – WPA, WPA2, and formerly WEP – are methods of authentication in a managed network such as a home or business network. A VANET represents a different scenario in which vehicles engage in ad-hoc communicate with each other, but at the same

time they are connected to a greater city-wide network through the application of RSUs. As Samara et al. [79] notes in their research, there are many varieties of attacks that can take place in a VANET, including denial of service attacks in which an attacker overloads the network using packet injection, thereby preventing any vehicles from receiving safety messages. A Sybil attack could also occur, in which a hacker could create dozens of false identities and trick the network into thinking that a traffic jam has taken place, thereby forcing drivers to take alternate routes. While the 802.11p standard does not currently include any methods for preventing such attacks from taking place, Wang and Jiang [80] recommended creating a separate class of RSUs called authentication RSUs, whose sole purpose was to verify the identity of all cars that drive through that section of the road. Upon verifying the identity of a car through communicating with a central certificate authority, the car would be assigned with a temporary certificate, and only certified vehicles would be able to participate in the VANET. This would prevent Sybil attacks from taking place by ignoring any false units (who would presumably be unable to attain certificates), and it would create a mechanism in which attackers performing denial of service attacks could be traced and reported. Additionally, the use of temporary certificates as opposed to permanent certificates would allow drivers to retain their anonymity while participating in the VANET.

It is important to note that while DSRC's ad-hoc nature lends itself to vehicular applications, there are disadvantages to using an ad-hoc network as opposed to a managed network. In a managed network with a central base station, each node is aware of every member's existence. Therefore, information can be disseminated universally, and any disputes between nodes can be resolved efficiently. However, in an ad-hoc network, each node is only aware of those neighbors that are within its communication range. This could lead to a scenario in which a vehicle receives one set of information from an infrastructure unit and a conflicting set of information from an ambulance (to provide one example). The vehicle would not know which set of information is accurate, and it would be

difficult to resolve the dispute if the ambulance and the infrastructure unit are unable to communicate with each other directly. A similar issue is the “hidden transmitter” scenario in which the vehicle receives packets from the infrastructure and the ambulance (using the example described above) simultaneously, leading to packet collisions and possible data corruption. While neither of these issues are necessarily debilitating in collision prevention applications, they would become potentially detrimental in the emergency response application discussed in this thesis (where signals must travel for much larger distances).

Additionally, coverage issues may result if there is an insufficient number of DSRC-equipped vehicles and infrastructure units. The path between the collision and the ambulance must have complete coverage with vehicles properly spaced throughout. If a scenario occurs in which the collision site and the ambulance exist in two separate ad-hoc networks, it will not be possible for the ambulance to use DSRC attain any information. In order for such a scenario to be avoided, DSRC adoption rates among vehicle manufacturers must be sufficiently high, and municipal governments must ensure that infrastructure units are spaced in such a way that minimizes discontinuities in coverage.

Finally, while DSRC’s exclusive use of the 5.9 GHz band allows it to avoid congestion issues to an extent, it is important to acknowledge that congestion can still occur, particularly in densely populated urban areas with hundreds of vehicles attempting to send status updates several times per second. If an accident were to occur in such an environment, there is a possibility that vehicles would be unable to process the large amount of packets being sent to them. This would ultimately lead to a loss of service and a failure to deliver crucial updates regarding the physiological parameters of accident victims. Packet routing and prioritization techniques would have to be employed to reduce the likelihood of such a scenario.

## **3.2. The Four Most Prevalent Low-Power Wireless Communication Systems**

### **3.2.1. Bluetooth**

As discussed in Chapter 2, Bluetooth has been a popular wireless communication protocol in the development of health monitoring systems and WBAN applications. The Bluetooth Special Interest Group (SIG) created the system to be robust, low cost, easy to use, and capable of small form factors. These benefits have contributed greatly to Bluetooth's popularity among researchers and manufacturers. Bluetooth's operation within the 2.4 GHz ISM band allows it to be used in almost every country in the world, while its prevalence in computers, tablets, and mobile phones allows for WBANs to be easily interfaced with existing devices. While WBAN applications typically don't require very high data rates, Bluetooth is capable of 1 Mb/s at its standard rate and 2-3 Mb/s when using the Enhanced Data Rate (EDR) capability, which makes it useful for a wide range of applications extending beyond health monitoring. The 10 m range offered by Bluetooth also makes it acceptable for WBAN systems, in which wireless nodes are typically less than a meter apart.

Bluetooth operates at 2.4 GHz, though Bluetooth devices don't remain in one fixed channel during communication. Instead, Bluetooth uses a technique called Frequency Hopping Spread Spectrum (FHSS) in which transmissions perform a pseudo-random hopping of 79 frequencies, each of which are separated by 1 MHz. Frequency hopping allows Bluetooth to co-exist in the same physical channel as other 2.4 GHz devices such as 802.11g or 802.15.4 transceivers without signal degradation or unwanted packet collisions. Furthermore, Bluetooth devices can utilize a feature called adaptive hopping, in which heavily occupied channels are excluded entirely from the hopping scheme. When Bluetooth devices engage in a network with one master unit and any number of slaves, the hopping sequence for all transmissions is created based on the address of the master unit. The hopping sequence is then exclusive to this specific network. The phase of the

hopping sequence is determined by the clock of the master node. This allows different Bluetooth networks to operate in the same spectrum with a decreased likelihood of collisions [81]. In addition to having different hopping patterns, data packets from different Bluetooth networks are preceded with network-specific access codes in order to account for those instances in which two Bluetooth devices from different networks occupy the same channel at the same time instance.

As previously stated, Bluetooth networks consist of one master unit and one or more slave units. This is known as a piconet configuration. In such a network, slaves are not permitted to form physical links with other slaves - they can only communicate back and forth with their master. A Bluetooth device can be involved in more than one piconet, but because the FHSS hopping sequence and phase are mapped to the address of a master unit, a given Bluetooth device is not permitted to be a master of more than one piconet. However, it is permitted for a unit to be a master of one piconet and a slave of another. Furthermore, it is permitted for a unit to be a slave to more than one master unit. If a Bluetooth device is a member of two or more piconets, it is said to be involved in a scatternet, an example of which is shown in Figure 3-6. In this example, unit A is a master with B, C, and D as its slaves. However, C is a master to E and F, while D is a slave to H. This scatternet is a combination of three different piconets, and they each have their own FHSS hopping pattern determined by the address and clock phase of their respective masters.

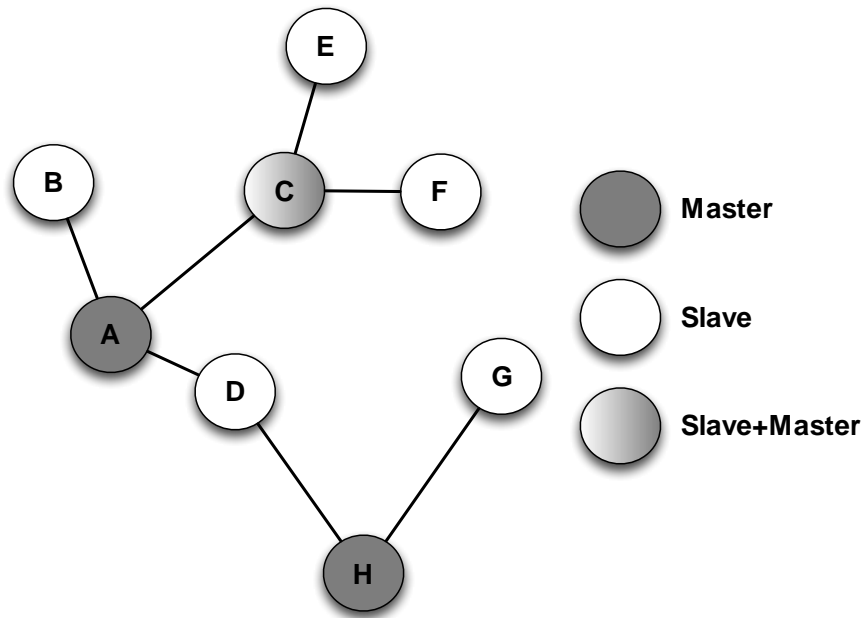


Figure 3-6: Bluetooth scatternet example

The packet structure for Bluetooth is shown in Figure 3-7. As previously mentioned, the channel access code is used to differentiate between piconets. The packet header contains the logical transport address of the recipient unit in the piconet (a unit that is participating in more than one piconet would have different logical transport addresses for each piconet). If the Bluetooth unit is using EDR, the packet header is followed by a guard interval for the rejection of inter-symbol interference (ISI). The payload header contains the size of the payload along with various other pieces of information, and the payload itself contains the user data. Finally, Bluetooth packets use a CRC in order to check for any transmission errors that may have occurred in the channel [81].

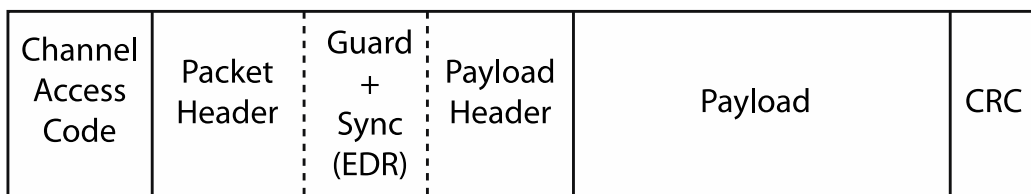


Figure 3-7: Bluetooth packet structure

Bluetooth's primary form of security is its pairing process, in which a six decimal digit passkey is exchanged between two units when they establish a connection. In Bluetooth 2.0 + EDR and prior versions, this was a four-digit passkey, but it was updated in order to achieve compliance with the United States' Federal Information Processing Standards (FIPS). The six-digit passkey is created using the Elliptic Curve Diffie Hellman (ECDH) technique, and the resulting security scheme is referred to in the Bluetooth standard as Secure Simple Pairing [81]. ECDH is a key generation algorithm in which two or more devices generate the same secret key  $K$  based on an elliptical curve in which the individual private keys of the two devices are points on the curve along along with a base point  $G$  [82]. This security scheme was chosen by the Bluetooth SIG in order to create a compromise between computational complexity (the ECDH technique is less complex than other popular encryption techniques) and eavesdropping prevention.

### **3.2.2. ZigBee**

Though Bluetooth's interoperability has made it a popular choice among researchers, its high power consumption is a serious drawback, especially in WBAN applications that require operation for days or weeks. This high power consumption has motivated many researchers and industry manufacturers to pursue ZigBee wireless communication. The ZigBee Alliance has described their wireless communication system as a low-cost, low-power system [83], and researchers performing comparisons with Bluetooth and ZigBee have found that the latter system provides significant power savings [84]. The range achieved by ZigBee devices has been found to be over eight meters, which makes them suitable for short-range WBAN applications [42]. Additionally, ZigBee's maximum data rate of 250 kb/s is more than sufficient for physiological monitoring, where packets typically contain less than 1 kb of data.

The ZigBee wireless communication is built on top of the IEEE 802.15.4 protocol, as shown in Figure 3-8. The PHY and MAC layers of the stack are fully

defined by 802.15.4 and are discussed in further detail below. The network (NWK) layer is the first ZigBee-defined layer, and it is meant to serve as an interface between the MAC layer and the application layer. The NWK layer facilitates certain functions within ZigBee such as the ability to configure a new device, establish a new network, join a network, and discover optimal routing paths through a network. Finally, the Application Support Sublayer (APS) layer and the ZigBee Device Object (ZDO) layers are also defined by ZigBee, and these two layers interface directly with the end manufacturer's application [83].

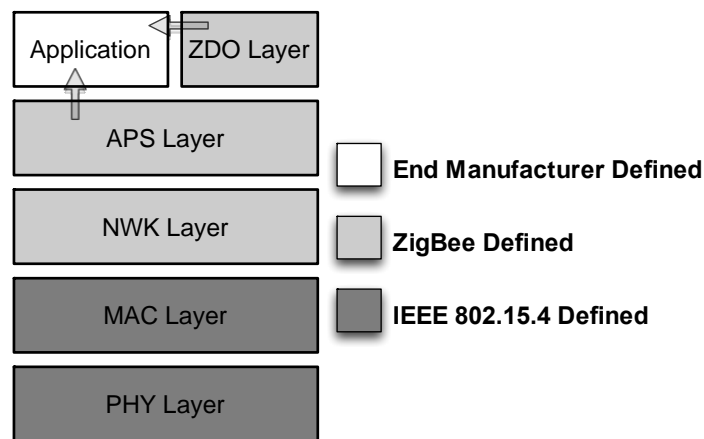


Figure 3-8: ZigBee stack (simplified view)

The PHY layer of 802.15.4 allows for operation in three different frequency bands. Channel 0 of ZigBee operates at 868.3 MHz, which is used in some European countries. Any transmissions that take place at this channel are modulated with BPSK and therefore have the smallest maximum data rate of 20 kb/s. Channels 1 through 10 operate in the 915 MHz band (from 906 MHz to 924 MHz), which is used primarily in the United States and Canada. These channels also use BPSK, though they can achieve a slightly higher bit rate of 40 kb/s. However, the most popular ZigBee channels are 11 through 26, which operate in the 2.4 GHz ISM band between 2405 MHz and 2480 MHz and are therefore usable in almost every country in the world. Transmissions on these channels are modulated using offset QPSK (O-QPSK) and can achieve a maximum bit rate of 250 kb/s [85].

Rather than using frequency hopping or multi-carrier techniques like Bluetooth and DSRC, ZigBee utilizes its available channel bandwidth with a technique called Dynamic Sequence Spread Spectrum (DSSS). In DSSS, the modulated data signal  $S(t)$  is multiplied by a spreading signal or spreading code  $S_c(t)$ , thereby resulting in a bandwidth of  $B_c+B$ , which is a larger bandwidth than what is required for data communication. This use of excessive bandwidth allows a transmitted signal to reject ISI and multipath interference. DSSS and FHSS mitigate interference using two completely different approaches in which the former suppresses the effects of strong interferers and the latter avoids these interferers altogether [76].

The ZigBee network topology has more flexibility than the Bluetooth topology, as it can operate in a star, tree, or mesh arrangement. The star topology is similar to the starbus from Bluetooth in that a single ZigBee coordinator sets up the network, and all other nodes in the network report back to the coordinator while never communicating with each other. The tree topology is shown in Figure 3-9, and it uses routers to move messages from the coordinator to the nodes at the bottom, but it still follows a hierarchy in which messages flow strictly from the top to the bottom or vice-versa. The mesh topology is completely ad-hoc, similar to the IBSS network used in DSRC. In this configuration, communication within the personal area network is peer-to-peer, with no hierarchy and no routers [83].

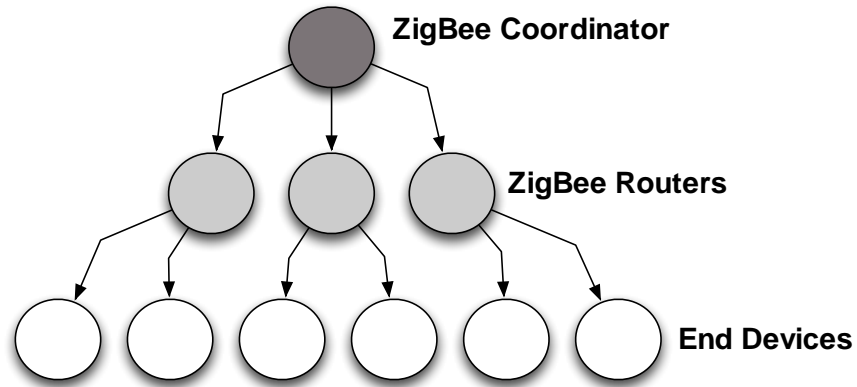


Figure 3-9: ZigBee tree topology

Figure 3-10 shows the packet structure that is used in ZigBee. The frame control field is two bytes long, and it contains some miscellaneous information about the packet, including whether or not security is enabled and whether or not it requires an acknowledgement. The one-byte sequence number is used to match certain packets together. For example, if the packet requires an acknowledgement, the sequence number of the data packet and the acknowledgement would match, in order to ensure that the end manufacturer application can associate one with the other. The personal area network (PAN) of ZigBee and 802.15.4 is used to differentiate between ZigBee networks that may be communicating on the same physical channel. The PAN is two bytes long, and each ZigBee packet has fields for the source PAN and the destination PAN, though in a typical usage scenario, these PANs would be identical, as units in different PANs are usually not expected to communicate with each other. The address of a ZigBee unit can be either two bytes long or eight bytes long, and it is essentially the same as a MAC address in 802.11 units. The address is used to uniquely identify each unit in a ZigBee PAN. The payload is of variable length, and it contains the actual data to be transmitted. Finally, the frame control sequence (FCS) contains a CRC similar to DSRC and Bluetooth to check for any errors that may have occurred from within the channel [85].

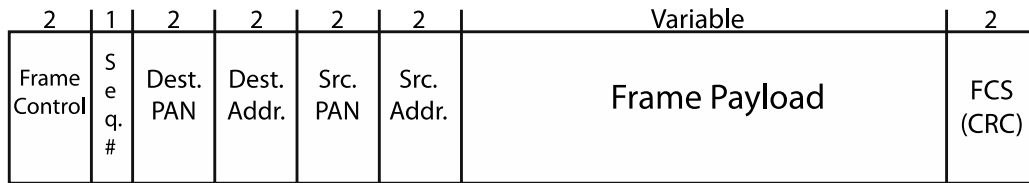


Figure 3-10: ZigBee packet structure

The security features of ZigBee are implemented either in the NWK or APS layers of the stack (i.e. the ZigBee layers as opposed to the 802.15.4 layer). ZigBee's security system is based on three kinds of keys called link keys, network keys, and master keys. Link keys are acquired from key establishment using the master keys, whereas network keys and master keys are pre-installed by the manufacturer. These keys are used to encrypt either the NWK or APS layers of the stack (though encryption is never applied on both), and only ZigBee units with the proper keys can remove the encryption and read the frame contents inside.

### 3.2.3. ANT

Although ZigBee and Bluetooth have both become widely used 2.4 GHz wireless communication systems for WBAN applications, there have been some attempts at creating proprietary systems that operate inside the ISM band. One example is the ANT wireless system created by Dynastream Innovations Inc. The manufacturer of ANT claims that the low stack overhead of the system is what allows it to have lower power consumption than larger systems like ZigBee and Bluetooth. Furthermore, unlike standards-based wireless systems that need to be applicable to a wide range of applications, Dynastream has designed and optimized ANT specifically for wireless sensor network applications. The ANT protocol is available in various devices such as the nRF51422 system-on-a-chip (Nordic Semiconductor, Norway), and these devices can achieve data rates of up to 2 Mbps.

Similar to ZigBee, ANT is capable of the star, tree, and mesh network topologies. However, ANT differs from ZigBee in how the master/slave relationship between two units operates. In ANT, the fundamental building block for a network is the channel. Unlike other communication systems like Bluetooth and ZigBee, the word “channel” in ANT does not refer to a physical frequency assignment. Rather, a “channel” in ANT refers to the link that is created between a master node and its slave node. The channel in ANT can have certain characteristics assigned to it, including whether it’s a transmit-only channel (where slaves can only send data) or a receive-only channel (where slaves can only receive data) and the channel message rate (the rate at which packets will be sent by the master, which ranges from 0.5 Hz to over 200 Hz) [86]. In a network of ANT units, each connection is its own channel, and each channel has its own master-slave relationship. One example of an ANT network is the starbus network in Figure 3-11. In this example, all three channels share a common master. However, each channel has its own unique characteristics, and in this case, channel 0 is a transmit-only channel whereas channels 1 and 2 are bidirectional slave channels, in which the master primarily receives data from the slave, but it can still send data to the slave if it is required to.

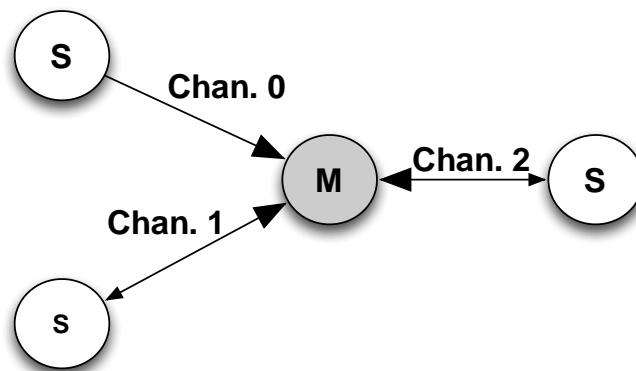


Figure 3-11: ANT starbus network example

ANT uses a technique called frequency agility to improve its coexistence with other 2.4 GHz devices in the vicinity. However, unlike Bluetooth’s FHSS

technique that hops across a pseudo-random sequence of frequencies during every transmission, a radio using frequency agility remains in one frequency while continuously monitoring the link quality. If the link quality degrades, ANT will automatically alter the operating frequency of the channel in order to compensate. ANT has 124 different operating frequencies ranging from 2400 MHz to 2524 MHz, which is an improvement over the 26 channels of ZigBee or the 79 channels of Bluetooth, though ZigBee's 5 MHz channel bandwidth is larger than what ANT provides.

Compared to Bluetooth and ZigBee, the MAC packet frame for ANT is very simple, as shown in Figure 3-12. The sync byte is a single byte with a fixed value, the message length indicates how many bytes are present in the payload (i.e. the value of  $N$ ), and the message ID indicates whether or not the packet is performing a special command (such as setting the channel RF frequency, setting the transmit power, setting the timeout, etc.). After the message ID, the payload is sent as  $N$  data bytes. The check sum at the end of the packet is simply the XOR of every bit in the packet (excluding the checksum itself).

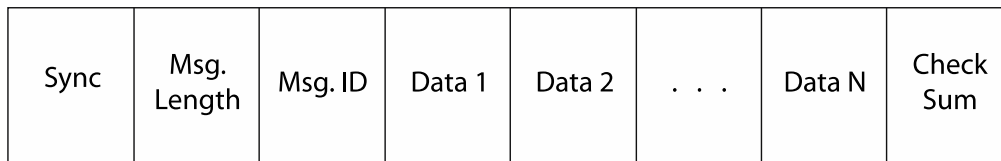


Figure 3-12: ANT packet structure

ANT is just one example of a proprietary 2.4 GHz communication system. Systems such as ANT have the advantage of being able to form their communication characteristics around a specific application. In the case of ANT, the application is wireless body area networks. However, proprietary systems are not as robust as standards-based systems like ZigBee and Bluetooth, and they also cannot provide the interoperability of a standards-based system. Additionally, the ANT standard does not include any built-in security, and there are no

countermeasures against eavesdropping or man-in-the-middle attacks. This lack of interoperability and security is a large drawback that must be taken into consideration if the end manufacturer's application requires interaction with any external devices.

#### **3.2.4. Bluetooth Low Energy**

From Chapter 2, it is clear that many wireless physiological monitoring systems have been researched and developed in the literature. However, researchers are still attempting to design systems that satisfy all of the design requirements of health care applications. In Omre's review of health monitors [87], he identified interoperability, low power consumption, minimization of electromagnetic interference (EMI), and secure data transmission as being the four most important requirements of a health monitor. IEEE 802.11 WiFi-based systems provide excellent interoperability and security features (assuming the implementation of a system like WPA2), and its operation in the 5 GHz spectrum (assuming the use of 802.11a or n) reduces the possibility of EMI. However, WiFi systems have extremely high power consumption when compared to the other wireless systems. Classic Bluetooth has the same issue of power consumption, though the problem is not as severe as it is in the case of WiFi. ZigBee and ANT are both capable of low-power operation, but they do not have the interoperability of WiFi or Bluetooth. Phones, tablets, and laptops are not typically manufactured with ZigBee or ANT transceivers, thereby creating the need for external radios that may not even be available for different platforms. ANT in particular suffers due to its lack of built-in security, thereby requiring an implementation much higher up in the stack.

In light of these challenges, Bluetooth Low Energy (BLE) shows considerable promise as an optimal wireless protocol for physiological monitoring applications. The goal of BLE is to offer the same interoperability, EMI rejection, and comparable security features of classic Bluetooth while greatly reducing

transmit/receive power consumption. While BLE operates in the EMI-heavy 2.4 GHz ISM band, it operates at 0 dBm output power, and it uses short transmission bursts to ensure that it is only transmitting for 1% of its total operating time [87]. Another way that BLE avoids EMI is through the same FHSS technique used by classic Bluetooth. However, while classic Bluetooth uses 79 channels in its hopping pattern, BLE only uses 40 channels – 37 of which are used for data while the other 3 are used for advertising events. BLE also has the same adaptive hopping capability as classic Bluetooth, in which heavily occupied frequencies can be removed from the pseudo-random hopping order entirely. In addition to FHSS, BLE uses a similar approach to classic Bluetooth in order to prevent unwanted collisions between uncorrelated devices. However, while classic Bluetooth uses access codes (as discussed in section 3.2), BLE devices use randomly generated addresses to differentiate between different piconets [81]. BLE can achieve data rates of 1 Mb/s and ranges of up to 10 m, which are comparable to classic Bluetooth (assuming that EDR is not being used), and more than adequate for WBAN applications.

The Bluetooth SIG aims to achieve interoperability in BLE by facilitating the development of single-mode and dual-mode BLE devices. Single-mode transceivers are only capable of communicating with other BLE devices, but they offer very low power consumption. These single-mode transceivers are intended for installation into low-power devices such as physiological monitors, watches, or sensors in order to allow them to last for weeks or months at a time. Dual-mode transceivers are capable of communicating with either BLE or classic Bluetooth devices, though they sacrifice their low-power capabilities in order to gain this feature. Dual-mode transceivers are intended for installation into phones, tablets, and laptop computers, where ultra low power is not a significant concern. Furthermore, because most of these devices already include classic Bluetooth transceivers, changing to dual-mode Bluetooth transceivers will ideally require minimal extra design effort on the part of the engineers.

Unlike classic Bluetooth or ZigBee, BLE is only capable of the piconet topology. Specifically, this means that while one BLE master unit can have multiple slaves, it is not permitted for one unit to be a slave in multiple piconets, nor is it permitted for a unit to be a master of one piconet and a slave of another (in other words, scatternet configurations are not permitted in BLE). Furthermore, it is not possible for BLE units to change roles (i.e. from master to slave or vice-versa) once a connection has been established. However, Bluetooth Specification 4.0 is the first version of the standard to include support for BLE, and the standard has indicated that these restrictions could be relaxed in the future in order to allow additional flexibility in BLE's network topologies [81].

From Figure 3-13, it is apparent that Bluetooth Low Energy uses a simpler packet structure than classic Bluetooth. The preamble consists of a fixed pattern of bits for synchronization purposes, while the access address is used to differentiate between physical links that exist within the same channel (i.e. it performs the same function as the channel access code in classic Bluetooth). The PDU header's contents depend on whether the specific packet is an advertising packet or a data packet, though its intended purpose is to provide miscellaneous information regarding the payload contents, including the length of the payload. Finally, the payload contains the actual data to be transmitted, while the CRC is used for error checking.

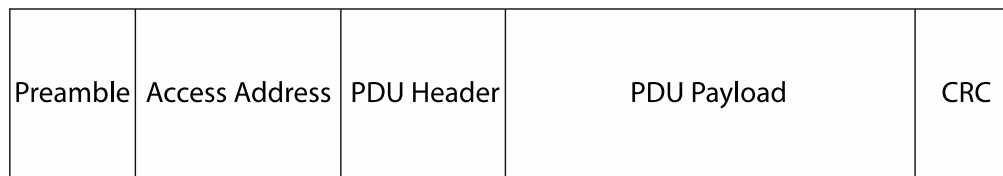


Figure 3-13: Bluetooth Low Energy packet structure

BLE uses a similar security scheme as classic Bluetooth. A passkey system is used to prevent unwanted eavesdropping and man-in-the-middle attacks in a connection. However, Bluetooth does not use the ECDH system used by classic

Bluetooth in order to keep processor loads and power consumption as low as possible. Instead, key generation is performed by the host of the connection, and the generated key is independent of any other BLE device. In addition to key generation, BLE also has support for AES-128 encryption for further protection against eavesdropping [81].

Table 3-2 contains a comparison of the four low-power wireless communication systems discussed in this chapter. From the table, Bluetooth has higher power consumption than ZigBee, ANT, or BLE, and this makes it a poor choice for an in-car physiological monitor that must be able to operate for as long as possible in life threatening emergency situations. ANT is inferior to the other three systems when taking security into consideration, and this is an important concern for a monitoring device that will be transmitting physiological parameters. Between the remaining two systems, ZigBee and BLE are both suitable for in-car monitoring, but the interoperability of BLE with dual-mode Bluetooth devices allows for integration with mobile phones or tablets as a possible method of downloading and displaying recorded data.

Bluetooth Low Energy has the potential to be a suitable wireless system for in-car physiological monitoring when compared to the other three discussed protocols, though there are no existing systems that combine DSRC with BLE communication. There are numerous challenges associated with creating an in-car safety system that uses these two wireless protocols together, and these challenges are discussed in the next chapter.

	<b>Bluetooth</b>	<b>ZigBee</b>	<b>ANT</b>	<b>Bluetooth Low Energy</b>
<b>Power consumption</b>	High	Low	Low	Low
<b>Interoperability</b>	High	Low	Low	High
<b>Maximum data rate</b>	1-3 Mb/s	250 kb/s	2 Mb/s	1 Mb/s
<b>Spectrum Modulation</b>	FHSS	DSSS	Frequency Agility	FHSS
<b>Number of channels</b>	79	27	124	40
<b>Frequency band</b>	2.4 GHz	868.3 MHz, 915 MHz, 2.4 GHz	2.4 GHz	2.4 GHz
<b>Network topologies</b>	Piconet, scatternet	Star, tree, mesh	Star, tree, mesh	Piconet
<b>Security</b>	Pairing, passkeys	Encryption keys	None	Pairing, passkeys

Table 3-2: Comparison of low-power wireless communication systems

# CHAPTER 4. SYSTEM DESIGN<sup>1</sup>

## 4.1. System Overview

As previously stated, the objective of this research is to determine whether 5.9 GHz DSRC is a viable system for transmitting a vehicle occupant's vital signs in the event of a car accident or medical emergency. If elderly drivers had their physiological parameters monitored during driving or while sitting in a car as a passenger, DSRC could potentially be used to transmit these parameters to EMS (or to other authorized vehicles) in the event of an accident, thereby allowing EMS to prioritize their emergency response efforts. Although DSRC has the potential to work in an application such as this, the IEEE 802.11p standard has only recently been ratified, and its use in practical, high priority scenarios is unproven. This research involves designing an in-car system that combines DSRC vehicular communication with physiological monitoring. The developed system is a research tool that will be used to investigate whether DSRC can satisfy the low latency, low packet loss, and high reliability criteria that a vehicular communication system requires in accident prevention situations.

A block diagram of the complete system is shown in Figure 4-1. From the figure, the complete system is comprised of two primary components – a DSRC vehicular communication system and a Bluetooth Low Energy-based physiological monitor. The developed DSRC system is capable of joining an ad-hoc network with all other vehicles in the vicinity, and it can send messages to nearby vehicles using an in-car user interface. To increase the system's power efficiency and to reduce the possibility of EMI in densely populated urban environments, the DSRC system should be able to adjust the transmission power between 0 and 28 dBm, as required by the FCC's restrictions in the United States [75]. A small form factor and ease of installation into an automobile are also

---

<sup>1</sup> Material in this chapter has been presented at the *AUTO 21 Annual Conference 2011* and the *25th IEEE Canadian Conference on Electrical and Computer Engineering (CCECE) 2012*

important design parameters. Additionally, the system must be user friendly, as the target candidates are elderly drivers who may not feel comfortable adopting new technologies. Finally, the designed DSRC system can serve as an on-board unit in a vehicle or as a road-side infrastructure unit.

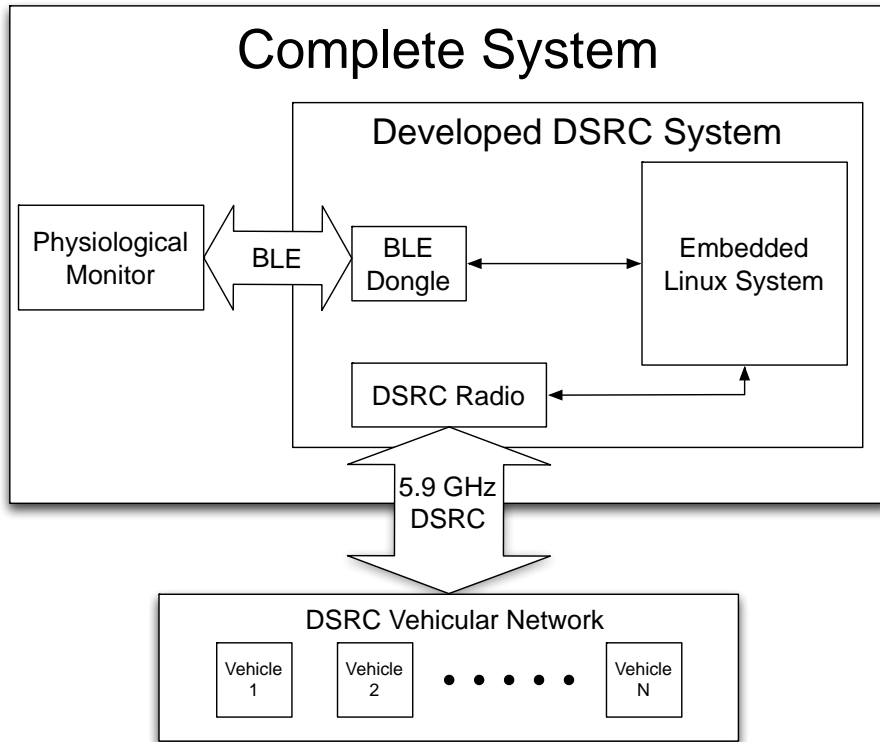


Figure 4-1: Block diagram of in-car integrated system

The physiological monitor is designed to be worn during driving. The use of wires must be kept to a minimum to avoid creating distractions for the driver. Therefore, wireless communication between the sensors and the developed DSRC system is essential. In addition to reducing distractions, using wireless communication allows the system to be expanded with new sensor nodes. However, the wireless sensor nodes must consume very low power to preserve the system's battery life. As discussed in Chapter 3, ZigBee, Bluetooth Low Energy, and ANT are all capable of low power consumption, but the added advantage of interoperability makes BLE a good choice for the wireless protocol in the physiological monitor.

Furthermore, the choice of physiological parameters to monitor is considered carefully. It is important to choose parameters that can be measured inside a vehicle while providing minimal distraction for the driver. At the same time, these parameters should provide useful information to EMS during emergencies. The parameters that have been chosen are heart rate, body temperature, and blood oxygen saturation ( $SpO_2$ ), and all three of these will be discussed in Section 4.3.2.

The remainder of this chapter consists of an in-depth description of the system design. The design of the developed DSRC system and physiological monitor will be discussed, as will the process of integrating the two individual components into a complete system.

## **4.2. DSRC Vehicular Communication System**

### **4.2.1. Hardware Selection**

A block diagram of the DSRC vehicular communication system is shown in Figure 4-2. Each of the individual subsystems in the block diagram will be discussed in detail below, with the exception of the Bluetooth Low Energy dongle, which will be discussed in Section 4.3.3.

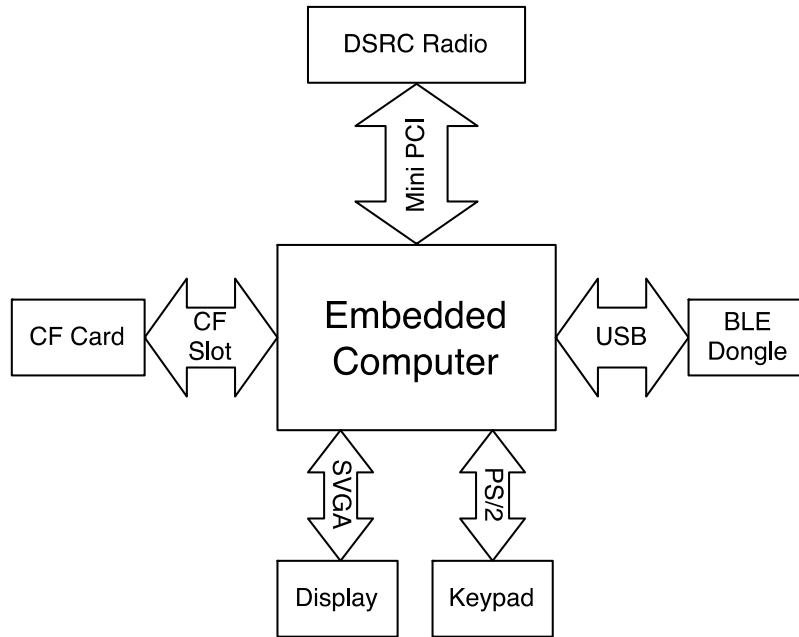


Figure 4-2: Block diagram of developed DSRC system

The most important component of the vehicular communication system is the DSRC radio. As previously stated, the IEEE 802.11p standard was ratified in 2010 and therefore, there are very few commercially available DSRC radios. From the literature review in Chapter 2, software radio implementation of 802.11p is a possibility. Specifically, the USRP software radio system (Ettus Research, USA) used in [35] has been shown to be capable of reproducing the key OFDM parameters of 802.11p in the 5.9 GHz frequency band. However, the USRP software radio system must connect to an embedded computer through Ethernet, because the transmitter code is compiled and executed inside the embedded computer. Moreover, the embedded computer would be required to run the in-car user interface. The USRP software radio system has physical dimensions of 18 cm x 21 cm x 5.5 cm, and embedded computers typically have similar dimensions. This would lead to a form factor consisting of two enclosures, which is not ideal for easy installation into an automobile. Another possibility for implementing DSRC is to re-tune an 802.11a chipset for operation in the 5.9 GHz range. The MAX2829 (Maxim, USA) discussed in Chapter 2 is one example of an 802.11a chipset that has been shown to be capable of DSRC operation [36].

Though the MAX2829 would have to be integrated into an embedded system in order to provide a user interface for the vehicle occupants, it is still a far more viable option for miniaturization than the software radio approach, due to its 8 m x 8 m footprint. However, a radio that has been designed specifically for 802.11p operation is preferable to a re-tuned 802.11a radio. One of the only 802.11p radios available is the DCMA-86P2 (Unex Technologies, Taiwan). The DCMA-86P2 is a Type III mini-PCI wireless radio that contains a high-rejection RX filter that is designed to operate in the frequency range of 5.85 – 5.92 GHz. The radio has dimensions of 5.96 cm x 5.08 cm, and its mini-PCI interface allows it to be integrated with an embedded computer into a single enclosure. For these reason, the DCMA-86P2 was chosen as the DSRC radio for the system.

The DCMA-86P2 DSRC radio requires 1.4 A when transmitting with a Tx power of 24 dBm, 0.75 A when transmitting at a Tx power of 5 dBm, and 0.3 A when the transmitter is idle. As mentioned in Chapter 3, the OFDM subcarriers of DSRC need to be able to support symbols modulated with BPSK, QPSK, 16-QAM, and 64-QAM, and the DCMA-86P2 supports all of these modulation techniques along with a 10 MHz bandwidth in order to achieve theoretical data rates from 3 Mb/s to 27 Mb/s. The DCMA-86P2 has been rated for operation between  $-40^{\circ}\text{C}$  to  $85^{\circ}\text{C}$ , which makes it an appropriate radio for road-side infrastructure units in a wide range of climates. Even at the extreme ends of this temperature range, the receiver is still capable of very low sensitivity levels. In the worst case of operation at  $-40^{\circ}\text{C}$  with the maximum theoretical data rate of 27 Mb/s, the receiver can still detect signals as weak as  $-77.5$  dBm.

Figure 4-3 shows a block diagram of the DCMA-86P2 DSRC radio. This radio contains an AR5414 WLAN CMOS chip (Qualcomm Atheros, USA) and all of the required RF circuitry such as the Rx filter and the Micro Miniature Coaxial (MMCX) female connector for the antenna. The AR5414 is a dual-band RF transceiver designed for operation in both the 2.4 GHz and 5 GHz frequency bands in order to comply with 802.11a/b/g standards, but it also supports

operation within the DSRC frequency range of 5.85 – 5.92 GHz. As previously discussed, the RF filter in the DCMA-86P2 has been designed specifically for high rejection of any frequencies that fall outside of the DSRC band. The radio also uses a 40 MHz crystal, though in the case of DSRC, the frequency synthesizer inside of the AR5414 is responsible for generation a 10 MHz signal from this crystal.

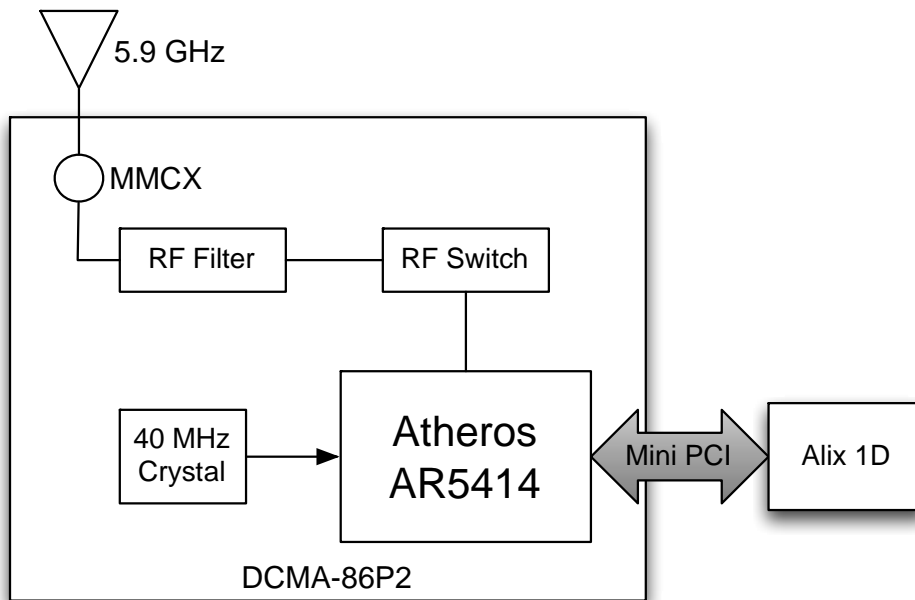


Figure 4-3: RF system for DCMA-86P2 DSRC radio

The DCMA-86P2 communicates with the host using a Type III mini-PCI interface, and therefore, an embedded computer with a mini-PCI slot is required to control it. The embedded computer should have a small form factor and peripheral ports for devices such as the Bluetooth Low Energy USB dongle that is required to communicate with the physiological monitor. Table 4-1 contains a comparison of several embedded computers that are capable of running Linux. From the table, the only embedded computers that include mini-PCI slots are the Alix machines (PC Engines, Switzerland). Furthermore, video support is required in order to create a user interface that the vehicle occupants can receive notifications on, and the only two machines to include video support in addition to

mini-PCI support are the Alix 1D and the Alix 3D3. Although the Alix 3D3 has a smaller form factor, the Alix 1D has a PS/2 port and general purpose input/output (GPIO) data lines, which makes it more flexible and more capable of future expansion. For this reason, the Alix 1D was chosen as the embedded computer for the DSRC system.

	<b>PC Engines Alix 1D</b>	<b>PC Engines Alix 2D13</b>	<b>PC Engines Alix 3D3</b>	<b>BeagleBoard XM</b>	<b>Raspberry Pi Model B</b>
<b>Mini-PCI Slots</b>	1	1	2	None	None
<b>USB Ports</b>	2	2	2	4	2
<b>Video Output</b>	VGA	None	VGA	DVI-D	HDMI
<b>Processor</b>	LX800 500 MHz	LX800 500 MHz	LX800 500 MHz	ARM Cortex 1 GHz	BCM2835 700 MHz
<b>Memory</b>	256 MB	256 MB	256 MB	512 MB	256 MB
<b>Peripherals</b>	PS/2, GPIO, RS232, Ethernet	RS232, Ethernet, I2C	RS232, Ethernet	I2C, GPIO, Ethernet	GPIO
<b>Dimensions</b>	17 cm x 17 cm	15.2 cm x 15.2 cm	10 cm x 16 cm	8.5 cm x 8.6 cm	8.6 cm x 5.4 cm

Table 4-1: Comparison of embedded computers

The Alix 1D with the DCMA-86P2 DSRC radio is shown in Figure 4-4. The Geode LX800 is used by the embedded computer as its CPU core and its graphics processor. The LX800's 500 MHz clock speed is comparatively low compared to modern desktop and laptop computers, but for operating the DSRC radio and the user interface, it is sufficiently powerful. The Alix 1D also uses 256 MB of RAM and a 256 kB cache. In addition to this hardware, the Alix 1D also contains several other peripherals that are important for the DSRC system, including the CompactFlash card slot for storage of the operating system and software, a PS/2 port for the keypad (discussed below), and a USB port for the BLE dongle (as well as an additional USB port that could potentially be used for a GPS module in the future). The Alix 1D requires 12 V, and it consumes approximately 0.4 A with no mini-PCI cards or peripherals connected.

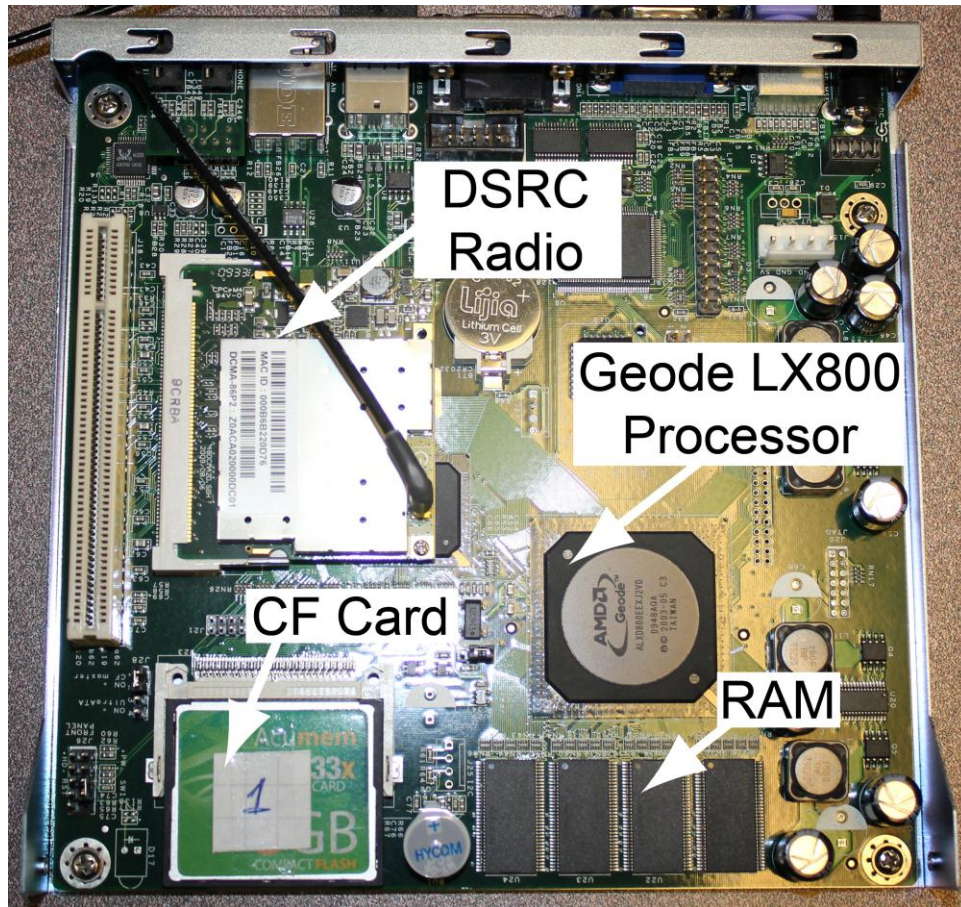


Figure 4-4: Alix 1D with DSRC radio and CF card

As previously stated in Chapter 2, when designing in-car systems that require occasional user interaction from elderly drivers, it is important to account for the user's slower response times and decreased physical strength. In particular, it was suggested in [22] to use large, distinguishable buttons as opposed to turning knobs or two-handed control mechanisms. Using a touchscreen display to control the DSRC system's user interface was initially considered, but the idea was eventually discarded due to the shortcomings of both capacitive and resistive touchscreens. Capacitive touchscreens are easy to operate with a minimal amount of force, which make them a good choice for elderly drivers with limited manual dexterity. However, these screens cannot be used with gloves on – they require bare skin for interaction, as the capacitance of the screen can only be altered through interaction with an external electrical conductor. Such a control

mechanism is inadequate for usage in cold climates where gloves are required for safety. Resistive touchscreens are capable of being used through gloves, but they require a greater amount of force in order to create contact between the two electrically resistive layers of the screen. This greater amount of force makes them a poor choice for elderly drivers. For this DSRC system, a keypad with mechanical switches – the ControlPad 683 (Genovation, USA) – was chosen as the input mechanism, and it is shown in Figure 4-5. The keys of the ControlPad 683 can be programmed for specific functions or commands, and this capability allows it to be used with the user interface. The keypad has dimensions of 15 cm x 9.5 cm x 3.5 cm, and as previously mentioned, it connects to the Alix 1D using the PS/2 peripheral port. The tactile feedback of the keypad makes it much more reliable than a resistive touchscreen.



Figure 4-5: Keypad for developed DSRC system

When serving as an on-board unit, the DSRC system requires feedback in order to notify the driver of certain events (a traffic jam, an incoming ambulance, etc). Additionally, entering commands into the system is easier when there is feedback in place that confirms the proper operation of the system. In order to provide this

feedback, a 5” LCD display (Accele, USA) was selected. The display connects to the Alix 1D’s SVGA port, though it requires its own dedicated power source, as the Alix 1D does not have any outputs that are capable of sourcing the 12 V and 270 mA required for operation. The maximum resolution of the display is only 640 x 480, though the user interface was designed to accommodate this.

When initially selecting RF antennas for this project, there were no 5.9 GHz DSRC antennas available, and therefore, a 5.8 GHz antenna designed for operation in the 802.11a frequency band was chosen. The 5.8 GHz antenna has a nominal gain of 3 dBi, and it connects to the DCMA-86P2 DSRC radio using a micro-miniature coaxial (MMCX) connector. Later in the project, the ECOM9-5500 antenna (Mobile Mark, USA) – an antenna designed specifically for 5.9 GHz DSRC applications – became commercially available. It was purchased to replace the 802.11a antenna due to its superior characteristics. This new antenna had a gain of 9 dBi, and a magnetic mount for easy attachment to the top of an automobile. Additionally, this antenna is weather proof, which is an important characteristic for on-board units and road-side units. A comparison between the ECOM9-5500 and the 802.11a antenna is shown in Table 4-2.

	<b>802.11a antenna</b>	<b>ECOM9-5500 antenna</b>
<b>Height</b>	15.3 cm	36 cm
<b>Gain</b>	3 dBi	9 dBi
<b>Cable Length</b>	1.52 m	3.04 m
<b>Weatherproof</b>	No	Yes

Table 4-2: Comparison of antennas

The complete DSRC system (with the 5.9 GHz antenna) is shown in Figure 4-6. Note that the Alix 1D has been placed in an enclosure (BOX 1C, PC Engines, Switzerland) for protection and ease of installation into an automobile.

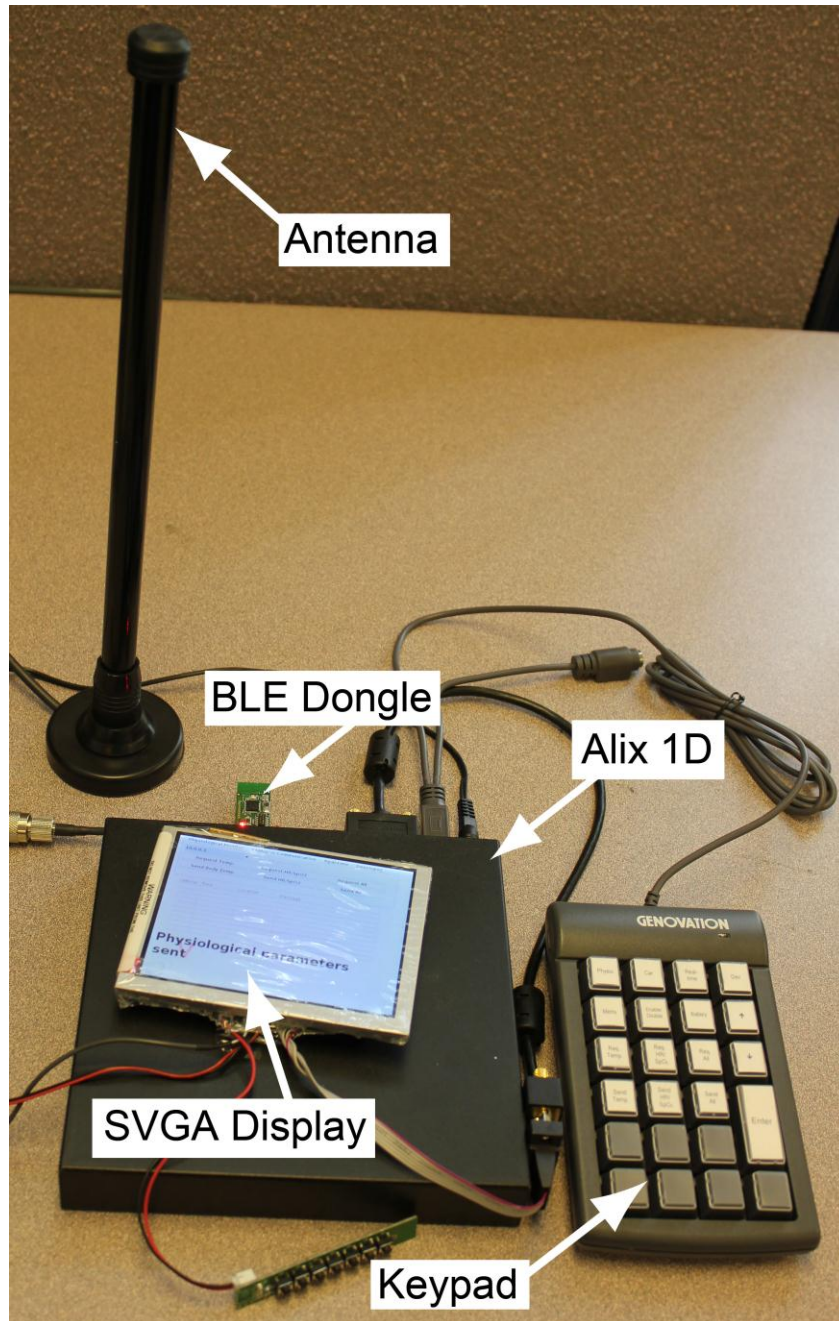


Figure 4-6: Complete DSRC system

#### 4.2.2. DSRC Radio Driver

The DCMA-86P2 DSRC radio can be purchased from the manufacturer, but there is no software driver provided to implement 802.11p functionality. Therefore, a custom software driver needed to be developed for this purpose. Fortunately,

there is an open-source Linux software driver available for several different Atheros transceivers called Ath5k. However, this Ath5k software driver was created with the intention of providing 802.11a/b/g WiFi support for Atheros chipsets. As previously discussed in Chapter 3, 802.11p DSRC does not drastically differ from 802.11a. Compared to 802.11a, DSRC operates at a higher frequency band (5.85 – 5.92 GHz as opposed to 5.170 – 5.835 GHz) and with a smaller bandwidth (10 MHz as opposed to 20 MHz). The developed DSRC software driver was based on Ath5k, though the software driver for this project was configured to meet the requirements of the 802.11p standard. The developed software driver works by adjusting the regulatory domain control implementation file within Ath5k. For example, the FCC in the United States recognizes 5.835 GHz as the maximum allowed frequency of an 802.11a wireless card, and therefore, the regulatory domain control implementation file in Ath5k sets this as the maximum frequency for US wireless cards. In order to unlock the DSRC frequency band, the regulatory domain control was adjusted to allow the AR5414 chipset to operate in the DSRC frequency range regardless of which regulatory domain the transceiver uses. It is important to note that this adjustment can only be performed on versions of the Linux kernel that are older than 2.6.28. Starting with Linux kernel 2.6.28, the Ath5k driver uses a new regulatory framework called Central Regulatory Domain Agent (CRDA) that can no longer be bypassed with this technique. Finally, the default 20 MHz bandwidth used by 802.11a/b/g was halved by manipulating the phase locked loop (PLL) control register at the PHY layer of the Ath5k driver. The DSRC driver was compiled into the Linux kernel, and this allowed Linux to operate the AR5414 in compliance with 802.11p.

Ath5k requires a Linux environment, and among the possible choices, Debian Linux 5.0.7 was chosen because of its low processor overhead and its support for various utility packages. The availability of utility packages became important when designing the user interface. Furthermore, Debian Linux 5.0.7 uses Linux kernel 2.6.26, which does not contain CRDA and therefore allows the DSRC

driver to successfully tune the radio for the required frequency band, as previously discussed.

### **4.2.3. In-car User Interface**

The Debian Linux installation serves not just as a foundation for the DSRC software driver, but also as a platform for the in-car user interface. One of the advantages of using Debian Linux is the built-in graphics support for the Alix 1D. This allows usage of the 5” LCD display discussed in Section 4.2.1 to display a graphical user interface (GUI) that the vehicle occupants can interact with. This GUI was created using the Swing Java toolkit of Eclipse. Swing is a platform-independent toolkit that installs into the Eclipse integrated development environment (IDE), and it is used to create GUIs using the Java programming language. Swing was chosen as the GUI builder for the user interface due to its low system resource requirements. As previously mentioned, the Alix 1D only has a single-core 500 MHz processor and 256 MB of RAM, and therefore Swing's lightweight resource consumption allows the user interface to achieve acceptable performance. Additionally, the Swing toolkit and the Eclipse IDE are both freely available without the need for a software license.

The in-car user interface can be seen in Figure 4-7. The button layout inside of the user interface has been designed to match the button layout on the keypad. In order to avoid clutter and to accommodate the low 640 x 480 resolution supported by the display, the user interface is organized into tabs of various categories: “Physiological Monitoring” for all non-DSRC functions pertaining to the monitor, “Vehicular Communication” for all DSRC-related tasks, “Real-time” for real-time operation of the physiological monitor (discussed further in Section 4.3.3), and “Developer” for test functions that were used during development. These tabs are activated by using the top row of buttons on the keypad, and within each tab view, the specific functions are activated by using the appropriately labeled keys on the keypad. The bottom of the user interface contains a notification area in which

crucial messages can be displayed for the vehicle occupants to read. The most recent notification is displayed in large letters for easy reading, while past notifications are displayed above the most recent notification. For example, if an ambulance is requesting physiological parameters from a specific vehicle, they would enter the “Vehicular Communication” tab, select the target vehicle from the drop-down menu, and press the “Request All” button on the keypad. This action causes the user interface to send a message over DSRC to the target vehicle, and when the target vehicle receives this message, it automatically reacts by reading the physiological parameters from the vehicle occupant’s monitor over BLE. These parameters are then transmitted back to the ambulance over DSRC. Once these parameters are received by the ambulance, the notification area is updated to display these parameters, as shown in Figure 4-7. Ideally, the user interface should be able to provide notifications to the vehicle occupants while requiring as little intervention as possible.

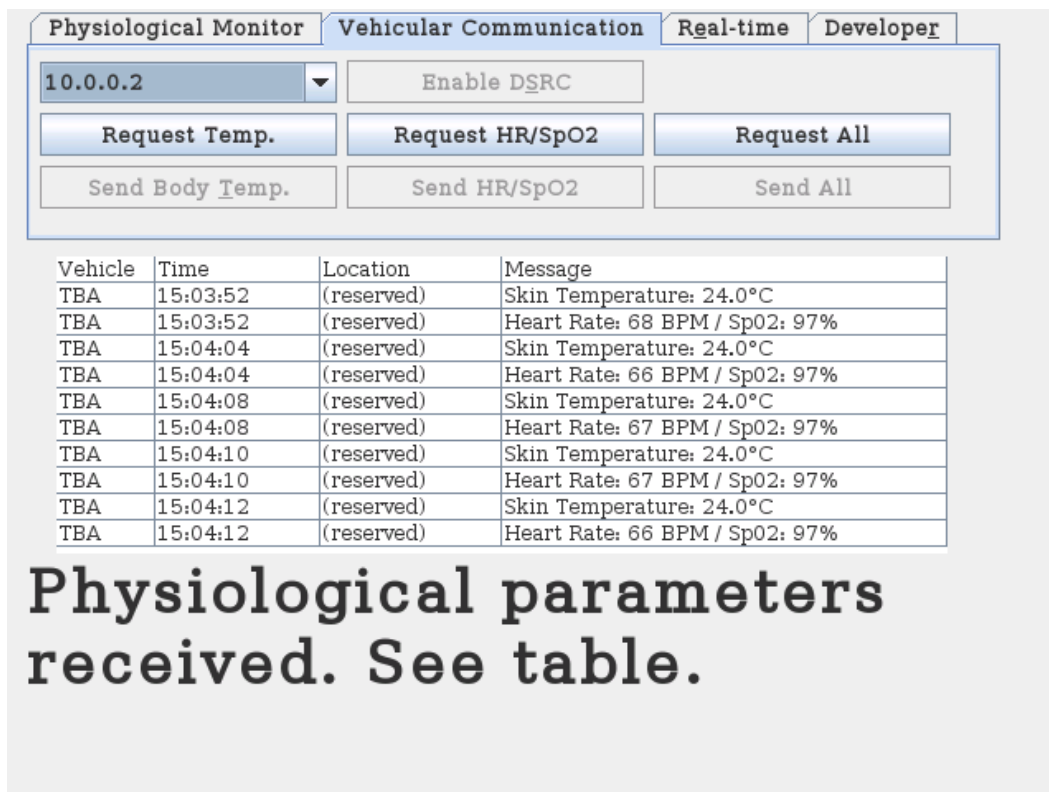


Figure 4-7: In-car user interface

Sending messages via DSRC is performed by using the IP addresses of each individual DSRC unit. In order for the user interface software to detect which vehicles are present in the vicinity, the Java program accesses Debian Linux's nmap utility via a ProcessBuilder object (ProcessBuilders are responsible for running Linux shell script within Java and returning the output of these scripts). The user interface runs nmap every thirty seconds in a dedicated thread, and whenever a new vehicle is detected in the same ad-hoc cell, its IP address is added to a drop-down menu where it can be selected using the keypad. In a practical implementation of the DSRC system, these IP addresses can be combined with license plate numbers and the location information provided via an on-board GPS. In addition to the thread running nmap, a second thread inside of the user interface constantly monitors for new DSRC messages that are received.

### 4.3. Physiological Monitoring System

Figure 4-8 shows a block diagram of the physiological monitor. Each of the individual components of the monitor will be discussed in detail in this section.

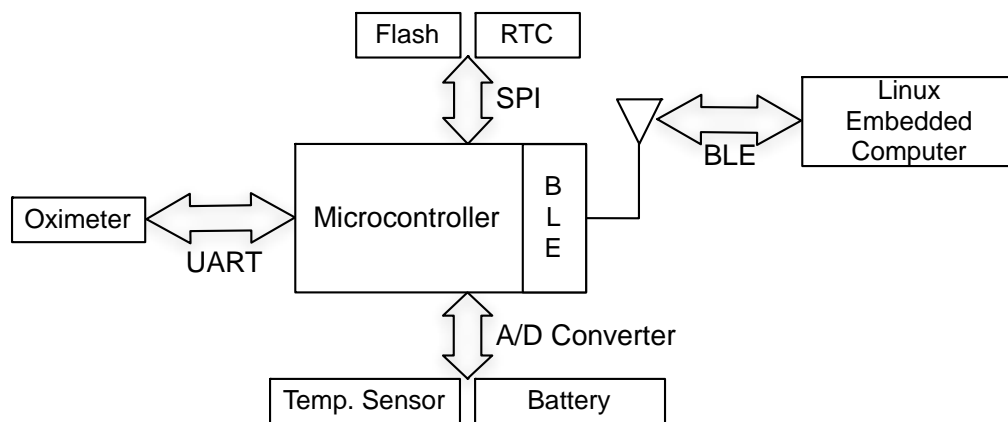


Figure 4-8: Block diagram of physiological monitor

### 4.3.1. Bluetooth Low Energy Radio

The choice of Bluetooth Low Energy radio for this project was a choice between the CC2540 (Texas Instruments, USA), and the nRF8001 (Nordic Semiconductor, Norway). A comparison of the two radios is shown in Table 4-3. From the table, the nRF8001 has smaller peak currents for transmitting and receiving BLE packets. The sleep current of the nRF8001 is higher, though this difference is negligible. Furthermore, the nRF8001 has a smaller footprint than the CC2540. However, the largest difference between the two radios is that the nRF8001 is a standalone BLE transceiver that connects to a microcontroller using the SPI interface, and the CC2540 is a System-on-a-Chip (SoC) that contains a microcontroller with an 8051 core, a BLE radio, and several peripherals. The nRF8001 is a good choice for a BLE radio if a particular design requires a specific microcontroller or peripherals that are not present in the CC2540. For instance, if a particular design requires a microcontroller with I2C capability or 32-bit numerical processing along with BLE, the nRF8001 would be the preferable radio, as the CC2540 does not have either of these features. However, CC2540 includes all of the peripherals needed for the design of the physiological monitor, and it also contains sufficient processing power. While the nRF8001 consumes less current than the CC2540 while transmitting and receiving, having a separate microcontroller interfacing with the nRF8001 would diminish any advantages in power efficiency. Additionally, having a microcontroller and a BLE radio on the same chip with the CC2540 requires less space on the printed circuit board than the two-chip solution required in the case of the nRF8001. This is an important design consideration in the physiological monitor, since it is worn on the arm, and it should therefore be small in order to minimize distraction. In order to maximize power efficiency and minimize physical board space, the CC2540 was chosen over the nRF8001 as the BLE radio for the physiological monitor.

	<b>TI CC2540</b>	<b>Nordic nRF8001</b>
<b>Voltage</b>	2 - 3.6 V	1.9 - 3.6 V
<b>TX current at 3.3 V</b>	24 mA	12.7 mA
<b>RX current at 3.3 V</b>	19.6 mA	14.6 mA
<b>Sleep current at 3.3 V</b>	0.4 $\mu$ A	0.5 $\mu$ A
<b>Type</b>	System-on-a-Chip	SPI
<b>Package</b>	QFN40	QFN32
<b>Dimensions</b>	6 mm x 6 mm	5 mm x 5 mm

Table 4-3: Comparison of Bluetooth Low Energy radios

The CC2540 contains 256 kB of on-board flash memory, which was used to store the application along with the BLE stack. Additionally, the CC2540 contains a 12-bit A/D converter with eight channels. These A/D channels were used to monitor the temperature sensor's output and the battery voltage level. The CC2540 also contains two serial peripheral ports which can either be used for SPI or UART, the latter of which is used to communicate with the OEM III pulse oximeter. Finally, the 21 general purpose I/O pins available on the SoC were sufficient for the various devices being used in the monitor.

#### 4.3.2. Sensors

It is important to choose sensors for the physiological monitoring system that provide useful information to EMS in the event of a car accident or medical emergency. Furthermore, as this system is designed primarily for elderly drivers, the physiological parameters being measured should be relevant to the elderly population.

Heart rate was chosen as a parameter to measure because it has been shown to be an important indicator for detecting life-threatening cardiovascular dysfunction following serious injuries such as those caused by car accidents [88]. Furthermore, SpO<sub>2</sub> is commonly used for monitoring critical patients, and it has been shown that oxygen saturation levels below 93% can be used as an indicator for acute heart failure [89]. Therefore, SpO<sub>2</sub> was also chosen as a parameter to

monitor with the system. In order to measure heart rate and SpO<sub>2</sub>, the PureLight 8000J Flex Sensor (NONIN, USA) was used. The sensor contains an infrared LED and a photodiode, and it is worn by the user with the LED on one side of their finger and the photodiode on the other side. When the infrared LED emits pulses of light into the finger, some of the photons from these light pulses are absorbed by the hemoglobin and some of them are received by the photodiode. The signal created from this absorption of light pulses is called a photoplethysmographic (PPG) signal, and it can be used to determine the heart rate and SpO<sub>2</sub> of the user. The Flex Sensor connects to a separate module called the OEM III (NONIN, USA), and this module is responsible for performing the signal processing of the PPG signal and calculating the heart rate and SpO<sub>2</sub>. The OEM III calculates the heart rate and SpO<sub>2</sub> using a 4-byte exponential moving average, and the calculated values – which were updated inside the OEM III on every pulse beat – were transmitted over UART once per second. It is important to note that the 1 Hz transmission rate is a limitation of the OEM III's UART interface. While logging heart rate values at a rate of 1 Hz is sufficient for some measurements (i.e. measuring long-term heart rate decrease following an accident), determining heart rate variability (HRV) requires much higher sampling rates. If HRV is being tracked as a mortality predictor following a heart attack, or if HRV is being used to detect autonomic nerve damage in a diabetes patient, a sampling rate of at least 250 Hz is required [90], [91]. This oximeter is incapable of sampling at 250 Hz, and so it is limited in the number of symptoms it can detect. The pulse oximeter system consumes 8.79 mA on a 3.3 V supply, it has a SpO<sub>2</sub> accuracy of  $\pm 3\%$  and a heart rate accuracy of  $\pm 3$  beats per minute assuming no motion and  $\pm 5$  beats per minute during motion. This oximeter system was chosen because the sensor uses a flexible form factor that allows it to be integrated into a glove. If the sensor and the connecting wire are concealed into a glove, it could be worn by the vehicle occupant without interfering with any driving tasks.

The use of the arm band to support the monitor makes body temperature sensing possible. When looking at the available temperature sensors, the AD22103 (Analog Devices, USA) is an ideal choice for a physiological monitoring application. The sensor has a small footprint of 5 mm x 4 mm and can easily be mounted on a printed circuit board. The sensor is accurate to within 1°C when operating in the range of 0°C to 100°C. Furthermore, the sensor has low current consumption of 500  $\mu$ A when using a 3.3 V supply.

### **4.3.3. Data Acquisition System**

When operating in the real-time sampling mode while connected to the developed DSRC system, the physiological monitor would not require any on-board data storage or time keeping. The Alix 1D embedded system already includes a real-time clock (RTC), and the CompactFlash card in the DSRC system provides adequate space to store all logged information. However, for instances where the monitor is being used as a standalone device, or for instances where the DSRC system is unable to log data (due to an error or other such circumstances), a 4 MB flash (M25P32, Numonyx, Switzerland) was added to the physiological monitor to log samples from the user. This flash chip has dimensions of 6 mm x 5 mm, and it consumes 8 mA, 15 mA, and 50  $\mu$ A during read, write, and standby modes, respectively. The individual data samples of the physiological monitor are 12 bytes in size (5 bytes for the time stamp, 3 bytes for the pulse oximeter, 2 bytes for temperature, and 2 bytes for the battery voltage), and therefore the 4 MB flash can sustain a maximum of 349,525 samples.

The timestamp for these samples is provided by a M41T93 real-time clock (ST Microelectronics, Switzerland). This RTC chip has dimensions of 4 mm x 4 mm, and it consumes 0.5-2 mA during operation (varies depending on read/write speed), and 6.5  $\mu$ A during standby. For instances where the monitor is being used without the DSRC system, the RTC is also capable of providing external interrupts to the CC2540 at periodic intervals in order to wake it from sleep mode.

This allows the monitor to operate in a low-power state with its radio off, thereby preserving battery power. Finally, the RTC also contains 7 bytes of volatile SRAM to be used for any purpose required by the application.

All of the individual components of the physiological monitor require a 3.3 V supply. In order to provide power to the system, a 3.7 V, 850 mAh lithium polymer battery was regulated to 3.3 V using power management circuitry. The lithium polymer battery was chosen due to its low profile, its high capacity, and its ability to be recharged using on-board charge circuitry and an AC adapter. Test results and battery life information for this battery are discussed in Section 5.5.3.

The physiological monitor and its battery were placed into an enclosure in order to protect the circuit board from damage. However, because the temperature sensor is soldered to the PCB, a medical grade silicone (Dow Corning 3140, Dow Corning, USA) was applied on top of the sensor in order to allow for conductivity between the sensor and the user's skin. The complete physiological monitoring system without the case attached is shown in Figure 4-9. The board has physical dimensions of 5.4 cm x 4.8 cm x 1.5 cm.

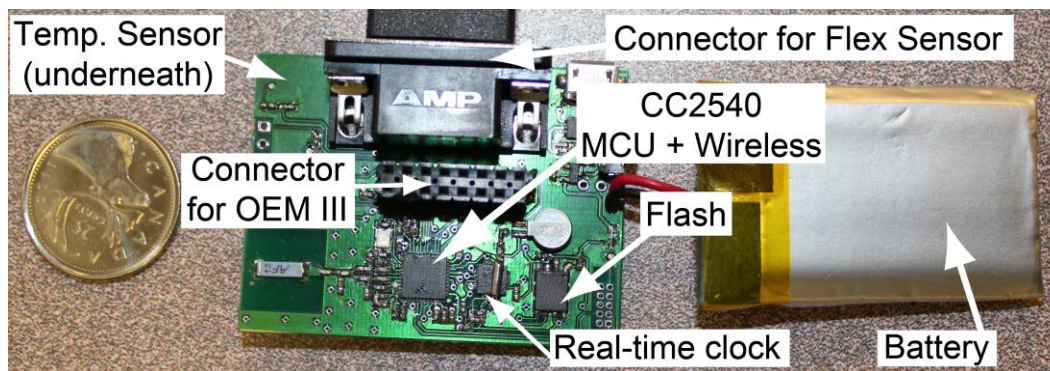


Figure 4-9: Physiological monitor PCB with battery

The physiological monitor is the slave of the BLE starbus network, and a USB dongle on the DSRC system acted as the master of the network. The USB dongle was provided by Texas Instruments, and it also uses the CC2540 for communication. The dongle is recognized by the DSRC system as a serial device,

and it communicates with the DSRC system by sending bytes that correspond to different BLE instructions (discussed in further detail in the next section). This dongle was chosen because it uses the CC2540 for BLE communication, which eliminates the possibility of any hardware incompatibilities between the physiological monitor and the USB dongle. Furthermore, the dongle is able to communicate with the Linux operating system with the proper software libraries.

#### **4.3.4. Firmware Design**

To develop a system that is BLE-compliant and able to communicate with any other BLE device, the firmware of the developed physiological monitor integrated with the Bluetooth Low Energy protocol stack. Figure 4-10 shows the task hierarchy of the Operating System Abstraction Layer (OSAL) provided by Texas Instruments. The OSAL tasks all comprise the main polling or event loop of the physiological monitor's firmware. In the OSAL, the BLE protocol stack elements run at the lower levels, and the physiological monitoring application runs at the top level. The following section explains the individual stack elements.

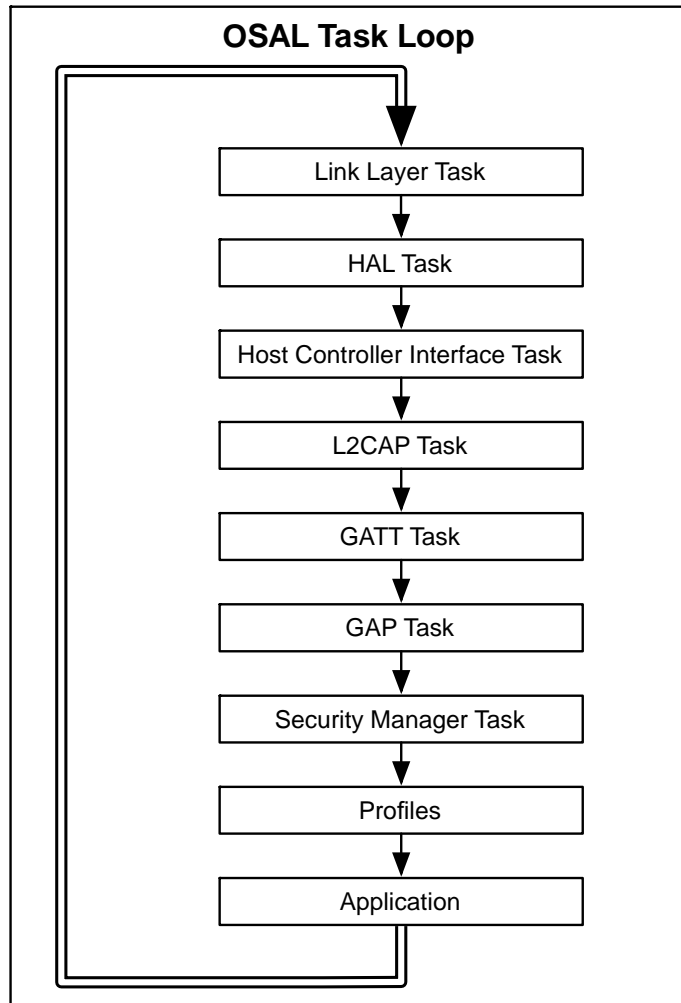


Figure 4-10: BLE stack OSAL task loop

**Link Layer:** Controls the RF state of the device: standby, advertising, scanning, initiating, or connected.

**Hardware Abstraction Layer (HAL):** Responsible for linking the firmware with the hardware of the chip, which means providing access to the chip's various peripherals (ADC, UART, SPI, etc.).

**Host Controller Interface (HCI):** Facilitates communication between the PHY layer of the radio and the higher level layers, namely the L2CAP and the profiles.

**Logical Link Control and Adaptive Protocol (L2CAP):** Provides data encapsulation for the upper layers.

**Generic Attribute Protocol (GATT):** Allows the device to communicate its attributes such as its characteristic values to another device.

**Generic Access Protocol (GAP):** Handles various tasks, including device discovery and connection events.

**Security Manager (SM):** Handles the pairing of devices, if it is enabled.

**Profiles:** Defines the application-specific GATT table, including all characteristic values. All data communication between the physiological monitor and the DSRC system is performed through reading and writing of these characteristic values.

**Application:** The developed application, which in this case is the physiological monitoring application. The application layer is discussed in further detail below.

The GATT layer of the OSAL is especially important for communication between the physiological monitor and the developed DSRC system. When data transfers between the physiological monitor and the DSRC system, the physiological monitor assumes the role of the GATT server, and the DSRC system assumes the role of the GATT client. These roles are completely independent of the master/slave relationship in the network (recall that the DSRC system is the master and the physiological monitor is the slave). Devices that are set up to act as GATT servers contain a structure called a GATT table. The GATT table contains special registers called characteristic values. The GATT server can load data into a characteristic value, which can then be read by a client device. Likewise, a client device can send information to a GATT server by writing a value into one of the server's characteristic values.

As previously mentioned, the Application layer of the OSAL in this case is the physiological monitoring application. The flowchart for the physiological monitor firmware is shown in Figure 4-11. Each of the three branches of the flowchart will be discussed in further detail below.

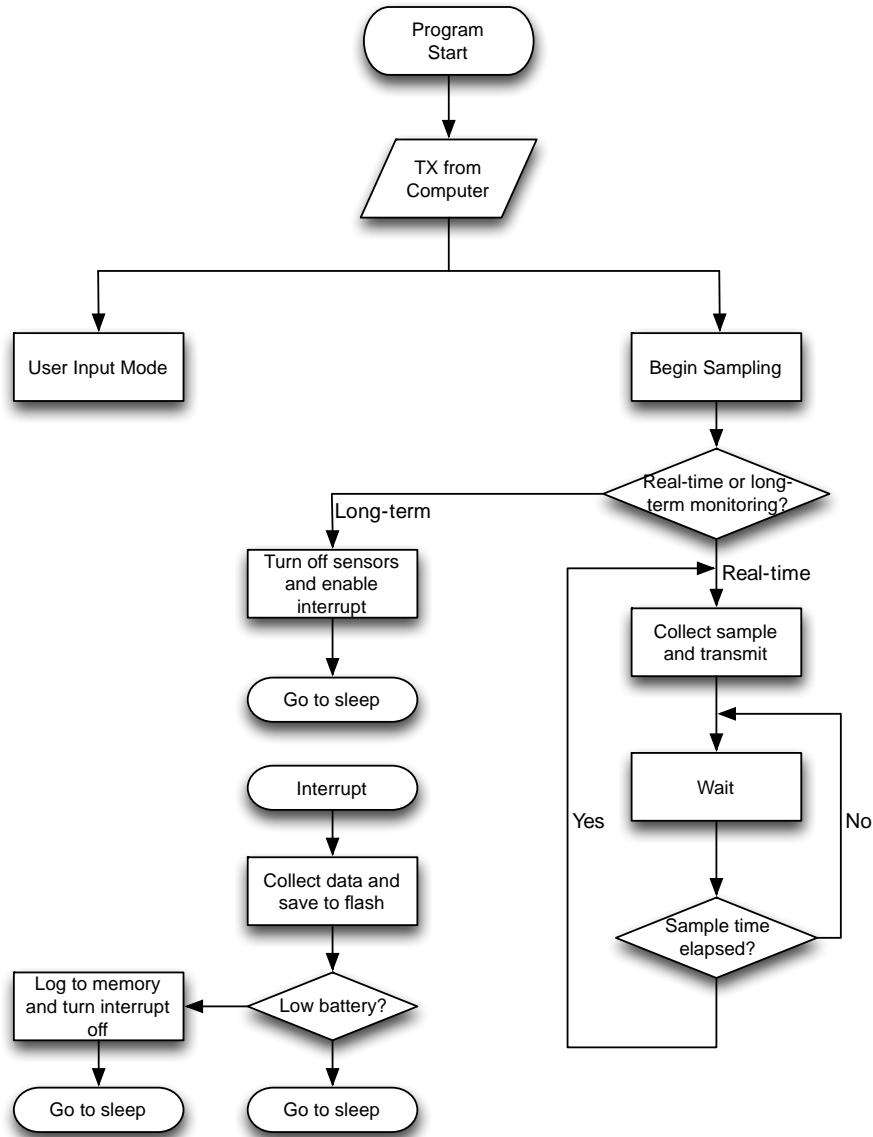


Figure 4-11: Physiological monitor application layer

When the monitor establishes a connection with the DSRC system, the device begins in user input mode, where the DSRC system can request certain pieces of data from the monitor, including (but not limited to) the heart rate and SpO<sub>2</sub> values, the body temperature, the battery voltage, or error flags. When real-time sampling mode is initiated by the in-car user interface, the monitor enters a loop where it retrieves and sends the physiological parameters of the vehicle occupant over BLE at a rate of one sample per second. This sample rate is adjustable, but it

is limited by the pulse oximetry module, which cannot retrieve heart rate and SpO<sub>2</sub> data faster than once per second. In this mode, the monitor sends the requested data continuously, thereby ensuring that the DSRC user interface is always updated with the most recent physiological data, which saves time in the event that an EMS vehicle requests this data. The third mode of operation in the Application layer is the long-term sampling mode, in which the monitor breaks the BLE connection to the DSRC system, turns off all of its sensors, and goes into a low power mode. At periodic intervals that are adjustable while in user input mode, the RTC wakes up the processor, the processor collects samples from all of the physiological sensors, stores the combined sample in the flash memory, and then the monitor goes back into the low-power mode. The monitor also checks the voltage level of the battery when it receives an interrupt, and if the battery voltage is below a threshold voltage (3.5 V), the monitor stores a low battery message into the flash before transitioning into a deep sleep that can only be woken up with a hardware reset. This battery check is only used in long-term sampling mode, because a loss of power while writing to the flash memory could potentially damage the flash. When the monitor is operating in the real-time mode (where the flash memory is never used), the system shuts off at the battery's discharge cutoff voltage of 2.75 V. The long-term sampling mode is designed for acquiring data over a large period of time, and is not used in conjunction with the DSRC system. However, this long-term sampling mode allows the physiological monitor to be used as a standalone device if the user is out of their vehicle but still needs to have their physiological parameters monitored.

#### **4.4. Integrated System**

One of the key challenges in implementing Bluetooth Low Energy on the developed DSRC system was getting the CC2540 BLE dongle to work with the Debian Linux operating system. The BLE dongle manufacturer (Texas Instruments) only supports Windows-based operating systems. Therefore, in order to make the Java user interface communicate with the BLE dongle, the open

source RXTX Java library was used with Linux's Java Runtime Environment (JRE). The RXTX library contains functions for sending and receiving commands to and from a serial device such as the BLE dongle (a serial device is a device that is recognized by the operating system as a serial port). However, Texas Instruments' BLE dongle uses serial port `/dev/ttyACM0` or greater on a Linux machine, and this is not a serial port that is supported by default in RXTX. Therefore, in order to communicate with the BLE dongle in Java, it was necessary to modify the source code of the RXTX library by adding in support for this serial port. After this, the new library files were recompiled and installed into the JRE. This modified RXTX library allowed full control of the BLE dongle inside of the DSRC Java user interface. Texas Instruments provided documentation that discusses how to use serial commands in order to communicate directly with the HCI layer of the BLE stack, and the commands from that documentation were used with the RXTX library's functions to implement all of the communication between the user interface and the physiological monitor. Inside the user interface software, the BLE receiver operates in its own dedicated thread where it constantly checks the serial port for new messages from the BLE dongle and takes the appropriate actions when new messages are received.

As discussed in Section 4.3.4, the physiological monitor primarily works with the DSRC system by using the real-time sampling mode. In this mode, the monitor checks the parameters of the vehicle occupant every second (the sampling rate is limited by the OEM III pulse oximeter, as discussed in Section 4.3.4) and transmits this information to the DSRC system. When the system receives a new BLE data packet from the physiological monitor, it puts a timestamp on that sample and stores it into a log file. In addition to this, it also displays the most recent physiological parameters of the driver in the "Real-time" tab of the user interface. Inside the "Vehicular Communication" tab of the interface, the vehicle's driver or passenger can send the most recent physiological parameters to a vehicle using the "Send All" button. If the most recent parameters in the user interface are more than one second old, the interface requests new data from the

monitor over BLE before communicating with the recipient vehicle over DSRC. Additionally, the vehicle's driver or passenger is able to request physiological parameters from a target vehicle by pressing the "Request All" button. For testing purposes, the requesting of physiological parameters currently works with any vehicle.

## **CHAPTER 5: SYSTEM VALIDATION AND RESULTS<sup>1</sup>**

To evaluate the functionality and performance of the developed DSRC system and the physiological monitor, laboratory and road tests have been performed. For the DSRC system, compliance with the IEEE 802.11p standard had to be validated, and the latency and packet loss of the system had to be measured in indoor, vehicle-to-vehicle (V2V), and vehicle-to-infrastructure (V2I) settings. For the physiological monitor, the temperature sensor, pulse oximeter, Bluetooth Low Energy (BLE) radio, battery life, and long-term data acquisition needed to be tested. Finally, the integrated system needed to be evaluated in a V2V setting to determine if DSRC could be used to transmit physiological parameters with an acceptable rate of success. This chapter describes the tests used to evaluate the individual systems and the integrated system. After this, results for each of the tests are presented.

### **5.1. DSRC System Test Methods**

#### **5.1.1. DSRC Frequency Spectrum Test**

To verify that the DSRC radio is compliant with the IEEE 802.11p specifications, a spectrum analysis of the transmitted DSRC signal was performed. A Spectran HF-6065 (Aaronia, Germany) spectrum analyzer was used to determine if the developed DSRC system could communicate within the frequency range of 5.86 – 5.92 GHz with a signal bandwidth of 10 MHz. The spectrum analyzer was also used to determine if the DSRC system was capable of adjusting its transmission power. The DSRC antenna and the spectrum analyzer antenna were placed approximately 5 cm away from each other, as shown in Figure 5-1. The antennas were placed close to each other to maximize the clarity of the received signal. At transmission powers of 1 dBm, 12 dBm, and 24 dBm, the DSRC system was configured to send 64-byte packets to another system at a rate of approximately

---

<sup>1</sup> Material in this chapter has been presented at the *AUTO 21 Annual Conference 2012*

400 Hz using Linux's built-in ping command. These ping messages were sent for approximately ten minutes while the spectrum analyzer repeatedly performed sweeps across a 25 MHz span. All of the spectrum analyzer's sweeps during the ten-minute period were averaged together to form an image of the transmitted signal's frequency spectrum. This test was conducted at the DSRC frequencies of 5.86 GHz, 5.90 GHz, and 5.92 GHz.

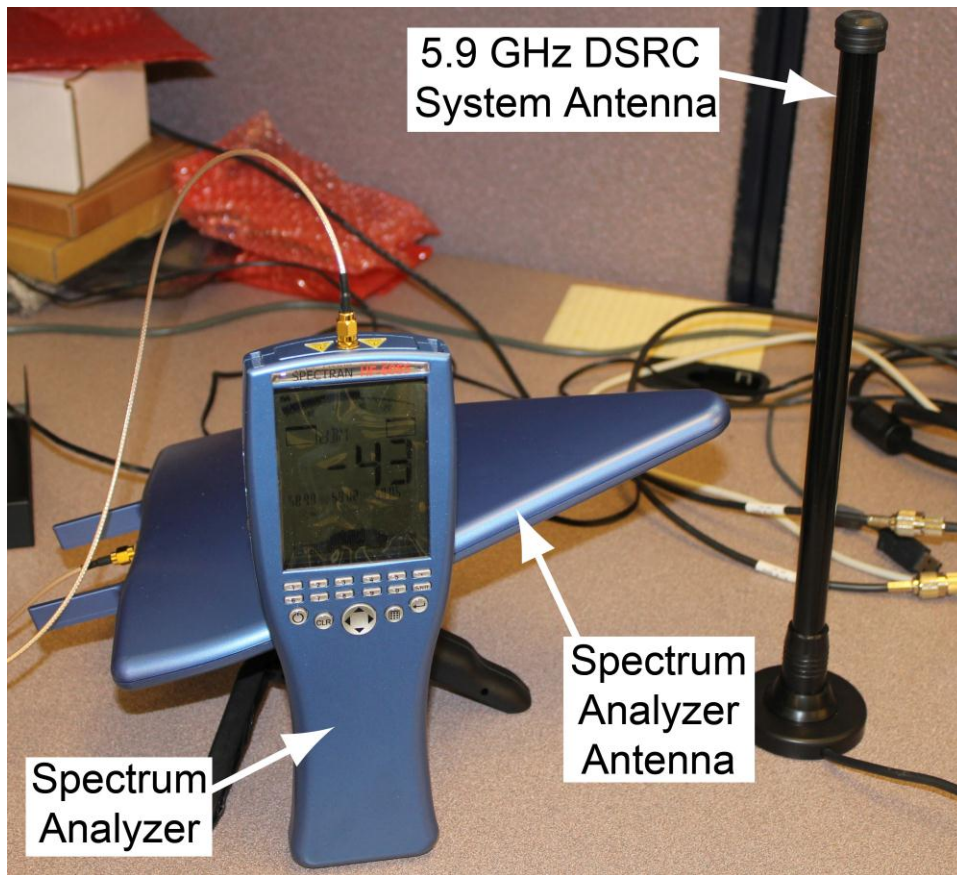


Figure 5-1: Spectrum analyzer test setup for DSRC system

### 5.1.2. Indoor Test

To determine the latency and packet loss of the DSRC system in a stationary, short range setting, an indoor test was performed in a laboratory environment. In this test, two DSRC systems with the 5.9 GHz antennas were placed approximately 20 m apart. The radios in both systems were tuned to a center

frequency of 5.9 GHz. The antennas of the two systems had line-of-sight with each other, but there were metal filing cabinets along the path. In Part A of the test, 10,000 64-byte packets were sent from one system to the other at a rate of approximately 400 Hz using the ping command. Once all 10,000 packets were sent, the Linux terminal reported the average communication latency, and this value was recorded. Note that “latency” in this test (and all other latency tests discussed in this chapter) refers to the length of time for the packet to be sent plus the length of time for the acknowledgement to be received. In Part B of the test, Linux’s iperf command was used to send approximately 2,500 1.4 kilobyte packets at a rate of 1 Mbps from one DSRC system to the other, and the number of lost packets was recorded. The iperf command provides a much more realistic indication of packet loss than the ping command, since iperf uses UDP packets, which do not incorporate the retry mechanism of the Internet Control Message Protocol (ICMP) packet type used by ping. Part A and B were run three time each, and both parts were run at 10 MHz and 20 MHz bandwidths to observe how DSRC’s narrow channel bandwidth impacted the performance of the connection.

### **5.1.3. Vehicle-to-Vehicle Tests**

The performance of the system in a moving vehicular environment was measured in two separate V2V tests. The first V2V test used the 5.8 GHz 802.11a antennas and a 20 MHz channel bandwidth and the second test used the 5.9 GHz DSRC antennas and a 10 MHz channel bandwidth.

#### Test 1: V2V with 5.8 GHz antennas, 20 MHz bandwidth

The purpose of this test was to determine the average latency of DSRC communication in a V2V setting with 20 MHz bandwidth, to see how the latency is affected by movement. Additionally, the test was also used to determine the range where ping messages stop being acknowledged between vehicles, which would provide an indication of the system’s range capabilities. This test used the

5.8 GHz antenna because they were the first available; the 5.9 GHz antennas were not commercially available at the time of testing. DSRC systems were placed into two vehicles with the antennas attached to the roof, and both systems were tuned to a center frequency of 5.9 GHz. In Part A of the test, the two vehicles drove together in an environment with buildings and parked cars on either side of the road, as shown in Figure 5-2. The vehicles were separated by a distance between 100-150 m, and they were travelling at approximately 60 km/h. While the vehicles were driving, the trailing vehicle sent 64-byte packets to the leading vehicle using the ping command at a rate of approximately 400 Hz, and the average communication latency was recorded. Part A of the test was performed twice, though the environment was slightly different in each trial. In Part B of the test, one vehicle drove away from a stationary vehicle, and the moving vehicle sent ping messages to the stationary vehicle. The passenger in the moving vehicle recorded the vehicle's location when it stopped receiving acknowledgements, and this location was used to determine the maximum transmission distance. Part B of the test was also performed twice.

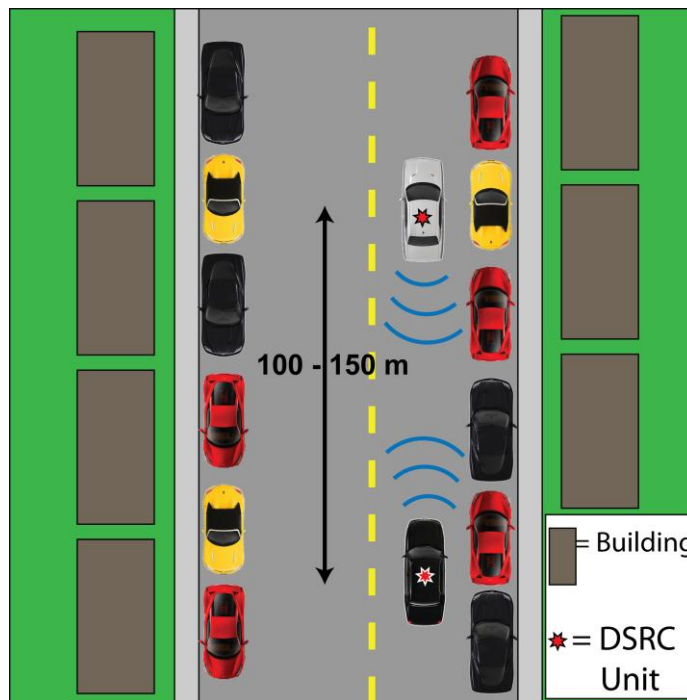


Figure 5-2: Environment for V2V Test 1, Part A

#### Test 2: V2V with 5.9 GHz antennas, 10 MHz bandwidth

This test was conducted in order to determine how the latency in a channel with 10 MHz of bandwidth is affected by movement in a vehicular environment. At the time of testing, the 5.9 GHz antennas were commercially available, and were therefore used instead of the 5.8 GHz antennas. In this test, two vehicles travelled together on a road that is approximately 740 m long, and they maintained a speed of approximately 60 km/h. Buildings were on both sides of the road, but there were no cars parked on the road until the final 100 m. In Part A of the test, the trailing vehicle sent 64-byte ping messages to the leading vehicle at a rate of 100 Hz, and the average latency was recorded. Part A was performed three times, though trials 1 and 2 had a vehicle separation of 50-100 m, and trial 3 had a separation of 100-150 m. In Part B of the test, the iperf command was used to measure the packet loss when the trailing vehicle sent approximately 2,500 UDP packets to the leading vehicle at a data rate of 1 Mbps. Part B was repeated four times, though trials 1 and 2 had a vehicle separation of 50-100 m and trials 3 and 4 had a vehicle separation of 100-150 m.

#### **5.1.4. Vehicle-to-Infrastructure Tests**

Three tests were used to validate the communication in a V2I configuration. The first test used the 5.8 GHz 802.11a antennas and a 20 MHz channel bandwidth, the second test used the 5.9 GHz DSRC antennas and a 20 MHz channel bandwidth, and the third test used the 5.9 GHz DSRC antennas and a 10 MHz channel bandwidth.

#### Test 1: V2I with 5.8 GHz antennas, 20 MHz bandwidth

The purpose of this test was to determine the latency of V2I communication with a 20 MHz bandwidth and the maximum range of V2I communication with the 802.11a antennas. In this test, one DSRC system was installed in a vehicle with

the antenna mounted on the roof and the other DSRC system was installed on the side of the road with the antenna raised 2.3 m above the ground. The center frequency of both DSRC systems was tuned to 5.9 GHz. The environment for this V2I test is shown in Figure 5-3. Note that in this test, the vehicle drove in two different directions (eastbound and northbound) to observe how the environment changed the latency and range. These directions are shown in Figure 5-3 as separate vehicles, though there was only one vehicle used for this test. The vehicle drove away from the infrastructure unit while sending 64-byte ping messages at a rate of approximately 400 Hz. The maximum transmission distance was recorded, as was the average latency of the ping messages. This test was performed three times – once in the eastbound direction of Figure 5-3 and twice in the northbound direction.

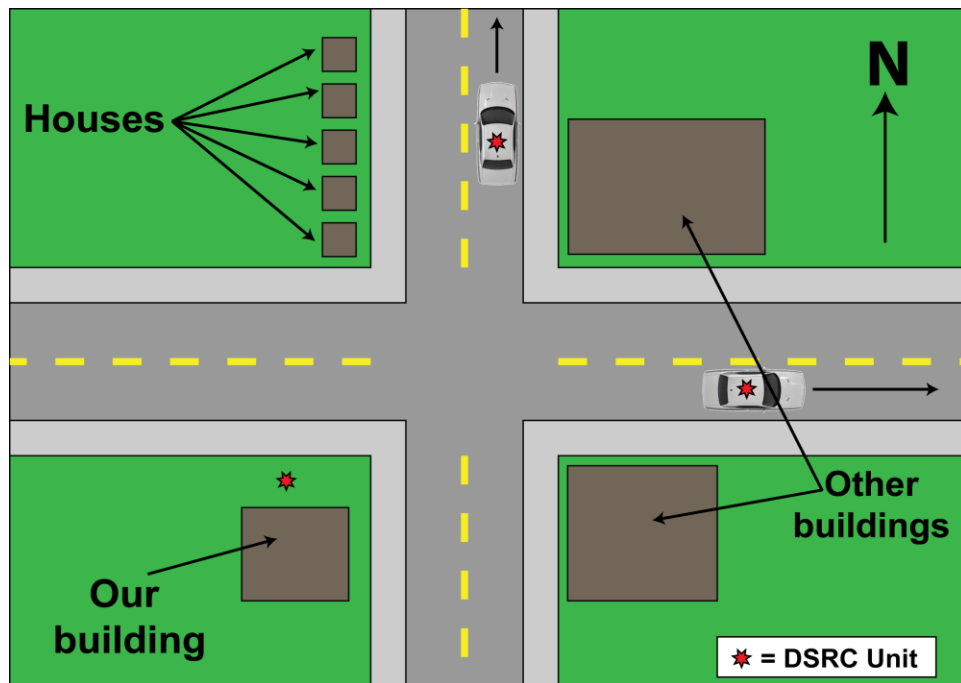


Figure 5-3: Environment for V2I Test 1

Test 2: V2I with 5.9 GHz antennas, 20 MHz bandwidth

In order to determine how the 5.9 GHz DSRC antennas improve the communication range when compared to the 802.11a 5.8 GHz antennas, another

V2I test was performed. One DSRC system was installed into a vehicle and the other DSRC system was at the side of the road with the antenna approximately 1.87 m above the ground. Similar to the previous test, the vehicle sent ping messages to the infrastructure unit at a rate of approximately 400 Hz while driving away, and the maximum transmission distance was recorded in two environments – the same northbound environment shown in Figure 5-3, and a different road with a longer line-of-sight between the vehicle and infrastructure. Each direction was performed twice.

### Test 3: V2I with 5.9 GHz antennas, 10 MHz bandwidth

V2I Test 3 observed the performance of the DSRC connection at long distances under stationary conditions. The vehicle and infrastructure DSRC systems both had 5.9 GHz antennas, 10 MHz channel bandwidths, and a 5.9 GHz center frequency, and the test was carried out in a setting with a continuous line-of-sight from the infrastructure unit to the vehicle. The infrastructure antenna was placed at a height of 0.66 m from the ground. The environment used in Test 3 had a clear line of sight between the vehicle and infrastructure for over 250 m, and therefore antenna height was not considered to be an important factor in this test (i.e. there was no shadowing to overcome), hence the low infrastructure antenna height that was chosen. In Part A of the test, 2,000 64 byte ping messages were sent from the vehicle to the infrastructure at a rate of 100 Hz at set distances: 5 m, 48 m, 96 m, 145 m, and 194 m. These distances were marked by street lamps along the side of the road, i.e. the first lamp was 5 m away from the infrastructure unit, the next lamp was 48 m away, and so forth. At each distance, the average latency of the ping messages was recorded. This test was performed six times. In Part B of the test, the iperf command in Linux was used to send packets at a data rate of 1 Mbps to determine the packet loss at the same distances as Part A. This test was performed three times.

## **5.2. Physiological Monitor Test Methods**

### **5.2.1. Skin Temperature Test**

The accuracy and thermal response of the temperature sensor was tested by comparison with the thermocouple attachment of a Fluke 179 multimeter. This thermocouple had an accuracy of  $\pm 1\%$  of the measurement reading and its resolution was  $0.1^{\circ}\text{C}$  in the temperature range of  $-40^{\circ}\text{C}$  to  $400^{\circ}\text{C}$ . The first temperature test compared the sensor and thermocouple under a heat lamp, and the second temperature test compared the sensor and thermocouple on a volunteer's arm.

#### Test 1: Physiological monitor and thermocouple under heat lamp

The purpose of this test was to evaluate the thermal response of the temperature sensor under heating and cooling conditions. The temperature sensor and thermocouple were both placed 10 cm underneath a lamp and the temperature was increased from room temperature ( $24^{\circ}\text{C}$ ) to approximately  $42^{\circ}\text{C}$ . The lamp was then turned off and both sensors were allowed to cool down to approximately  $27^{\circ}\text{C}$ . Temperature measurements for the thermocouple and the physiological monitor were taken every twenty seconds for twenty minutes (a total of 60 samples). The temperature range was chosen because it was similar to a typical range of body temperature.

#### Test 2: Physiological monitor and thermocouple on arm

The heat transfer from direct contact with skin differs compared to the heat transfer from radiation, and therefore a second temperature test was performed to evaluate the accuracy and thermal response of the physiological monitor's temperature sensor on skin. The physiological monitor and the thermocouple were placed on a volunteer's forearm until both sensors' temperatures stabilized. The

sensors were then removed, and temperature measurements were taken every twenty seconds for twenty minutes (a total of 61 samples). This test was performed twice, with trials being separated by a two-hour gap. This gap allowed the temperature sensor and the thermocouple to completely cool down and return to the ambient temperature, thereby ensuring that the trials were independent from one another. The temperature data from the two trials were averaged together for each time instance, and this data was observed in order to evaluate the thermal response of the temperature sensor.

### **5.2.2. Heart Rate and SpO<sub>2</sub> Test**

The objective of this test was to evaluate the accuracy of the physiological monitor's pulse oximeter by comparing it to the manufacturer's evaluation board. A volunteer wore two flex sensors simultaneously – one on the left index finger and one on the left middle finger. One sensor was connected to the physiological monitor, and the other was connected to the evaluation board. The two systems recorded heart rate and SpO<sub>2</sub> data every second for approximately six minutes (a total of 370 samples). The volunteer was sitting still for the duration of the test.

### **5.2.3. Current Consumption Test**

The current consumption test was performed to determine the battery life of the proposed lithium polymer battery based on the current consumption of the monitor and the specification ratings of the battery (3.7 V operating voltage, 850 mAh capacity). A Fluke 867B multimeter was used to measure the current consumption of the physiological monitor during the real-time and long-term sampling modes of operation. A laboratory power supply was adjusted for an output voltage of 3.7 V in order to simulate the selected battery.

#### **5.2.4. Bluetooth Low Energy Frequency Spectrum Test**

The purpose of the BLE spectrum analysis was to evaluate the RF performance of the physiological monitor's Bluetooth Low Energy radio at different transmission powers. The Spectran HF-6065 spectrum analyzer was used with the antenna placed approximately 5 cm away from the physiological monitor. The BLE radio of the physiological monitor was configured to continuously transmit a modulated signal at 2446 MHz (BLE channel 20). The analyzer performed approximately twenty sweeps across an 8 MHz span, and these sweeps were averaged together to produce an image of the transmitted signal's frequency spectrum. This test was performed at transmission powers of  $-6$  dBm, 0 dBm, and 4 dBm.

#### **5.2.5. Bluetooth Low Energy Range Test**

In order to evaluate the BLE radio's transmission distance, a range test was performed in a laboratory environment. The physiological monitor established a connection with a BLE USB dongle that was connected to a Windows computer. The physiological monitor was configured to transmit 100 packets of data (23 bytes per packet) to the BLE dongle at a transmission rate of 20 Hz. An application on the Windows computer was configured to count the number of packets successfully received by the BLE dongle. These packets were sent at set distances of 0 m (i.e. The physiological monitor and the BLE dongle were beside each other), 2 m, 4 m, 6 m, and 8 m. In each instance, the number of lost packets out of the 100 transmitted packets was recorded.

#### **5.2.6. Long-Term Sampling Test**

Once the individual subsystems of the monitor were tested, long-term sampling trials were conducted in order to evaluate the performance of the monitor while operating in the low-power mode. Four healthy subjects (male) with ages between 23 and 31 years wore the monitor on their arm and the pulse oximeter on their

index finger for three to five hours. None of the subjects performed any strenuous activities during the periods, and they were either working at a computer in a sitting position or walking outside the laboratory for leisure. The monitor collected physiological data every minute and the data was downloaded for analysis. Figure 5-4 shows the physiological monitor when being worn by one of the subjects.

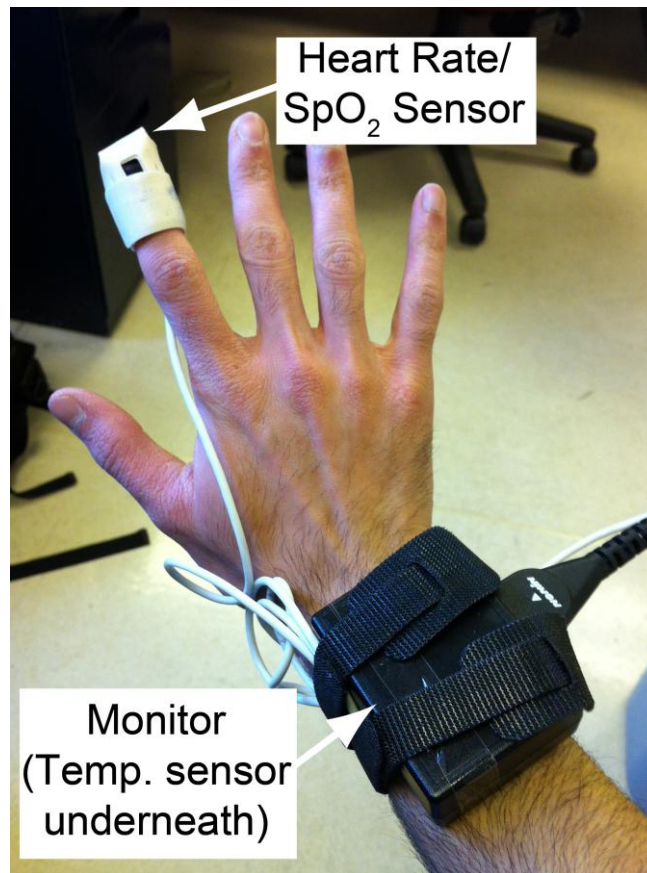


Figure 5-4: Physiological monitor on volunteer

### 5.3. Integrated System Test Methods

The purpose of this test was to determine if physiological data can be retrieved through DSRC, and to determine the reliability of the combined DSRC and physiological monitoring system. DSRC systems were installed into two vehicles, and the user interface discussed in Section 4.2.3 was installed on both. The DSRC

systems both used 5.9 GHz antennas, 10 MHz channel bandwidths, and center frequencies of 5.9 GHz. In the leading vehicle, a volunteer wore a pulse oximeter connected to the physiological monitor. The physiological monitor was not worn on the volunteer's wrist for the majority of the test, but it was instead placed on the car seat. The physiological monitor was communicating with the DSRC system using the Bluetooth Low Energy protocol, and real-time sampling was used to transmit sensor data to the in-car user interface once per second. The trailing vehicle drove approximately 50-100 m away from the leading vehicle, with both vehicles travelling between 30-60 km/h, depending on the speed limits of particular roads. The passenger in the trailing vehicle repeatedly requested the sensor data from the leading vehicle, and this sensor data was recorded. Additionally, if the interface failed to return any sensor data, or if the sensors returned invalid data, these instances were recorded as well. This test was performed three times, with trials 1 and 2 spanning a distance of 1,740 m each and trial 3 spanning a distance of 2,070 m. Trial 1 had 16 data requests, trial 2 had 19 data requests, and trial 3 had 25 data requests.

## **5.4. DSRC System Test Results**

### **5.4.1. DSRC Frequency Spectrum Test Results**

The frequency spectra of the DSRC system at center frequencies of 5.86 GHz, 5.90 GHz, and 5.92 GHz are shown in Figure 5-5, Figure 5-6, and Figure 5-7, respectively. In all three cases, the spectrum confirmed that the DSRC software can retune the center frequency with 10 MHz of signal bandwidth. Furthermore, the spectra have confirmed that the software driver is capable of adjusting the transmission power of the DSRC radio. Each of the measured signals exhibit a -3 dBm bandwidth (in which the signal's power is halved) that is within the 10 MHz bandwidth allocated for the channel.

Figure 5-5, Figure 5-6, and Figure 5-7 also include the Class C FCC spectral mask, which is the FCC’s requirement for limiting the out-of-band interference of a DSRC transmitter (only the highest Tx powers are shown, but similar trends exist for the lower powers) [75]. At all three center frequencies, it is apparent that the DSRC radio does not filter the out-of-band energy to the extent required by the FCC’s requirement. This is likely a consequence of the DCMA-86P2’s Tx filter, which may not have been designed and tested specifically for the FCC’s requirement. If this system is to be used in the United States, additional Tx filtering or a different radio built to FCC specifications will be required.

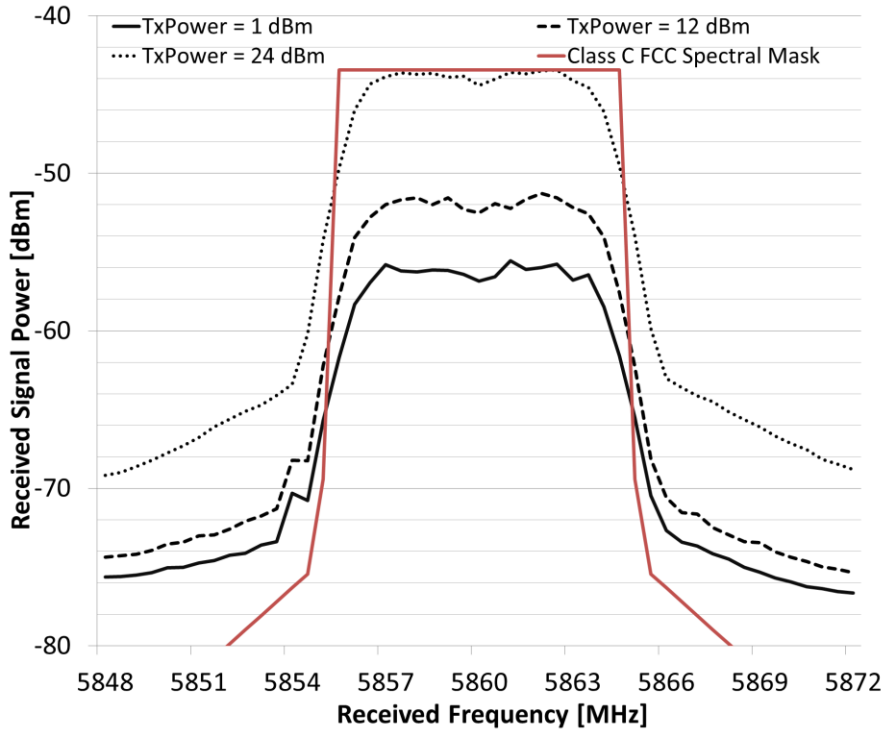


Figure 5-5: Frequency spectrum of DSRC radio at 5.86 GHz

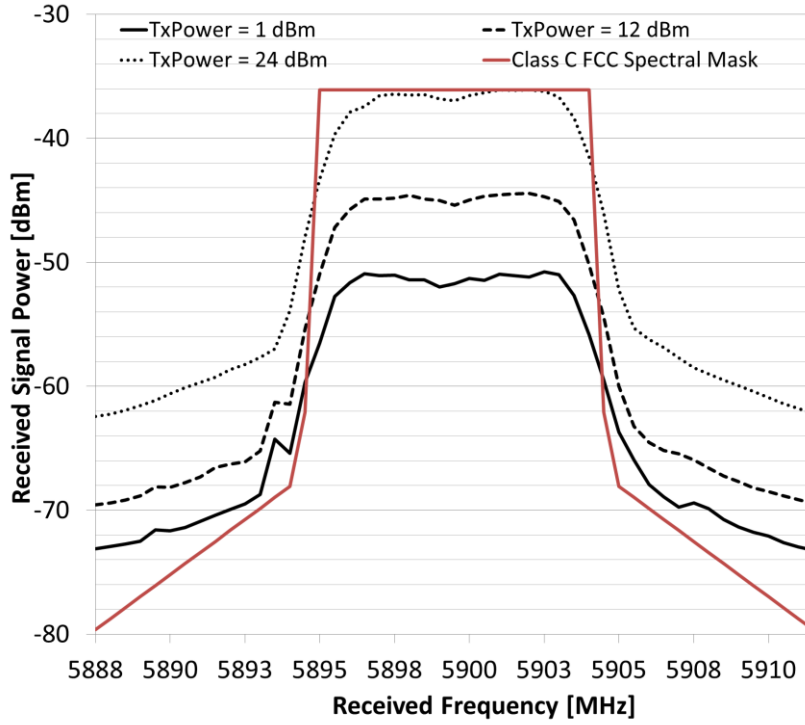


Figure 5-6: Frequency spectrum of DSRC radio at 5.90 GHz

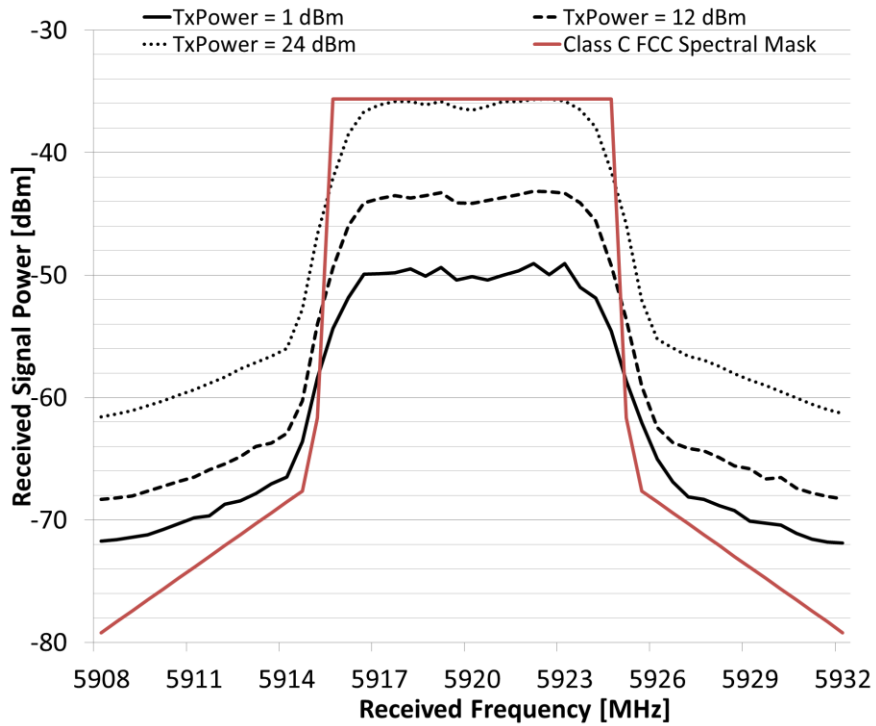


Figure 5-7: Frequency spectrum of DSRC radio at 5.92 GHz

At each transmission power and each center frequency tested, the received signal powers are shown in Table 5-1. From these results, the radio exhibits superior performance at the higher frequencies, particularly at TxPower = 24 dBm, where the 5.92 GHz spectrum is 7.9 dBm stronger than the 5.86 GHz spectrum. This could be caused by the Rx filter in the radio favouring higher frequencies over lower frequencies, thereby resulting in some attenuation of the transmitted signal in the 5.86 GHz case. Furthermore, the spectrum analyzer used in this test has a measurement error of  $\pm 3$  dBm, which possibly contributes to the differences in received signal power at different center frequencies.

	<b>5.86 GHz</b>	<b>5.90 GHz</b>	<b>5.92 GHz</b>
<b>TxPower = 1 dBm</b>	-56.9 dBm	-51.9 dBm	-50.1 dBm
<b>TxPower = 12 dBm</b>	-52.9 dBm	-45.3 dBm	-44.2 dBm
<b>TxPower = 24 dBm</b>	-44.4 dBm	-37.0 dBm	-36.5 dBm

Table 5-1: Received signal power for DSRC spectrum analysis

#### 5.4.2. Indoor Test Results

The Part A latency test results for both the 10 MHz and 20 MHz bandwidths are shown in Table 5-2. Across trials 1, 2, and 3, the DSRC systems had an average latency of  $1.147 \pm 0.0015$  ms at 10 MHz bandwidth and  $0.587 \pm 0.002$  ms at 20 MHz bandwidth. Narrowing the channel bandwidth to 10 MHz has caused the latency of packets to be approximately doubled, thereby halving the throughput of the system, as trials 1, 2, and 3 of both tests involved 64-byte packets transmitted at a rate of approximately 400 Hz.

	<b>Trial 1</b>	<b>Trial 2</b>	<b>Trial 3</b>	<b>Average <math>\pm</math> SD</b>
<b>10 MHz bandwidth</b>	1.164 ms	1.137 ms	1.140 ms	$1.147 \pm 0.015$ ms
<b>20 MHz bandwidth</b>	0.586 ms	0.589 ms	0.586 ms	$0.587 \pm 0.002$ ms

Table 5-2: Recorded latencies for indoor test

For the packet loss test in Part B, a combined 7,655 packets were sent across all three 10 MHz bandwidth trials and 7,657 packets were sent in the 20 MHz bandwidth trials, and there were no lost packets at either bandwidth configuration.

### **5.4.3. Vehicle-to-Vehicle Test Results**

#### Test 1: V2V with 5.8 GHz antennas, 20 MHz bandwidth

In Part A of the test (with two vehicles travelling together), the trailing vehicle sent a total of 275,787 packets, and it received acknowledgements for 275,710 of those packets. The average latency of these packets was 0.658 ms, which is 71  $\mu$ s longer than the 0.587 ms average latency from the indoor tests, representing a performance degradation of 12.1%. Possible reasons for this latency increase include the greater separation between vehicles, the speed of the vehicles (which results in faster channel fading and lower channel capacity due to higher Doppler spreads), and the reflections caused by other cars and buildings in the vicinity. In Part B of the test (with one vehicle driving away from the other), the moving vehicle drove 230 m away from the resting vehicle in both trials before the pings stopped being acknowledged. At this distance, the moving vehicle had already lost line-of-sight with the resting vehicle.

#### Test 2: V2V with 5.9 GHz antennas, 10 MHz bandwidth

In Part A of the test, the trailing vehicle recorded the average latencies in trials 1, 2, and 3. These results along with comparisons to the indoor test results are shown in Table 5-3. In trials 1 and 2, with the vehicle separation between 50-100 m, the average latency increased by approximately the same amount of time recorded in Part 1 when 20 MHz of bandwidth was used. However, this represents a smaller percentage of the overall latency, due to the increased latency in the 10 MHz bandwidth. With the vehicles separated by 100-150 m in trial 3, the latency experienced a very large increase, and some of the ping messages sent by the

trailing vehicle were never acknowledged by the leading vehicle. At a sufficiently large distance and speed, it appears that DSRC experiences significant performance degradation over the stationary case.

	<b>Trial 1</b>	<b>Trial 2</b>	<b>Trial 3</b>
<b>Received packets/Sent packets</b>	3972/3972	4672/4672	3851/3875
<b>Average latency (ms)</b>	1.225	1.231	1.947
<b>Increase over indoor test (μs)</b>	78	84	800
<b>Increase over indoor test (%)</b>	6.8	7.3	69.7

Table 5-3: Latency test results for V2V Test 2, Part A

In Part B of Test 2, when testing packet loss with a 50-100 m vehicle separation, there were 2 lost packets out of 2,552 (.078% packet loss) in trial 1 and 1 lost packet out of 2,553 (.039% packet loss) in trial 2. These results are essentially identical to the indoor test. However, when the vehicles were separated by 100-150 m for trial 3, the iperf utility inside Linux returned a time-out error due to missing ten packets in a row (iperf does not return any packet loss data if it exits due to a time-out error). When this was repeated in trial 4, there were 21 lost packets out of 2,557 (0.82% packet loss). Similar to the latency, the packet loss increased significantly when the vehicle separation increased, and based on the time-out error in trial 3, instances of lost packets do not appear to be uncorrelated.

#### 5.4.4. Vehicle-to-Infrastructure Test Results

##### Test 1: V2I with 5.8 GHz antennas, 20 MHz bandwidth

The latency and range results for each of the three trials (eastbound, northbound 1, and northbound 2) are shown in Table 5-4. Similar to the V2V tests, the latencies that occurred while driving away from the infrastructure are greater than those exhibited in the stationary indoor setting, though the average increase of 16.6% is higher than the 12.1% increase from V2V Test 1 Part A in Section 5.4.3. This is possibly due to the lost line-of-sight that occurred in the northbound and eastbound directions due to buildings in the vicinity. Note from the table that the

number of lost ping messages is higher in the V2I tests than in V2V Test 1. Across the three trials, there were 1,288 lost packets out of 87,558, for a total loss of 1.47%. However, unlike the V2V tests, the V2I tests were run until ping packets stopped being acknowledged, and therefore the higher number of lost packets was expected. With the 5.8 GHz antennas, the maximum range achieved by the DSRC system was 182 m in the northbound direction, though line of sight was already lost before this distance was reached.

	<b>Eastbound</b>	<b>Northbound 1</b>	<b>Northbound 2</b>
<b>Received packets/Send packets</b>	32940/33182	32246/33012	21084/21364
<b>Average latency (ms)</b>	0.677	0.714	0.663
<b>Increase over indoor test (µs)</b>	90	127	76
<b>Increase over indoor test (%)</b>	15.3	21.6	12.9
<b>Maximum range (m)</b>	145	182	182

Table 5-4: Latency test results for V2I Test 1

#### Test 2: V2I with 5.9 GHz antennas, 20 MHz bandwidth

When the 5.9 GHz antennas were used, the vehicle was able to travel in the northbound direction for approximately 360 m in both trials before eventually losing communication with the infrastructure unit. This is approximately twice as far as the distance achieved using the 5.8 GHz antennas. When travelling on a different road with a longer line-of-sight between the vehicle and infrastructure, the vehicle travelled for approximately 460 m in both trials before losing communication with the infrastructure unit. The average distance from the combined four trials was approximately 410 m, which is an improvement of 228 m over first northbound V2I test. Furthermore, this is a 180 m improvement when compared to V2V Test 1 Part B when the 5.8 GHz antennas were used. Similar to V2I Test 1, the communication range in this case may have been adversely affected by shadowing from buildings in the test environment.

### Test 3: V2I with 5.9 GHz antennas, 10 MHz bandwidth

In Part A of the test, the observed average latency values at all five distances for all six trials were recorded, and the results are shown in Table 5-5. The *ping* tool in Linux provided minimum, average, and maximum latency values for each trial, along with the standard deviation ( $\sigma$ ). Note that the cells of the table labeled as “N/A” in trial 1 and trial 5 are instances where the connection between the vehicle and the infrastructure unit was lost. Throughout this test, there were instances where the connection between the vehicle and the infrastructure would be lost, and then regained once the vehicle was driven slightly forward. This could be due to the presence of dead zones in the infrastructure unit’s coverage area. As discussed in Section 5.1.4, the infrastructure antenna was 0.66 m above the ground in this test, which is at a lower position than the infrastructure antennas in Tests 1 and 2. This low distance from the ground may have created dead zones in the antenna’s coverage area, and driving the car slightly forward may have moved the vehicle out of these dead zones. It is also important to note that the 145 m distance in trial 5 produced a very large average latency of 10.885 ms (the maximum and standard deviation are unusually large as well), which may have been caused by a poor link quality between the vehicle and the infrastructure. When excluding trial 1 and trial 5, it is shown that latency increases with distance, though none of the latency values in this test are as high as the latency values from V2V Test 2 (Table 5-3), even in the 194 m case, where the distance between the vehicle and the antenna is greater than the maximum distance of 150 m from V2V Test 2. It is unlikely that there is a direct correlation between the separation of Tx/Rx units and the recorded latencies. The time of flight at the distances measured is on the order of less than 1  $\mu$ s (for 194 m, the time of flight is 0.647  $\mu$ s). An increase in latency by approximately 100  $\mu$ s between 5 m and 194 m cannot be attributed to time of flight.

	5 m	48 m	96 m	145 m	194 m
<b>Trial 1</b> (min/avg/max/ $\sigma$ ) [ms]	1.005/ 1.177/ 49.119/ 1.533	1.006/ 1.132/ 10.851/ 0.470	1.006/ 1.120/ 3.548/ 0.296	N/A	N/A
<b>Trial 2</b> (min/avg/max/ $\sigma$ ) [ms]	1.006/ 1.086/ 25.567/ 0.555	1.005/ 1.163/ 48.198/ 1.291	1.006/ 1.182/ 50.5/ 1.614	1.007/ 1.119/ 4.144/ 0.286	1.006/ 1.135/ 4.956/ 0.321
<b>Trial 3</b> (min/avg/max/ $\sigma$ ) [ms]	1.005/ 1.134/ 49.154/ 1.497	1.007/ 1.073/ 1.163/ 0.045	1.007/ 1.115/ 3.725/ 0.284	1.007/ 1.114/ 3.695/ 0.284	1.007/ 1.145/ 48.497/ 1.096
<b>Trial 4</b> (min/avg/max/ $\sigma$ ) [ms]	1.005/ 1.135/ 49.250/ 1.511	1.006/ 1.085/ 3.561/ 0.177	1.006/ 1.161/ 49.444/ 1.321	1.005/ 1.493/ 48.520/ 1.635	1.006/ 1.231/ 48.953/ 1.533
<b>Trial 5</b> (min/avg/max/ $\sigma$ ) [ms]	1.005/ 1.120/ 49.235/ 1.292	1.006/ 1.161/ 48.837/ 1.311	1.005/ 1.139/ 48.547/ 1.011	1.005/ 10.885/ 128.894/ 15.855	N/A
<b>Trial 6</b> (min/avg/max/ $\sigma$ ) [ms]	1.005/ 1.094/ 48.053/ 1.051	1.000/ 1.113/ 3.608/ 0.282	1.006/ 1.185/ 52.253/ 1.671	1.006/ 1.140/ 4.357/ 0.337	1.006/ 1.361/ 11.936/ 0.667
<b>Average <math>\pm \sigma</math> [ms]</b>	1.124 $\pm$ 0.033	1.121 $\pm$ 0.038	1.150 $\pm$ 0.030	3.150 $\pm$ 4.327	1.218 $\pm$ 0.105
<b>Average <math>\pm \sigma</math> excluding trials 1 and 5 [ms]</b>	1.112 $\pm$ 0.026	1.109 $\pm$ 0.040	1.161 $\pm$ 0.032	1.217 $\pm$ 0.185	1.218 $\pm$ 0.105

Table 5-5: Latency test results for V2I Test 3, Part A

When testing packet loss with the iperf utility in Part B, trial 1 experienced significant packet loss of 76% and 83% at the 145 m and 194 m distances, respectively. However, in trials 2 and 3, the packet loss was 0% for all five distances, with 2550-2553 packets sent at each distance. The large losses in trial 1 could also be explained by the presence of dead zones in the coverage area, where the link between the vehicle and infrastructure was either very weak or non-existent.

## **5.5. Physiological Monitor Test Results**

### **5.5.1. Skin Temperature Test Results**

#### Test 1: Physiological monitor and thermocouple under heat lamp

When analyzing the recorded temperature data for the full twenty minutes (i.e. the heating and cooling phases), the mean error and standard deviation between the Fluke 179 thermocouple and the temperature sensor was  $1.0^{\circ}\text{C} \pm 0.8^{\circ}\text{C}$ . Figure 5-8 shows the temperature measurements from both sensors ( $n = 1,205$ ). The heat lamp was turned off after 8 minutes and the temperature proceeded to drop. From the figure, a discrepancy exists during the cool-down periods – the thermocouple’s temperature dropped faster than the sensor’s temperature. Eventually, the measured temperatures of the thermocouple and the sensor stabilize around  $27^{\circ}\text{C}$ . When using the data within the first eight minutes (i.e. the heating phase), the measurement difference was only  $0.3^{\circ}\text{C} \pm 0.2^{\circ}\text{C}$ .

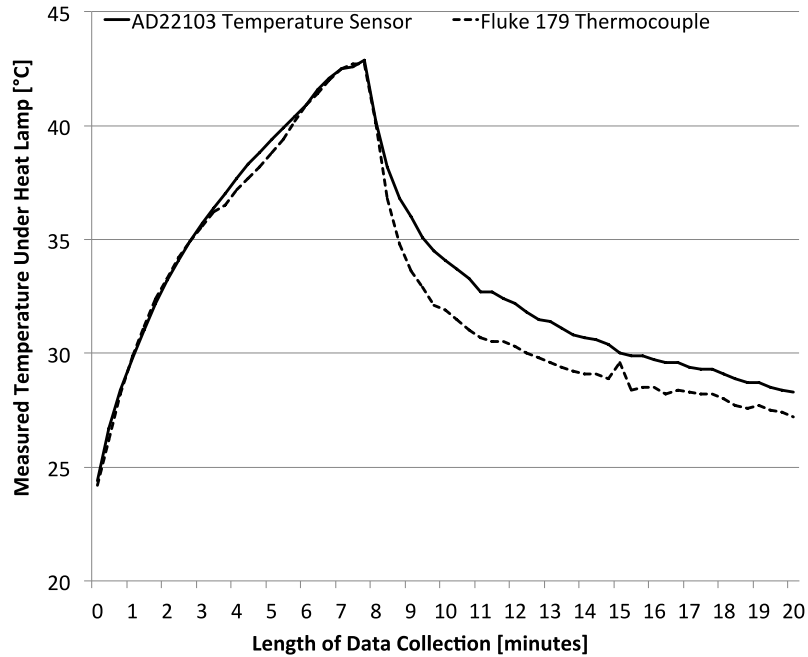


Figure 5-8: Temperature data for temperature test 1 (heat lamp)

Test 2: Physiological monitor and thermocouple on arm

With the sensors being worn by the volunteer, the average measured skin temperature across both trials was 32.5°C according to the temperature sensor and 32.6°C according to the thermocouple. Figure 5-9 shows the average temperature across both trials upon removing the sensors from the volunteer's skin, and once again the thermocouple responded to the temperature decrease much faster than the physiological monitor's temperature sensor. The mean and standard deviation of the temperature differences between the sensor and the thermocouple were 3.0°C ± 1.3°C.

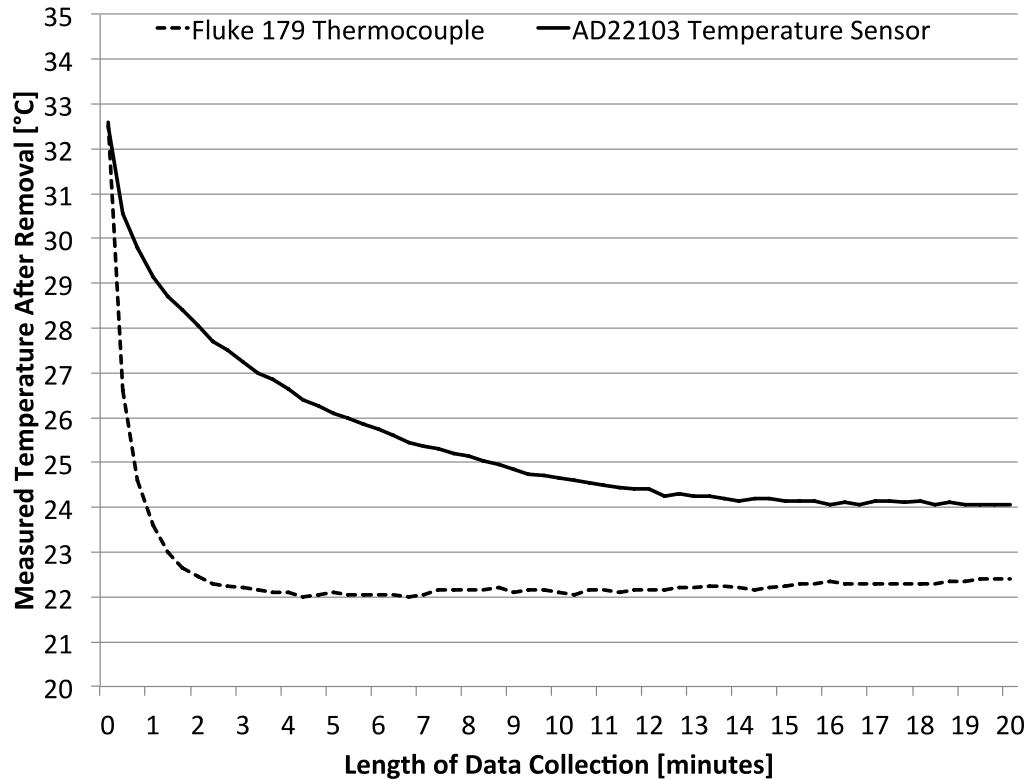


Figure 5-9: Temperature data for temperature test 2 (arm)

In Test 1 and Test 2, the thermocouple demonstrated a faster rate of cooling than the temperature sensor, particularly while measuring temperature directly on skin. Since the thermal response of the temperature sensor is dependent upon its airflow rate, the sensor takes a longer amount of time to react to changes in temperature when its airflow is restricted. This relationship between thermal response and airflow rate could possibly explain why the temperature difference during cool-down was much greater than the temperature difference during the heating phase of Test 1 or the initial state of Test 2. The temperature underneath the heat lamp and on the volunteer's arm increased gradually, but it fell rapidly once the lamp was shut off and once the sensor was removed from the arm. Therefore, any differences in thermal response between the physiological monitor's temperature sensor and the thermocouple would have been far more pronounced under cooling conditions.

### 5.5.2. Heart Rate and SpO<sub>2</sub> Test Results

Over the approximately six-minute time span, the two pulse oximeters recorded one sample per second, and the mean and standard deviation values of these samples are shown in Table 5-6. The mean and standard deviation of absolute error between the heart rate values measured by the two units was  $0.5 \pm 0.8$  beats per minute. Likewise, the mean and standard deviation of absolute error between the SpO<sub>2</sub> values was  $1.0\% \pm 0.7\%$ . It was also observed that 92% of data had an absolute heart rate difference of 1 beat per minute or less, and 81% of data had an absolute SpO<sub>2</sub> difference of less than 1%. This degree of accuracy for the physiological monitor is more than adequate for the application of in-car physiological monitoring.

	<b>Physiological Monitor</b>	<b>NONIN Evaluation Board</b>
<b>Heart rate (beats/second)</b>	$78.1 \pm 4.6$	$78.3 \pm 4.9$
<b>Oxygen saturation (%)</b>	$96.6 \pm 0.8$	$95.6 \pm 0.5$

Table 5-6: Mean and standard deviation of pulse oximeters

### 5.5.3. Current Consumption Test Results

When measuring the current consumption of the physiological monitor, the multimeter measured 16.9 mA while the monitor was connected with the USB dongle through Bluetooth Low Energy with the oximeter and the temperature sensor active. This was the mode of operation that the monitor used when inside a vehicle and transmitting physiological data. From the datasheet for the battery, draining the fully charged battery at 172 mA to the cutoff voltage of 2.75 V gives a battery life of  $\geq 5$  hours. If a similar discharge trend is assumed for a current consumption of 16.9 mA, this would result in a battery life of  $\geq 50.9$  hours with the monitor operating in the real-time sampling mode.

The current consumption of the monitor during sleep mode (long-term sampling) was measured to be 0.612 mA. However, the monitor must wake up every minute to take a sample, and the oximeter must be on for an average of 7 seconds to attain valid heart rate and SpO<sub>2</sub> data. This results in a discharge rate of 2.51 mAh. Again, assuming that the discharge trend doesn't change from the datasheet's specification, this leads to a total battery life of  $\geq 340.8$  hours (14.2 days).

#### **5.5.4. Bluetooth Low Energy Frequency Spectrum Test Results**

The frequency spectra captured by the analyzer at the three tested transmission powers are shown in Figure 5-10. In all three cases, the received signal power peaked at the expected center frequency of 2446 MHz. For TxPower = -6 dBm, 0 dBm, and 4 dBm, the received signal powers on the analyzer were -53.4 dBm, -47.2 dBm, and -43.4 dBm, respectively when the analyzer was located approximately 5 cm away from the monitor. This test confirmed that the radio can produce a signal at the expected center frequency, and that the radio is capable of adjusting its transmission power.

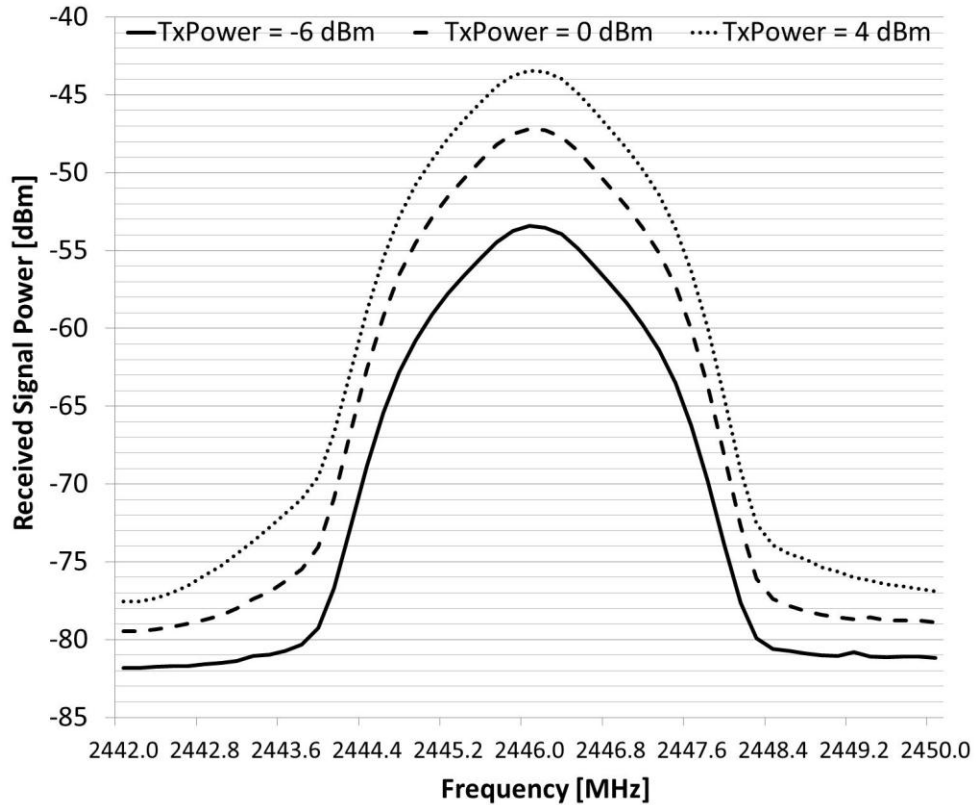


Figure 5-10: Frequency spectrum for Bluetooth Low Energy radio

### 5.5.5. Bluetooth Low Energy Range Test Results

During the communication range tests, there was no data loss between the distances from 0 to 8 m. The monitor correctly acknowledged all 500 data packets sent by the PC across the five distances measured. For an in-car physiological monitor, wireless BLE nodes will never be separated by a distance greater than 8 m, and therefore this transmission distance is more than adequate for this particular application.

### 5.5.6. Long-Term Sampling Test Results

Table 5-7 contains the test duration of each subject and the mean  $\pm$  standard deviation values of the physiological parameters measured. For each subject, the physiological monitor sampled once per minute. In all four long-term sampling

trials, the physiological monitor collected the correct number of samples, and samples were collected at the appropriate times based on the timestamps from the real-time clock. Figure 5-11 shows the skin temperature of subject 1 (n = 179) during the trial. The temperature was increasing at the beginning of the trial and stabilized between 30.5°C and 31.5°C. From the collected pulse oximeter data for subject 1, the average heart rate was  $68 \pm 7$  beats per minute and the average SpO<sub>2</sub> was between  $98\% \pm 0.8\%$  of oxygenation. In all four long-term sampling trials, the physiological parameters of the subject were within the range expected from healthy males.

	<b>Subject 1</b>	<b>Subject 2</b>	<b>Subject 3</b>	<b>Subject 4</b>
<b>Trial duration (minutes)</b>	179	247	263	281
<b>Skin temperature (°C)</b>	$33.8 \pm 0.5$	$31.7 \pm 0.6$	$33.5 \pm 0.4$	$34.5 \pm 0.5$
<b>Heart rate (beats/second)</b>	$68 \pm 7$	$56 \pm 7$	$68 \pm 7$	$77 \pm 11$
<b>Oxygen saturation (%)</b>	$98 \pm 0.8$	$98 \pm 1.2$	$97 \pm 1.2$	$98 \pm 0.9$

Table 5-7: Long-term sampling test results

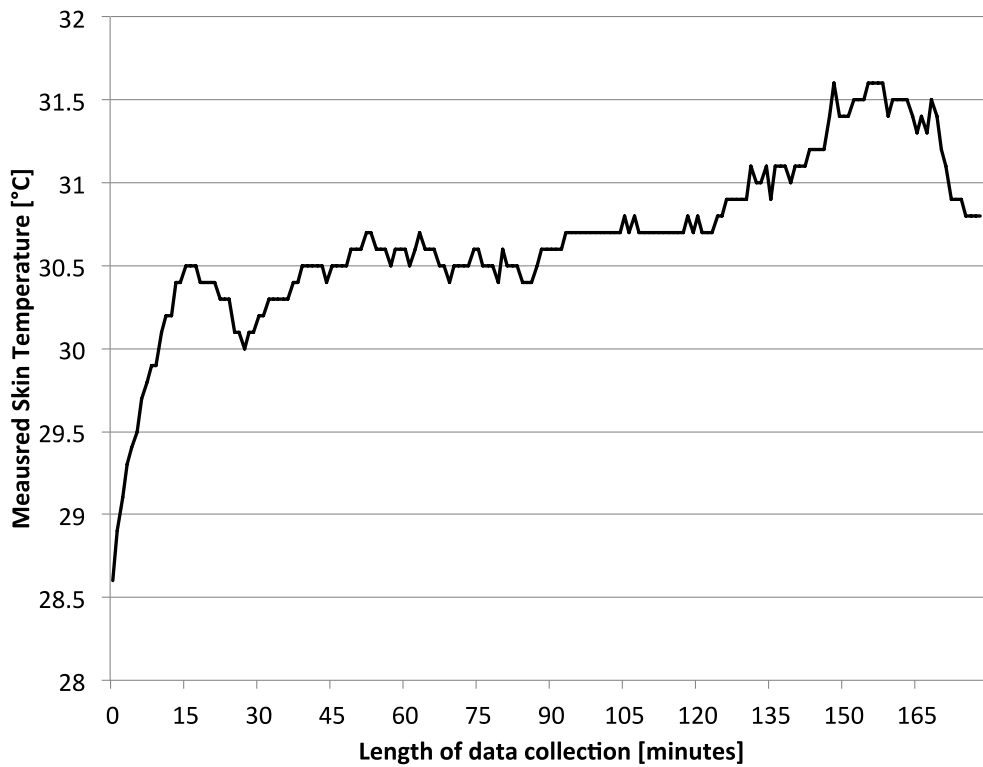


Figure 5-11: Skin temperature of subject 1 during long-term trials

## 5.6. Integrated System Test Results

In trial 1 of the integrated system test, the trailing vehicle received physiological monitor data for all 16 data requests that were sent, and all of these transmissions contained valid temperature and oximeter data. In trial 2, there was 1 request that did not return physiological monitor data. Furthermore, of the 18 successfully received physiological data messages, there was one message that did not contain valid heart rate or SpO<sub>2</sub> data, due to an improper fit of the pulse oximeter's fingertip sensor. In trial 3, there were 2 failed data requests and 23 successful requests, though 7 of these successful data requests had oximeter errors caused from a loose fit of the passenger's fingertip sensor. Across all three trials, there were 3 failed data requests out of 60, for a failure rate of 5%.

The average temperature recorded by the trailing vehicle was 28.6°C, the average heart rate of the passenger was 60.8 beats per second, and the average SpO<sub>2</sub> of the passenger was 97.6%. The temperature data retrieved via DSRC is shown in Figure 5-12 (n = 57). In trial 3, the passenger in the leading car moved the physiological monitor from the car seat to his forearm while the vehicle was in motion, thereby resulting in the sudden temperature increase between data points 42 and 43, as well as the continued increase in temperature lasting until the end of trial 3.

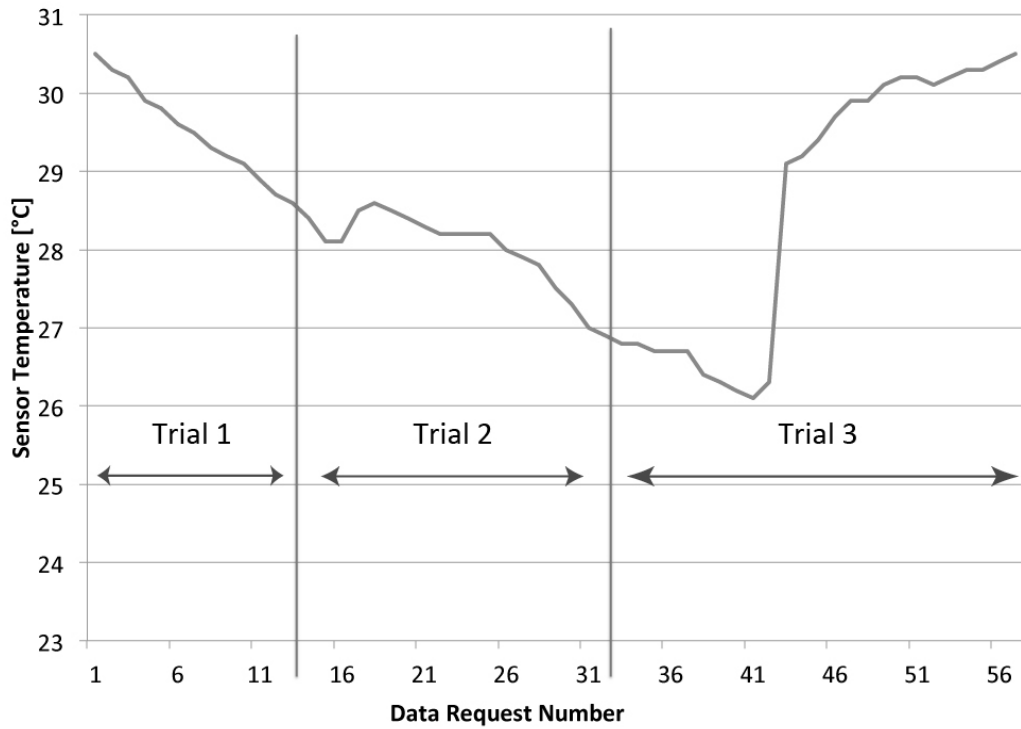


Figure 5-12: Temperature data for integrated system test

## **CHAPTER 6:**

# **CONCLUSIONS AND RECOMMENDATIONS**

### **6.1. Conclusions**

This thesis explored the possibility of using 5.9 GHz Dedicated Short Range Communication (DSRC) as a method of wirelessly transmitting physiological parameters out of a vehicle in the event of a car accident or medical emergency. This research was motivated by the need for new methods of protecting elderly drivers, particularly those with increased fragility. Studies have shown that elderly drivers are more likely to suffer serious injuries and fatalities in motor vehicle accidents when compared to younger drivers, despite the fact that they are statistically less likely to be involved in a collision. For those elderly drivers who still possess a sufficient degree of skill, it is preferable to keep them on the road, as driving cessation can have an adverse impact on quality of life. One possible way to improve vehicle safety for drivers and passengers is to combine in-car physiological monitoring with vehicular communication. This would allow Emergency Medical Services (EMS) to be notified of each crash victim's condition before arriving at the scene of an accident, thereby allowing them to prioritize their emergency response in favour of those who are at the greatest risk of dying. A major objective of this thesis was to determine the potential advantages of DSRC when compared to cellular communication systems such as WiMAX, UMTS, LTE. More importantly, this thesis investigated whether these advantages are beneficial in the specific application of emergency response.

In order to evaluate DSRC as a system for transmitting physiological parameters out of a vehicle, a combined DSRC and physiological monitoring system was designed and tested. The DSRC system was built with an embedded computer and a 5.9 GHz wireless radio, both of which were purchased off-the-shelf. A custom Linux driver was developed and tested to implement the 802.11p DSRC

communication protocol. An in-car user interface was also developed for Linux using the Java Swing toolset. This interface used a display and a keypad (both of which were purchased) to allow the vehicle occupants to receive important notifications and to send messages, if necessary.

The in-car physiological monitoring system was worn by the user with an armband, and it contained sensors (all of which were purchased off-the-shelf) for monitoring body temperature, heart rate, and blood oxygen saturation ( $\text{SpO}_2$ ). These parameters were chosen due to their importance in determining the physical and mental condition of a vehicle driver. A printed circuit board (PCB) was created to connect each of these sensors to a microcontroller, and firmware was written to sample data from each of these sensors and transmit them over Bluetooth Low Energy (BLE). BLE was used to facilitate communication between the physiological monitor and the DSRC system. The BLE protocol was chosen over other low-power wireless systems such as Bluetooth, ZigBee, and ANT due to its low power consumption and interoperability with other BLE-capable devices.

The developed DSRC system and the in-car physiological monitor were tested both individually and together as an integrated system. Spectrum analysis of the DSRC system revealed that the designed software driver was capable of operating in the 5.9 GHz frequency band with 10 MHz of signal bandwidth as required by the IEEE 802.11p specification. Furthermore, the software driver was capable of adjusting the transmission power of the DSRC radio. However, the chosen wireless radio was unable to conform to the spectral mask provided by the United States' Federal Communications Commission (FCC). The FCC requires Class C DSRC devices (which comprise the majority of vehicles that would use DSRC) to limit out-of-band transmitter energy by -26 dBm. In other words, the energy out of the 10 MHz band must be at least 26 dBm lower than the energy in the band, and this energy drops even further when moving away from the center frequency.

However, the DSRC system was unable to produce such a sharp attenuation in energy.

Additional tests verified that each of the DSRC units were capable of serving as on-board units and as road-side units, demonstrating low latency, low packet loss, and distances of up to 460 m. In a vehicle-to-vehicle scenario, the system was able to communicate with packet loss under 1% at 60 km/h and with a vehicle separation of up to 150 m. Furthermore, with a vehicle separation between 50-100 m, the average latency of communication was 1.228 ms, which represents an increase of 7.05% over the latency when both vehicles are stationary. This latency increased to 1.947 ms (a 69.7% increase over the stationary distance) when the vehicle separation increased to 100-150 m. In the vehicle-to-infrastructure tests, communication between a stationary vehicle and the infrastructure unit increased by 100  $\mu$ s, though there is currently insufficient V2I test data to draw any conclusions as to why this latency increase occurred.

The physiological monitor was found to be capable of measuring the body temperature, heart rate, and SpO<sub>2</sub> of a vehicle occupant with a sufficiently high degree of accuracy. Additionally, the monitor's operating current consumption results in a battery life of 50 hours. The Bluetooth Low Energy radio in the monitor was shown to be capable of communicating at 8 m, which is more than adequate for use inside of a vehicle, and the RF circuitry of the monitor was capable of transmitting a sufficiently strong signal in the BLE frequency range. Finally, the integrated system was capable of transmitting a vehicle occupant's vital signs out of the vehicle at distances over 100 m while the sending and receiving vehicles were simultaneously moving at 60 km/h.

While the research presented in this thesis demonstrates that DSRC has the potential to be used for emergency service applications, the benefits and drawbacks of DSRC must be taken into consideration when comparing it to existing cellular communication systems. From the vehicle-to-vehicle and

vehicle-to-infrastructure tests discussed in Chapter 5, it was shown that DSRC is capable of communicating with latencies of less than 2 ms. Moreover, the literature review in Chapter 2 showed packet latencies of 350 ms for UMTS, 50-100 ms for LTE, and 30-50 ms for WiMAX. This latency advantage makes DSRC a useful communication protocol for collision prevention applications, particularly those where vehicles are moving very fast and must be able to receive updates on vehicle proximities and impending dangers as often as possible. However, this requirement for extremely low latency is not as crucial in emergency response applications. In a scenario where an ambulance has dispatched and is en-route to the scene of the accident, updates would presumably be sent periodically in order for EMS to remain aware of the physical condition of each victim. Whether these updates arrived with a 1 ms or 50 ms latency is not an issue of particular importance when the ambulance is still minutes away from its destination. In such a scenario, long range communication is of greater importance than latency. From the range test results discussed in Chapter 5, it was shown that DSRC is capable of reaching ranges between 400-500 m in an urban environment, which is considerably lower than the 900 m communication range of WiMAX. In order for a DSRC packet to reach an ambulance from an accident site several kilometres away, several hops would be required, which would either require the majority of vehicles to be equipped with DSRC radios, or it would require the environment to be equipped with infrastructure units at distances of at least 400 m. Both of these configurations are virtually non-existent at present, and whether they will ever exist depends on the adoption rate of DSRC among vehicle manufacturers and municipal governments. DSRC has an advantage over cellular systems in that its frequency band is exclusively dedicated to vehicular applications, and it would likely be less susceptible to congestion than the highly populated UMTS and LTE networks in urban environments. However, this advantage has to be weighed against the two largest disadvantages that DSRC has compared to cellular systems - range and availability. From the results presented in this thesis, it can be concluded that DSRC is capable of being used in emergency response applications where physiological parameters are transmitted

out of the vehicle. However, it is too early in DSRC's adoption cycle to make any definitive statements on whether DSRC can provide any significant advantages over cellular systems for any applications outside of collision response.

## **6.2. Future Recommendations**

In order to transmit a signal over very large distances, DSRC must be capable of using other vehicles and roadside units in the vicinity as repeaters. This feature should be incorporated into future DSRC systems, as it will be necessary to communicate with EMS vehicles that are located several kilometres away. However, in order for a signal to reach its intended recipient, it will be necessary to add a Global Positioning System (GPS) transceiver to the developed DSRC systems to provide location awareness. GPS will also allow location information to be sent along with physiological parameters, thereby allowing EMS to locate specific victims in an emergency scenario.

In the V2I test results from Section 5.4.4, an increase in latency between the 5 m and 194 m distances was experienced (the increase was approximately 100  $\mu$ s). However, this increase cannot be attributed to time of flight of the DSRC packets (which is on the order of less than 1  $\mu$ s). This increase could be a consequence of the environment and the presence of reflectors, but it is difficult to make a definitive statement without more V2I tests. Additional V2I tests should be conducted at a professional test track where the presence of external environmental interferers can be mitigated. Additionally, tests should be conducted to determine the effects of poor SNR environments on packet processing time (which would in turn impact the latency of the channel). It is known that the 802.11 standard employs Forward Error Correction (FEC) [77], and this error correction would theoretically take a longer time to process in a noisy channel. Tests in varying SNR conditions should be performed to determine the significance (if any) of these processing delays.

Using the keypad with the in-car user interface requires visual contact, which creates a risk by taking the vehicle driver's attention away from the road. It would be preferable to replace the keypad with a form of interaction that does not require the driver to look away. A voice recognition engine would work well for this purpose. In addition to reducing driver distraction, voice recognition would also be easier to use for elderly drivers who have difficulty memorizing button placements for specific commands on a keypad.

The physiological monitor should incorporate a security system such as the Advanced Encryption Standard (AES-128) in order to protect the parameters of the vehicle occupant. If the system is left unsecured, it creates a significant threat to the user's privacy through eavesdropping and packet sniffing. Additionally, an encryption protocol should be incorporated into the developed DSRC system. This is especially important for scenarios in which other vehicles must serve as relays during transmission. Moreover, authentication of emergency service vehicles is also extremely important for privacy. Only authorized emergency service vehicles should be able to request physiological parameters from other vehicles.

Future researchers should consider adding a sensor for detecting the systolic blood pressure of a victim. Blood pressure is an important indicator for determining the amount of blood loss that a person has experienced following a car accident. However, every blood pressure sensor currently in use is inadequate for an in-vehicle monitor. Inflating blood pressure cuffs need to be placed at the same vertical level as the user's heart in order to attain accurate readings. In an accident scenario, it cannot be assumed that the cuff is in this position. Moreover, ring or finger-type blood pressure sensors are greatly influenced by motion. This makes such sensors unreliable in a moving vehicle or even in a stationary vehicle where the victim is conscious and moving. If a blood pressure sensor could provide reliable readings during motion and regardless of its position relative to the heart, it would be a valuable addition to the physiological monitor.

As previously mentioned, the transmission rate of the OEM III pulse oximeter is limited to 1 Hz. If a faster transmission rate is required (for example, to perform frequency spectrum analysis of HRV signals), a different oximeter should be selected, or the signal processing and filtering stages of the oximeter should be implemented in a custom circuit (i.e. without the use of the OEM III). This custom circuit could still utilize the fingertip flex sensor, though the DB9 connector for the flex sensor should be removed to reduce the size of the physiological monitor. All of the signal lines required for the sensor should be directly connected to the printed circuit board.

Additionally, a pilot study involving volunteer drivers would be required. Initially, volunteers – particularly elderly drivers – should use the system and provide feedback on which characteristics of the integrated system they consider difficult to use. Once the system is fine-tuned based on this user feedback, long-term studies with elderly drivers and EMS should be performed to determine the benefits of DSRC in collision prevention as well as in facilitating faster and more effective emergency response after an accident.

## REFERENCES

- [1] Transport Canada, "Canadian Motor Vehicle Traffic Collision Statistics" Available: <http://www.tc.gc.ca/eng/roadsafety/resources-researchstats-menu-847.htm>. [Accessed: 13-June-2012]
- [2] United States Government National Highway Traffic Safety Administration, "Fatality Analysis Reporting System" Available: <http://www-fars.nhtsa.dot.gov/Crashes/CrashesTime.aspx>. [Accessed: 24-May-2012].
- [3] L. Evans, *Traffic Safety and the Driver*. Van Nostrand Reinhold, pp. 25–28, 1991.
- [4] G. Adler and S. Rottunda, "Older adults' perspectives on driving cessation," *Journal of Aging Studies*, vol. 20, no. 3, pp. 227–235, 2006.
- [5] L. D'Angelo, J. Parlow, W. Spiessl, S. Hoch, and T. Liith, "A system for unobtrusive in-car vital parameter acquisition and processing," presented at the *4th International Conference on Pervasive Computing Technologies for Healthcare (PervasiveHealth)*, pp. 1–7, 2010
- [6] S. Heuer, B. Chamadiya, A. Gharbi, C. Kunze, and M. Wagner, "Unobtrusive in-vehicle biosignal instrumentation for advanced driver assistance and active safety," presented at the *IEEE EMBS Conference on Biomedical Engineering and Sciences (IECBES)*, pp. 252–256, 2010
- [7] H.-S. Shin, S.-J. Jung, J.-J. Kim, and W.-Y. Chung, "Real time car driver's condition monitoring system," presented at the *IEEE Sensors Conference*, pp. 951–954, 2010
- [8] C.-M. Yang, C.-C. Wu, C.-M. Chou, and T.-L. Yang, "Vehicle driver's ECG and sitting posture monitoring system," presented at the *IEEE International Conference on Information Technology and Applications in Biomedicine*, pp. 1–4, 2009.
- [9] D. Valerio, F. Ricciato, P. Belanovic, and T. Zemen, "UMTS on the road: broadcasting intelligent road safety information via MBMS," presented at

- the *IEEE Vehicular Technology Conference Spring*, pp. 3026–3030, 2008.
- [10] A. Costa, P. Pedreiras, J. Fonseca, J. N. Matos, H. Proenca, A. Gomes, and J. S. Gomes, “Evaluating WiMAX for vehicular communication applications,” presented at the *IEEE International Conference on Emerging Technologies and Factory Automation*, pp. 1185–1188, 2008.
- [11] D. Jiang, V. Taliwal, A. Meier, W. Holfelder, and R. Herrtwich, “Design of 5.9 ghz dsrc-based vehicular safety communication,” *IEEE Wireless Communications*, vol. 13, no. 5, pp. 36–43, 2006.
- [12] D. Jabaudon, J. Sztajzel, K. Sievert, T. Landis, and R. Sztajzel, “Usefulness of ambulatory 7-day ECG monitoring for the detection of atrial fibrillation and flutter after acute stroke and transient ischemic attack,” *Stroke*, vol. 35, no. 7, pp. 1647–1651, 2004.
- [13] S. Ullah, H. Higgins, B. Braem, B. Latre, C. Blondia, I. Moerman, S. Saleem, Z. Rahman, and K. S. Kwak, “A comprehensive survey of wireless body area networks,” *J Med Syst*, pp. 1–30, 2010.
- [14] R. Welsh, A. Morris, A. Hassan, and J. Charlton, “Crash characteristics and injury outcomes for older passenger car occupants,” *Transportation Research Part F: Traffic Psychology and Behaviour*, vol. 9, no. 5, pp. 322–334, 2006.
- [15] H. Sjögren, U. Björnstig, and A. Eriksson, “Elderly in the traffic environment: analysis of fatal crashes in northern Sweden,” *Accident Analysis & Prevention*, pp. 177-188, 1993.
- [16] V. Bansal, C. Conroy, D. Chang, G. T. Tominaga, and R. Coimbra, “Rib and sternum fractures in the elderly and extreme elderly following motor vehicle crashes,” *Accident Analysis & Prevention*, vol. 43, no. 3, pp. 661–665, 2011.
- [17] C. Peek-Asa, B. B. Dean, and R. J. Halbert, “Traffic-related injury hospitalizations among California elderly, 1994.,” *Accident Analysis & Prevention*, vol. 30, no. 3, pp. 389–395, 1998.
- [18] G. Li, E. R. Braver, and L.-H. Chen, “Fragility versus excessive crash

- involvement as determinants of high death rates per vehicle-mile of travel among older drivers,” *Accident Analysis & Prevention*, vol. 35, no. 2, pp. 227–235, 2003.
- [19] B. Freund, L. A. Colgrove, D. Petrakos, and R. McLeod, “In my car the brake is on the right: Pedal errors among older drivers,” *Accident Analysis & Prevention*, vol. 40, no. 1, pp. 403–409, 2008.
- [20] L. Evans, “Risks older drivers face themselves and threats they pose to other road users.,” *Int J Epidemiol*, vol. 29, no. 2, pp. 315–322, 2000.
- [21] L. P. Kostyniuk and J. T. Shope, “Driving and alternatives: Older drivers in Michigan,” *Journal of Safety Research*, vol. 34, no. 4, pp. 407–414, 2003.
- [22] S. A. Shaheen and D. A. Niemeier, “Integrating vehicle design and human factors: minimizing elderly driving constraints,” *Transportation Research Part C: Emerging Technologies*, vol. 9, no. 3, pp. 155–174, 2001.
- [23] J. Sixsmith and A. Sixsmith, “Older people, driving and new technology,” *Applied Ergonomics*, vol. 24, no. 1, pp. 40–43, 1993.
- [24] T. Mangel, T. Kosch, and H. Hartenstein, “A comparison of UMTS and LTE for vehicular safety communication at intersections,” *IEEE Vehicular Networking Conference (VNC), 2010*, pp. 293–300, 2010.
- [25] A. Ghosh, R. Ratasuk, B. Mondal, N. Mangalvedhe, and T. Thomas, “LTE-advanced: next-generation wireless broadband technology,” *IEEE Wireless Communications*, vol. 17, no. 3, pp. 10–22, 2010.
- [26] R. Colda, T. Palade, E. Puchita, I. Vermecan, and A. Moldovan, “Mobile WiMAX: System performance on a vehicular multipath channel,” presented at the *Proceedings of the Fourth European Conference on Antennas and Propagation (EuCAP)*, pp. 1–5, 2010.
- [27] C.-M. Chou, C.-Y. Li, W.-M. Chien, and K.-C. Lan, “A feasibility study on vehicle-to-infrastructure communication: WiFi vs. WiMAX,” presented at the *Tenth International Conference on Mobile Data Management: Systems, Services and Middleware*, pp. 397–398, 2009.

- [28] M. Jerbi, P. Marlier, and S. M. Senouci, "Experimental assessment of V2V and I2V communications," presented at the *IEEE International Conference on Mobile Adhoc and Sensor Systems*, pp. 1–6, 2007
- [29] M. Jerbi and S. M. Senouci, "Characterizing multi-hop communication in vehicular networks," presented at the *IEEE Wireless Communications and Networking Conference*, pp. 3309–3313, 2008.
- [30] J. P. Singh, N. Bambos, B. Srinivasan, D. Clawin, and Y. Yan, "Empirical observations on wireless LAN performance in vehicular traffic scenarios and link connectivity based enhancements for multihop routing," presented at the *IEEE Wireless Communications and Networking Conference*, vol. 3, pp. 1676–1682, 2005.
- [31] J. P. Singh, N. Bambos, B. Srinivasan, and D. Clawin, "Wireless LAN performance under varied stress conditions in vehicular traffic scenarios," presented at the *IEEE 56th Vehicular Technology Conference, VTC-Fall*, vol. 2, pp. 743–747, 2002.
- [32] J. Ott and D. Kutscher, "Drive-thru Internet: IEEE 802.11b for 'automobile' users," presented at *INFOCOM: Annual Joint Conference of the IEEE Computer and Communication Societies*, vol. 1, pp. 7–11, 2004.
- [33] R. Gass, J. Scott, and C. Diot, "Measurements of in-motion 802.11 networking," presented at the *IEEE Workshop on Mobile Computing Systems and Applications, WMCSA*, pp. 69–74, 2006.
- [34] IEEE, "IEEE Std 802.11p-2010 (Amendment to IEEE Std 802.11-2007) IEEE Standard for Information technology—Telecommunications and information exchange between systems—Local and metropolitan networks—Specific requirements—Part 11: Wireless LAN Medium Access Control (MAC) and Physical Layer (PHY) Specifications—Amendment 6: Wireless Access in Vehicular Environments," 802.11p, 2010.
- [35] P. Fuxjager, A. Costantini, D. Valerio, P. Castiglione, G. Zacheo, T. Zemen, and F. Ricciato, "IEEE 802.11p Transmission Using GNURadio," presented at the *6th Karlsruhe Workshop on Software*

- Radios*, pp. 83–86, 2010.
- [36] W. Xiang, Y. Huang, and S. Majhi, “The design of a wireless access for vehicular environment (WAVE) prototype for intelligent transportation system (ITS) and vehicular infrastructure integration (VII),” presented at the *IEEE Vehicular Technology Conference - VTC Fall*, pp. 1–2, 2008.
- [37] K. Ho, P. Kang, C. Hsu, and C. Lin, “Implementation of WAVE/DSRC devices for vehicular communications,” presented at the *International Symposium on Computer Communication Control and Automation (3CA)*, vol. 2, pp. 522–525, 2010.
- [38] C. Lin, B. Chen, and J. Lin, “Field test and performance improvement in IEEE 802.11p V2R/R2V environments,” presented at the *IEEE International Conference on Communications (ICC) Workshops*, pp. 1–5, 2010.
- [39] F. Bai and H. Krishnan, “Reliability analysis of DSRC wireless communication for vehicle safety applications,” presented at the *IEEE Intelligent Transportation Systems Conference (ITSC)*, pp. 355–362, 2006.
- [40] I. C. Msadaa, P. Cataldi, and F. Filali, “A comparative study between 802.11p and mobile WiMAX-based V2I communication networks,” presented at the *IEEE International Conference on Next Generation Mobile Applications, Services, and Technologies (NGMAST)*, pp. 186–191, 2010.
- [41] P. Belanovic, D. Valerio, A. Paier, T. Zemen, F. Ricciato, and C. Mecklenbrauker, “On wireless links for vehicle-to-infrastructure communications,” *IEEE Transactions on Vehicular Technology*, vol. 59, no. 1, pp. 269–282, 2010.
- [42] E. Lou, E. K. Brunton, F. Kamal, A. Renggli, K. Kemp, J. Lewicke, S. Dulai, J. M. Watt, and J. Andersen, “A low power wireless data acquisition device to monitor gait patterns for children with toe walking during daily activities,” *Journal of Medical Devices*, vol. 5, no. 2, pp. 1–6, 2011.

- [43] R. Matthews, N. J. McDonald, P. Hervieux, P. J. Turner, and M. A. Steindorf, "A wearable physiological sensor suite for unobtrusive monitoring of physiological and cognitive state," presented at the *IEEE International Conference of Engineering in Medicine and Biology Society EMBS*, pp. 5276–5281, 2007.
- [44] N. Oliver and F. Flores-Mangas, "HealthGear: A Real-time Wearable System for Monitoring and Analyzing Physiological Signals," *International Workshop On Wearable and Implantable Body Sensor Networks, 2006*, pp. 1–4, 2006.
- [45] M. Rofouei, M. Sinclair, R. Bittner, T. Blank, N. Saw, G. DeJean, and J. Heffron, "A Non-invasive Wearable Neck-Cuff System for Real-Time Sleep Monitoring," presented at the International Conference on Body Sensor Networks (BSN), pp. 156–161, 2011.
- [46] K. Ma, J. Khoo, and T. Brown, "Development of an ambulatory multi-parameter monitoring system for physiological stress related parameters," *Bioinformatics and Biomedical Technology (ICBBT), 2010, International Conference on*, pp. 324–328, 2010.
- [47] J. Kemp, E. I. Gaura, J. Brusey, and C. D. Thake, "Using Body Sensor Networks for Increased Safety in Bomb Disposal Missions," *IEEE International Conference on Sensor Networks, Ubiquitous and Trustworthy Computing*, pp. 81–89, 2008.
- [48] L. Xu, D. Guo, F. E. H. Tay, and S. Xing, "A wearable vital signs monitoring system for pervasive healthcare," presented at the *IEEE Conference on Sustainable Utilization and Development in Engineering and Technology (STUDENT)*, pp. 86–89, 2010.
- [49] D. C. Zheng and Y. T. Zhang, "A ring-type device for the noninvasive measurement of arterial blood pressure," presented at the *IEEE International Conference of the Engineering in Medicine and Biology Society*, vol. 4, pp. 3184–3187, 2003.
- [50] D. Park and S. Kang, "Development of Reusable and Expandable Communication Platform for Wearable Medical Sensor Network,"

- presented at the *Annual International Conference of the IEEE Engineering in Medicine and Biology Society*, pp. 5380–5383, 2004.
- [51] S.-N. Yu and J.-C. Cheng, “A wireless physiological signal monitoring system with integrated Bluetooth and WiFi technologies,” presented at the *IEEE International Conference of the Engineering in Medicine and Biology Society (EMBS)*, pp. 2203–2206, 2005.
- [52] F. Tsow, E. Forzani, A. Rai, R. Wang, R. Tsui, S. Mastroianni, C. Knobbe, A. J. Gandolfi, and N. J. Tao, “A wearable and wireless sensor system for real-time monitoring of toxic environmental volatile organic compounds,” *IEEE Sensors Journal.*, vol. 9, no. 12, pp. 1734–1740, 2009.
- [53] K. Malhi, S. Mukhopadhyay, J. Schnepper, M. Haefke, and H. Ewald, “A ZigBee based wearable physiological parameters monitoring system,” *IEEE Sensors Journal.*, vol. 12, no. 3, pp. 423-430, 2012.
- [54] N. Watthanawisuth, T. Lomas, A. Wisitsoraat, and A. Tuantranont, “Wireless wearable pulse oximeter for health monitoring using ZigBee wireless sensor network,” presented at the *IEEE International Conference on Electrical Engineering/Electronics Computer Telecommunications and Information Technology (ECTI-CON)*, pp. 575–579, 2010.
- [55] Z. Yan and Z. Jiaying, “Design and implementation of ZigBee based wireless sensor network for remote SpO<sub>2</sub> monitor,” presented at the *2nd International Conference on Future Computer and Communication (ICFCC)*, vol. 2, pp. 278-281, 2010.
- [56] T. Gao, D. Greenspan, M. Welsh, R. R. Juang, and A. Alm, “Vital signs monitoring and patient tracking over a wireless network,” presented at the *IEEE-EMBS 2005. 27th Annual International Conference of the Engineering in Medicine and Biology Society*, pp. 102–105, 2006.
- [57] S.-L. Chen, H.-Y. Lee, C.-A. Chen, H.-Y. Huang, and C.-H. Luo, “Wireless body sensor network With adaptive low-power design for biometrics and healthcare applications,” *IEEE Systems Journal*, vol. 3, no. 4, pp. 398–409, 2009.

- [58] J. Yoo, L. Yan, S. Lee, Y. Kim, and H.-J. Yoo, "A 5.2 mW Self-Configured Wearable Body Sensor Network and a 12 uW Wirelessly Powered Sensor for Continuous Health Monitoring System," *IEEE Journal of Solid State Circuits*, vol. 45, no. 1, pp. 178–188, 2009.
- [59] C.-T. Lin, C.-J. Chang, B.-S. Lin, S.-H. Hung, C.-F. Chao, and I.-J. Wang, "A real-time wireless brain–computer interface system for drowsiness detection," *IEEE Transactions on Biomedical Circuits and Systems*, vol. 4, no. 4, pp. 214–222, 2010.
- [60] A. Giusti, C. Zocchi, and A. Rovetta, "A noninvasive system for evaluating driver vigilance level examining both physiological and mechanical data," *IEEE Transactions on Intelligent Transportation Systems*, vol. 10, no. 1, pp. 127–134, 2009.
- [61] C. Zocchi, A. Rovetta, and F. Fanfulla, "Physiological parameters variation during driving simulations," presented at the *IEEE/ASME International Conference on Advanced Intelligent Mechatronics*, pp. 1–6, 2007.
- [62] H. J. Baek, H. B. Lee, J. S. Kim, J. M. Choi, K. K. Kim, and K. S. Park, "Nonintrusive biological signal monitoring in a car to evaluate a driver's stress and health state," *Telemed J E Health*, vol. 15, no. 2, pp. 182–189, 2009.
- [63] J. Healey and R. W. Picard, "Detecting stress during real-world driving tasks using physiological sensors," *IEEE Transactions on Intelligent Transportation Systems*, vol. 6, no. 2, pp. 156–166, 2005.
- [64] J. Healey and R. W. Picard, "SmartCar: Detecting Driver Stress," presented at the ICPR '00: Proceedings of the *International Conference on Pattern Recognition*, vol. 4, 2000.
- [65] C. Ramon, A. Clarion, C. Gehin, C. Petit, C. Collet, and A. Dittmar, "An integrated platform for the driver's physiological and functional states assessment," presented at the *30th Annual International Conference of the IEEE Engineering and Medicine and Biology Society*, pp. 506–509, 2008.

- [66] A. Clarion, C. Ramon, C. Petit, A. Dittmar, J. P. Bourgeay, A. Guillot, C. Gehin, E. McAdams, and C. Collet, “An integrated device to evaluate a driver’s functional state,” *Behavior Research Methods*, vol. 41, no. 3, pp. 882–888, 2009.
- [67] K. Murata, E. Fujita, S. Kojima, S. Maeda, Y. Ogura, T. Kamei, T. Tsuji, S. Kaneko, M. Yoshizumi, and N. Suzuki, “Noninvasive biological sensor system for detection of drunk driving,” *IEEE Transactions on Information Technology in Biomedicine*, vol. 15, no. 1, pp. 19–25, 2011.
- [68] Y.-C. Wu, Y.-Q. Xia, P. Xie, and X.-W. Ji, “The design of an automotive anti-drunk driving system to guarantee the uniqueness of driver,” presented at the *International Conference on Information Engineering and Computer Science*, ICIECS, pp. 1–4, 2009.
- [69] W. Dong, C. Q. Cheng, L. Kai, and F. Bao-hua, “The automatic control system of anti drunk-driving,” presented at the *International Conference on Electronics, Communications, and Control (ICECC)*, pp. 523–526, 2011.
- [70] A. Durresi, M. Durresi, and L. Barolli, “Wireless communications for health monitoring on highways,” presented at the *27th International Conference on Distributed Computing Systems Workshops*, pp. 37–45, 2007.
- [71] H. Yamagishi, H. Suzuki, and A. Watanabe, “Study of a remote monitoring system for senior drivers,” presented at the *IEEE Region 10 Conference (TENCON)*, pp. 1042–1047, 2010.
- [72] Federal Communications Commission, “FCC allocates spectrum in the 5.9 GHz range for intelligent transportation systems uses,” *Federal Communications Commission*. Federal Communications Commission, pp. 1–2, 1999.
- [73] C.-F. Lin, J.-C. Juang, E. Liang, and L.-Y. Ke, “Application of WAVE/DSRC for more efficient streetlamp control,” presented at the *Proceedings of SICE Annual Conference*, pp. 1381–1383, 2011.
- [74] D. Jiang and L. Delgrossi, “IEEE 802.11p: Towards an international

- standard for wireless access in vehicular environments,” presented at the *IEEE Vehicular Technology Conference - VTC Spring*, pp. 2036–2040, 2008.
- [75] J. B. Kenney, “Dedicated Short-Range Communications (DSRC) Standards in the United States,” *Proceedings of the IEEE*, vol. 99, no. 7, pp. 1162–1182, 2011.
- [76] A. Goldsmith, *Wireless Communications*, 1st ed. Cambridge University Press, pp. 1–644, 2005.
- [77] IEEE, “IEEE Std 802.11™-2012, IEEE Standard for Information technology—Telecommunications and information exchange between systems—Local and metropolitan area networks—Specific requirements—Part 11: WLAN MAC and PHY specifications,” 802.11-2012, 2012.
- [78] Y. Morgan, “Notes on DSRC & WAVE Standards Suite: Its Architecture, Design, and Characteristics,” *Communications Surveys & Tutorials, IEEE*, no. 99, pp. 1–15, 2010.
- [79] G. Samara, W. Al-Salihy, and R. Sures, “Security issues and challenges of Vehicular Ad Hoc Networks (VANET),” presented at the *International Conference on New Trends in Information Science and Service Science (NISS)*, pp. 393–398, 2010.
- [80] J. Wang and N. Jiang, “A simple and efficient security scheme for vehicular ad hoc networks,” presented at the *IEEE International Conference on Network Infrastructure and Digital Content (IC-NIDC)*, pp. 591–595, 2009.
- [81] Bluetooth SIG, “Bluetooth Specification Version 4.0,” 2010.
- [82] Y. Wang, B. Ramamurthy, and X. Zou, “The performance of elliptic curve based group Diffie-Hellman protocols for secure group communication over ad hoc networks,” presented at the *IEEE International Conference on Communications (ICC)*, vol. 5, pp. 2243–2248, 2006.
- [83] ZigBee Alliance, “ZigBee Specification,” 2008.

- [84] M. Benocci, E. Farella, L. Benini, and L. Vanzago, "Optimizing ZigBee for Data Streaming in Body-Area Bio-Feedback Applications," presented at the *International Workshop on Advances in Sensors and Interfaces, IWASI*, pp. 150–155, 2009.
- [85] IEEE, "IEEE Standard 802 Part 15.4: Wireless Medium Access Control (MAC) and Physical Layer (PHY) Specifications for Low-Rate Wireless Personal Area Networks (LR-WPANs)," 802.15.4, 2003.
- [86] Dynastream Innovations Inc., "ANT Message Protocol and Usage." Dynastream Innovations Inc., pp. 1–96, 2011.
- [87] A. H. Omre, "Bluetooth low energy: wireless connectivity for medical monitoring," *J Diabetes Sci Technol*, vol. 4, no. 2, pp. 457–463, 2010.
- [88] E. Chalari, G. Intas, P. Stergiannis, V. Paraskevas, and G. Fildissis, "The importance of vital signs in the triage of injured patients," *Crit Care Nurs Q*, vol. 35, no. 3, pp. 292–298, 2012.
- [89] J. Masip, M. Gayà, J. Páez, A. Betbesé, F. Vecilla, R. Manresa, and P. Ruíz, "Pulse Oximetry in the Diagnosis of Acute Heart Failure," *Revista Española de Cardiología (English Edition)*, pp. 1–6, 2012.
- [90] Task Force of the ESC/ASPE, "Heart rate variability. Standards of measurement, physiological interpretation, and clinical use," *European Heart Journal*, pp. 354-381, 1996.
- [91] T. Ziemssen, J. Gasch, H. Ruediger, "Influence of ECG sampling frequency on spectral analysis of RR intervals and baroreflex sensitivity using the EUROBAVAR data set" *Journal of Clinical Monitoring and Computing*, pp. 159-168, 2008.